PNC SN 241 71-55

Creep Tests of Experimental Fast Reactor Fuel Claddings

(Primary Test)

November, 1971

CREEP SUB-GROUP

FBR MATERIALS SUBCOMMITTEE

FBR FUEL DESIGN COMMITTEE

PNC

C O N T E N T S

1. Introduction

Fuel cladding tubes for fast experimental reactor (JOYO) are made of
AISI 316 steel. In using these tubes, a comprehensive analysis on
their

    (1) high temperature strength property,

    (2) irradiation property, and

    (3) behavior in Na

must be conducted to enhance their reliability.

In particular, reliable data are required in the analysis of the high
temperature strength property since the data are of urgent necessity
for reactor design and are the basis on which the analyses of the
other two factors (2) and (3) are conducted. Generally, there are
many high temperature strength data available on the AISI 316 steel
but few of them treat of thin and small tubes such as cladding tube.
It is not easy, therefore, to determine and establish an allowable
stress.

Then, the Material Construction Design Committee was established in
the Power Reactor & Nuclear Fuel Development Corporation (Hideyoshi
Utoguchi, Chairman) for the purpose of

    (i) determining basic provisions for reactor design, and

    (ii) investigating high temperature strength.

With respect to the item (ii) above, performance of creep test and
fatigue test on cladding tube itself and establishment of the
respective subgroups were intended, the planning and the performance
of such tests started in 1969, and the primary tests were completed
in March, 1971.

This report relates to the primary test on creep; in the Creep Sub-
group (led by Susumu Yoshida) tests National Research Institute for
Metals, Kobe Steel Ltd., Sumitomo Metal Industries Ltd., Hitachi,
Ltd. and the Power Reactor & Nuclear Fuel Development Corporation
joined and performed internal pressure creep-rupture tests and
uniaxial tensile creep rupture and uniaxial tensile creep tests on
primary trial manufactures (2 types of tube A and tube B) for
"JOYO" reactor. The tests were made at temperatures $600^{\circ}C$, $650^{\circ}C$,

$700^{\circ}C$ and $750^{\circ}C$ aiming at a maximum rupture time from 3,000 to 10,000 hours. The obtained data were statistically analyzed and the creep rupture strength, creep limit and limiting creep stress at 10,000th hour were estimated. The comparison between internal pressure creep rupture and uniaxial tensile creep rupture and the comparison among data of similar steel were also conducted.

In succession to these tests, the tests on the secondary trial cladding tubes are now under way where creep rate will be obtained in internal pressure creep test.

2. Test Pieces

2.1 Outline

As the trial manufactures in 1968 of fuel cladding tubes for fast experimental reactor, thin and small austenitic stainless steel tubes (2 types of tube A and tube B) conforming to the AISI 316 manufactured by Kobe Steel Ltd. and Sumitomo Metal Industries were used. (For purchasing specifications thereof, see Appendix.) The major features are as follows:

(1) Dimensions: Outside diameter 6.3 ± 0.03 mm,
            Inside diameter 5.6 ± 0.025 mm,
            Thickness 0.35 ± 0.03 mm

(2) Manufacturing process: Vacuum melting
            Cold working: approx. 10%

(3) Allowable defect: $25~\mu$ in depth

2.2 Chemical Composition

The chemical composition of the test pieces is shown in Table 1.

2.3 Nature

The optical microscopic structure, grain size, surface roughness and hardness of the test pieces are shown in Table 2. Fig. 1 (tube A) and Fig. 2 (tube B) show the results of the high temperature tensile tests, and Fig. 3 shows the results of the high temperature burst test.

3. Testing Method

3.1 Sampling of Test Pieces

The test pieces were sampled out of the same lot of cladding tubes of each type of tubes, A and B, respectively. They were further sampled out of those that were found acceptable through an ultrasonic flaw detecting inspection. Tests were made at random on the finally selected specimens.

3.2 Dimensions of Test Pieces

The dimensions of the internal pressure creep rupture test piece are shown in Fig. 4. The length of the test piece proper is 200 mm. The connections between the test piece and the closure head and between the test piece and the connecting tube were welded by T.I.G. welding.

Fig. 5 shows a uniaxial tensile creep test piece. The length of the test piece is 115 mm in case of creep test and 300 mm in case of creep rupture test. Portion of the test piece is drawn inward to avoid rupture from the T.I.G. weld. All the welds in the test piece were checked by X-ray non-destructive test for welding defect.

3.3 Testing Machine

The operating conditions of the internal pressure creep testing apparatuses and the uniaxial tensile creep testing apparatus are shown in Tables 3-1 and 3-2, respectively.

4. Test Conditions

The test conditions are shown in Table 4.

5. Test Results

5.1 Results of Internal Pressure Creep Rupture Test

The tests were performed at $600^{o}C$, $650^{o}C$, $700^{o}C$ and $750^{o}C$ respectively at each participant institute, whose results are as shown in Tables 5 and 6. Each parenthesized figure shows a

reference value of test piece ruptured at or near the weld. The figures marked with (● and O) show that they were used as data for statistic analysis of the relation between pressure and rupture time, and those marked with (●) indicate that they were used as data for statistical analysis of the relation between pressure and Larson - Miller parameter. The relations between pressure and rupture time of all the data except those parenthesized are graphed as shown in Fig. 6 and Fig. 7.

From the above results, differences in the individual data of each institute are seen undistinguishably mingled with the deviations of the data of all the institutes showing no significant characteristics, and no common distinct tendency is found among the data of the institutes. Also, there seems to be no significant difference in rupture time between the tests made in Ar gas atmosphere and the tests made in the air at temperatures $650^{\circ}C$ and $700^{\circ}C$ for less than 3,000 hours.

Creep rupture strength was higher with tube A than with tube B in the present tests made at the specified temperatures for the specified time.

5.2 Results of Uniaxial Tensile Creep Rupture and Creep Tests

Tables 7 and 8 show the results of uniaxial tensile creep rupture test and creep test conducted at $600^{\circ}C$, $650^{\circ}C$, $700^{\circ}C$ and $750^{\circ}C$ by a test agency.* Here, the figures marked with (● and O) also indicate same use as in the foregoing subsection. The relation between stress and rupture time of all the data obtained is shown in Fig. 8 which indicates that creep rupture strength under uniaxial tension was also higher for tube A than for tube B. Also, no significant difference in rupture time nor distinct tendency was found in the obtained test results of the creep rupture test pieces and creep test pieces.

---

* Material Testing Division, N.R.I.M.

6. Rearrangement of Test Results

6.1 Internal Pressure Creep Rupture

6.1.1 Pressure - Rupture Time

In relation to pressure ($\log P$) and time to rupture ($\log t_R$), curves were statistically applied to the following polynomial expression:

$$y_i = \beta_0 + \beta_1 \chi_i + \beta_2 \chi_i^2 + \cdots\cdots\cdots + \beta_n \chi_i^n + e_i$$

where, y_i : Dependent variable

χ_i : Independent variable

β_0 : Constant

$\beta_1 \quad \beta_2 \cdots\cdots\cdots , \beta_n$: Regression coefficient

e_i : Error in normal distribution $(0, \sigma_s^2)$

i : 1, 2, $\cdots\cdots\cdots$, m

In applying to the above expression, longarithm of pressure ($\log P$) was used for independent variable χ_1 and logarithm of rupture time ($\log t_R$) for dependent variable y_i. Regression line was estimated on the supposition that the dependent variable ($\log t_R$) will be normally distributed in a uniform variance.

In actual calculations, orthogonal polynomial expression was used for simplicity of calculation. The ratio $V_{k+1}/V_{E(k+1)}$ of mean square V_{k+1}, which is due to regression fluctuation induced by the addition of the k + 1 member to a k-degrees regression expression, to mean square $V_{E(k+1)}$, which is due to residual fluctuation for the (k+1)-degree expression, was calculated and the obtained value was compared with the value of F-distribution table at significance level of 5%. Studies were made to see if increase of degree would lead to some significant result and how correlation between χ_i and y_i would be intensified by increasing degree of regression. Thus, the location of a degree was deduced at which no further multiplication of degree would produce any significant effect in an orthogonal polynomial expression; a regression expression

up to a degree next preceding the degree thus deduced was chosen and the chosen degree expression was confirmed to be reasonable by the change of contribution.

Based on the above-stated statistic method, regression analysis was made on the relation between pressure and rupture time as shown in Table 9. In making up this table, the data of tube A and the data of tube B were separately analyzed regressively, and then regression analysis was made on both tubes A and B put together. In such a manner as aforementioned, ratio of mean square $/FO$ (RES)$/$ was compared with F-value at significance level of 5% $/F$ (0.05)$/$ and significant degree of regression equation (round mark in the table) was selected in reference to the change of contribution (r^2). The degree thus obtained was of the first degree in the analysis where the data of tubes A and B were separately regressed, while the equation was of the first degree at $600^{\circ}C$, $700^{\circ}C$ and $750^{\circ}C$ and of was the second degree only at $650^{\circ}C$ where the data of tubes A and B were analyzed together.

For relation between contribution and test temperature in regression equation of the degree selected on the data of the test pieces, the contribution was 67.2% at $600^{\circ}C$, and showed higher percentage 91.7%, 94.7% or 97.0% at test temperature $650^{\circ}C$ or higher. This tendency was seen common to the data for tube B and also to the combined data of tubes A and B. Therefore, as long as the contribution alone is concerned, it is known that deviation is greater at $600^{\circ}C$ than at $650^{\circ}C$ or higher temperature in both cases of A and B tube data. It is also indicated that contribution at each testing temperature is lower in the combined data of tubes A and B than in the single data of either tube A or B, suggesting the presence of a certain great difference between the data of tube A and those of tube B. Standard deviation $/SD$ (RES)$/$, an index of the deviation of data from regression line, showed a similar tendency.

Each regression curve of tube A, tube B, and tubes A and B, in relation to pressure vs. rupture time, is shown in Figs. 9, 10, and 11, respectively. Confidence interval at 95% confidence coefficient based on the deviation of data from each estimated regression value was also shown on each graph. These curves were graphed with a digital plotter (n244A) direct connected to an computor NEAC 5100. In tube A and tube B, all the regression equations selected were of the first degree and the regression coefficient of the first member of such equations had a tendency to become high as test temperature was increased. It means that the gradient of the curve of log P for log t_R at high temperature is gentle, that is, the gradient of the curve of log t_R for log P is steep. At 650°C in Fig. 11, the regression curves have sharp turn at long time portion. This is related to the adopted quadratic equation as a regression expression, but such regression curves are not desirable as tendency lines of data.

6.1.2 Pressure – Larson-Miller Parameter

Using the following Larson-Miller parameter the relation between pressure and rupture time was rearranged so that from the internal pressure creep rupture data obtained for test times up to 3,000 hours, pressure against specific rupture time for longer hours and rupture time against specific pressure for longer hours may be estimated.

$$LMP = T (C + \log t_R)$$

where, T : Absolute temperature (test temperature)

C : Parameter constant

Curves were applied to the pressure and LMP correlation in the same manner as applied to the pressure and rupture time correlation in the foregoing section 6.1.1.

It is important to have a parameter constant most suitable for interpolation and extrapolation. For this purpose, the regression curves of pressure and LMP were applied in an orthogonal polynomial equation method in accordance with

- 7 -

the method of least square in order to obtain sum of squares of residuals between the estimated regression value and actually measured rupture time (expressed in logarithm, respectively) was adopted as most suitable one among those thus obtained.

Table 10 shows a regression analysis for the relation between pressure and LMP with a most suitable parameter constant. The degrees of the regression equation was selected in the same manner as in section 6.1.1 to be determined quadratic for tube A, cubic for tube B, and quadratic for tubes A and B combined. Contribution at each significant degree was 89.2% with tube A, 93.5% with tube B, and 72.6% with tubes A and B, indicating that combined regression of tubes A and B is not suitable.

Confidence interval at 95% confidence coefficient and regression curve in a selected equation of significant degree with such parameter constant as adopted in a manner mentioned above are shown in Figs. 12, 13 and 14. The value (C) of the adopted parameter constant was 17.01 for tube A, 13.12 for tube B, and 14.20 for tubes A and B in combination. The regression curve of tube A (Fig. 12) and that of tube B (Fig. 13) showed different tendencies, the former tending to curve downward while the latter tending to curve upward at high temperature in long time test. The data plot of combined tubes A and B in Fig. 14 indicates that tube A has higher rupture strength compared with tube B. As the low contribution percentage of 72.8% indicates, the application of curve was unsuccessful. This is because there was a comparatively great difference between the rupture strengths of tube A and tube B.

It is also noted, as stated in section 5.1, that there was found no significant difference among the data of all the test institutes and that the difference of

atmospheric constituents in which test pieces were tested did not bring about difference upon the data.

6.1.3   Pressure — Temperature

From the selected regression curves and the confidence intervals in the relation of pressure and LMP, the highest and lowest limit values of confidence intervals and the estimated regression values of pressures at test temperatures for rupture time of 1,000, 3,000, 10,000 and 15,000 hours were obtained. The relation of pressure and temperature for each rupture time in tube A, tube B, and tubes A and B is shown in Figs. 15, 16 and 17, respectively. In these three figures, the full lines are of estimated values obtained from regression curves and the break lines are of values obtained from the lowest limits of the confidence intervals at 95% confidence co-efficient. The values of the lowest limits only are shown because they are considered important for design purpose, while those of the highest values are omitted to avoid complexity in the graphs.

In combined tubes A and B (Fig. 17), assumptions can be made in many ways including an assumption that rupture time will be normally distributed under a certain level of pressure, and they will lead to an assumptive conclusion that 50% of cladding tubes will rupture in 10,000 hours at $650^{\circ}C$ under pressure of approximately 150 kg/cm^2, and that 2.5% of cladding tubes will rupture in 10,000 hours under pressure of approximately 115 kg/cm^2.

6.2   Uniaxial Tensile Creep Rupture

6.2.1   Stress — Rupture Time

For the relation between stress ($\log \sigma$) and rupture time ($\log t_R$), the application of curves by polynomial equation was made in the same manner as in section 6.1.1.

Table 11 presents the regression analysis in the relation between stress and rupture time, in which the selected significant degrees of equation were both simple and quadratic. In every type of tubes at every test temperature, the contribution percentage is seen higher than in the case of the pressure vs rupture time correlation. One of the reasons is probably that these data were obtained by only one test institute. In the case of pressure vs rupture time the contribution percentage was lower at $600^{o}C$ than at other test temperatures, and the same phenomenon was found also in the correlation for combined tubes A and B.

Figs.18, 19 and 20 were drawn up by digital plotter of the confidence intervals at 95% confidence coefficient and the regression curves in the selected equation of the significant degree. Data deviation was higher for tubes A and B combined than for tube A and tube B.

6.2.2 Stress - Larson-Miller Parameter

Table 12 shows regression analysis results for the relation between stress and LMP obtained in the same manner as in section 6.1.2. The significant degree in the selected equation was quadratic for tube A, cubic for tube B, and quadratic for tubes A and B, same as in the pressure vs rupture time.

Figs.21, 22 and 23 present confidence intervals at 95% confidence coefficient and curves of selected regression equation of significant degree with a parameter constant adopted by statistic method. The tendencies of regression curves at high temperatures in long test time were different between tube A (Fig. 21) and tube B (Fig. 22) as in the pressure vs rupture time correlation. It is obvious that combined analysis of tube A and tube B does not bring about high contribution and that tube A has higher rupture strength than tube B.

6.2.3 Stress - Temperature

The relations between stress and temperature in 1,000 hrs, 3,000 hrs, 10,000 hrs, 15,000 hrs and 30,000 hrs obtained from the selected regression equation and the confidence intervals in the stress-LMP correlation are shown in Figs. 24, 25 and 26. In the case of tubes A and B combined (Fig. 26), the stress value from the regression curve at 650°C for 10,000 hours was 11.8 kg/mm² and the stress value from the lowest limit of the confidence interval at 95% confidence coefficient was 9.2 kg/mm².

6.3 Uniaxial Tensile Creep

6.3.1 Creep Curves

As an example of obtained creep curves, curves at 650°C are shown in Fig. 27. It indicates that where initial stress and test time are same, tube A has higher creep rate than tube B. In the strain calculation, the elongations between the edges of the test piece and the edges of the tight drawn spot are disregarded because the ratio of the elongation of this parts to the elongation measured between the edges of the test piece was less than 1/20 after rupture.

6.3.2 Stress - Minimum Creep Rate

Fig. 28 presents relation between stress and minimum creep rate. Curves were applied by the method of visual fit to the plots obtained in each type of material at each temperature. Apparent difference was seen between tube A and tube B, the former showing higher creep strength than the latter.

6.3.3 Stress - Time to Reach Specified Full Elongation

The relations between stress and time to reach full elongations of 0.5%, 1% and 2% are shown in Figs. 29 and 30. All the test pieces except 4 test pieces of tube B attained full elongation of 2% before they were ruptured.

6.3.4 Stress - Temperature

Of the relations between stress and temperature producing a fixed minimum creep rate, Fig. 31 presents the curves obtained from the stress vs minimum creep rate relations and Figs. 32 and 33 show the relation between stress and temperature that effects a full specified elongation in a fixed time; the former indicates creep limit at each temperature, while the latter indicates limiting creep stress at each temperature under each total strain. Both the creep limit and the limiting creep strees are seen higher in tube A than in tube B. The creep limit at which the minimum creep rate attained $10^{-4}\%$/hr at 650°C (Fig. 31) was 13.7 kg/mm^2 for tube A and 11.8 kg/mm^2 for tube B. The limiting creep stress at which full elongation of 1% was effected at 650°C for 10,000 hours was 13.0 kg/mm^2 for tube A (Fig. 32) and 10.4 kg/mm^2 for tube B (Fig. 33).

6.3.5 Rupture Time - Minimum Creep Rate

The relation between rupture time and minimum creep rate obtained at a same stress from uniaxial tensile creep test is shown in Fig. 34. The results for both tube A and tube B were approximated to a straight line, though somewhat deviated. Where the minimum creep rate is same, rupture time is seen longer for tube A than for tube B.

6.4 Correlation between Internal Pressure Creep Rupture and Uniaxial Tensile Creep Rupture

Since the practice of a uniaxial tensile creep rupture test is easier than that of an internal pressure creep rupture test, it will be convenient if the rupture time of the latter can be deduced from the data of the former by elucidating any usable correlation between the two types of ruptures.

For this purpose, test pressure in internal pressure creep rupture was replaced with hoop stress using the following experimental equations that represent the relation between the critical pressure of internal pressure cylinder and the tensile strength of material.

Equation of outside diameter : $\sigma = P\left(D_0/2t_k\right)$

Equation of average diameter : $\sigma = P\left(D_0/2t_k - 0.5\right)$

Equation of inside diameter : $\sigma = P\left(D_0/2t_k - 1\right)$

where, σ stands for hoop stress, P for test pressure, D_0 for outside diameter and t_k for thickness. The correlation between the tensile stress obtained in uniaxial tensile creep rupture test and the hoop stress obtained from the test pressure in internal pressure creep rupture test at same temperature for same rupture time is shown in Figs. 35 and 36.

Almost same results were obtained with tube A and tube B. Their indications are that hoop stress obtained from each equation is comparatively well related with tensile stress and, above all, that the closest correlation seems to come from the equation of average diameter which produces inter-mediary value between outside diameter and inside diameter plots. It seems generally reasonable, therefore, to relate internal pressure creep rupture with uniaxial tensile creep rupture by the medium of hoop stress calculated by the equation of average diameter for the purpose of the present test.

6.5 Comparison between Obtained Data and ISO Data

The uniaxial tensile creep rupture data and the data of internal pressure replaced with hoop stress in the equation of average diameter that were obtained in the present test were compared with the ISO data (ISO/TG17/WG10/EPT-SG) which contain tensile creep rupture data of tubes, plates and rods of same 316 steel as the present cladding tubes and which were collected from England, Japan, Sweden, Belgium and Italy, and the comparison results are shown in Figs. 37 and 38.

This comparison indicates that rupture strength at each test temperature is slightly higher in the data of the present test than in the ISO data. But the data of the present test tend to show approximation to the ISO data when tested for long time.

Then, another comparison was made, as shown in Fig. 39, between the estimated average rupture stress for 10,000 hours and 30,000 hours specified to each temperature by the ISO, and the estimated rupture stress for the same rupture hours that was obtained from regression curves in the correlation of stress and LMP where tube A and tube B were analyzed in combination. As this comparison figure shows, rupture strength of the present test is higher at 650°C and 700°C but lower at 600°C than the ISO's, but the difference in stress is within 1 kg/mm². The differences may be regarded, therefore, negligible when test time is long.

6.6 Estimated Values of Stress

The estimated values of rupture strength in 10,000 hrs and 15,000 hrs, creep limit at the minimum creep rate of $10^{-4}\%$/hr, and limiting creep stress to effect total strain of 1% in 10,000 hrs that were obtained through rearrangement and review of the above test results are shown in Table 13.

6.7 Test Pieces after Internal Pressure Creep Rupture

Photo 1 shows an example of the appearance of the test pieces after they underwent internal pressure creep rupture. These specimens were tested by a test institute in the atmosphere of air by the pressure medium of Ar gas. These photos show that the aspect of rupture in the breaks is "open-door" type at low temperatures. At high temperature, such aspect is seen to be "seam-like" or "pinhole" type as shown in Photo 2.
This difference in the aspect of breaks is thought to be in association with the ductility of the test pieces in each test condition.

Photo 2 shows an another example of the appearance of the test pieces tested for rupture by another test institute. They have "seam-like" type and "pinhole" type ruptures including "seam-like" breaks on symmetrical positions of a tube wall (tube A, 186-4, 280 kg/cm², 526.0 hrs) and 2 "seam-like" parallel breaks on the same spot of a tube wall (tube A, 186-5, 250 kg/cm², 876.1 hrs).

6.8 Dimensions of Test Pieces After Rupture

Increase in outside diameter ($^{\triangle D}/D_0$, %, mean value of several measurements) in the axial position of creep rupture test pieces after ruptured under internal pressure was studied and an example of the obtained results is shown in Fig. 40. Some difference of increases in outside diameter of test pieces is seen in these graphs depending on axial positions. Values of such increases in outside diameter of each test piece except at or near rupture were averaged under the consideration that such mean value will be almost equal to the increase in outside diameter of each test piece as a whole, and the mean value was plotted in relation to rupture time as shown in Fig. 41. From Fig. 41, such increase in outside diameter is seen slightly lower in tube B than in tube A. It also indicates that although increase in outside diameter is seemingly independent on rupture time, it tends to be slightly accelerated at 750°C in long rupture time.

Fig. 42 shows the relation between elongation and rupture time of creep test pieces ruptured under uniaxial tension, obtained by a test institute. Here, a certain relativity is seen between the elongation and rupture time, that is, the elongation tends to become high in short rupture time and to become low in long rupture time, and the curve in long rupture time is inclined to become easy at higher temperatures below 750°C, at which the elongation is seen higher to the contrary. This elongation is thought indicative of recrystallization started in long rupture time. The elongation of tube A is higher at low temperature but lower at high temperature in long rupture time than tube B. In general, the rupture time in which the elongation tendency is reversed appears to become shorter as temperature increases. Hence, recrystallization is though to start earlier in tube B than in tube A.

Anyhow, within the ranges of the temperatures and rupture time in the present test, there were found cases where increase in outside diameter and elongation can be very small, with the minimum increase value of 0.8% in outside diameter of test pieces (except at or near ruptures) creep-ruptured under internal pressure and

with the minimum elongation value of 0.6% in ruptures of creep test after tested under uniaxial tension.

6.9 Hardness of Test Pieces after Rupture

After rupture, hardness (H_v) of internal pressure creep rupture test pieces was measured in their axial positions. Fig. 43 shows those of tube A test pieces after long rupture time at $650^{\circ}C$ and Fig. 44 shows those of tube B test pieces after long rupture time at $650^{\circ}C$. Obtained hardness values (each plot represents the mean of several measurements) are somewhat varied; one of the causes may presumably be that measuring loads in the Vickers hardness measurements were not same in all the test institutes. Deviation in measured values was also found in different axial positions of a same test piece (except at rupture), but considering that such deviation may be slight and that such deviation may be of similar size at other temperatures, measured values of a same test piece were averaged. Thus, mean hardnesses of test pieces ruptured at 4 test temperatures in long rupture time were rearranged with Larson-Miller parameter (parameter constant fixed at 20) and put into Fig. 45. In Fig. 45, each plot is given with averaged values of longitudinal section and cross section in a same test piece, which result in high deviation. On the whole, however, hardness shows declining tendency within the parameter range 20 to 22.

Fig. 46 shows the relation between hardness $(H_v, 200g,$ average of several measurements) of test pieces creep ruptured under uniaxial tension at each temperature in long rupture time and Larson-Miller parameter (with fixed constant value of 20). The hardness of tube A is higher than that of tube B and is scarcely affected by the change of parameter values, while the hardness of tube B tends to become slightly lower when the parameter value is set between 22 and 24.3. This may be explained, as stated in the foregoing section of rupture elongation, from the presumable reason that recrystallization was taking place earlier in tube B at high temperature in long rupture time than in tube A.

6.10 Post-Rupture Structure

Photographs of photomicrographic structures taken on the fractured portions and the opposite sides of test pieces creep-ruptured under internal pressure are shown in Photo 3. Ruptures are seen in grain boundaries and numbers of grain boundary cracks are found in the vicinity of the fractured portion of tube B pieces at $700^\circ C$ for 815.0 hrs. In these photos, effect of cold working is noted still remaining on the longitudinal sections even after rupture took place. (For effects of cold working, see Table 2.)

Photographs of photomicrographic structures (in the vicinity of fractured portion) ruptured at each test temperature in long time are shown in Photo 4 (internal pressure creep ruptures) and Photo 5 (uniaxial tensile creep ruptures). As seen in these photos, precipitations are increasingly produced inside grain and on grain boundaries as temperature increases, σ-phase is precipitated at $750^\circ C$, and grain size is grown up through recrystallization. Except grain size, there can be seen no great structural difference between tube A and tube B.

The precipitation of carbide, the precipitation of σ-phase and the recrystallization are closely related with the behavior of the obtained creep rupture curves, creep curves, aspects of ruptures, rupture elongation and hardness.

7. Conclusion

The results of the internal pressure creep rupture test, the uniaxial tensile creep test and the creep rupture test made on fuel cladding tubes for fast experimental reactor under non-irradiation condition are summarized as follows:

1) Difference was found in the creep properties of type A tubes and type B tubes trial-manufactured by 2 domestic manufacturers.

2) Significant difference was not found among the data obtained by all the test institutes from internal pressure creep rupture tests. Also, the data obtained from the tests made at temperatures $650^\circ C$ and $700^\circ C$ in the atmosphere of Ar gas for 3,000 hours max. did not show difference by atmosphere.

3) Studies on the relation between the internal pressure creep rupture test and the uniaxial tensile creep rupture test indicate that the equation of average diameter can satisfactorily associate the two.

4) For creep rupture strength, the comparison between the present test data and the ISO data indicates that the strength in short rupture time is higher in the present test data than, and is approximated in long rupture time to, the ISO data which employed non-cold worked test pieces.

5) As a result of statistic analysis of the obtained test results, stress values as basic data for design purpose was obtained as shown in Table 13.
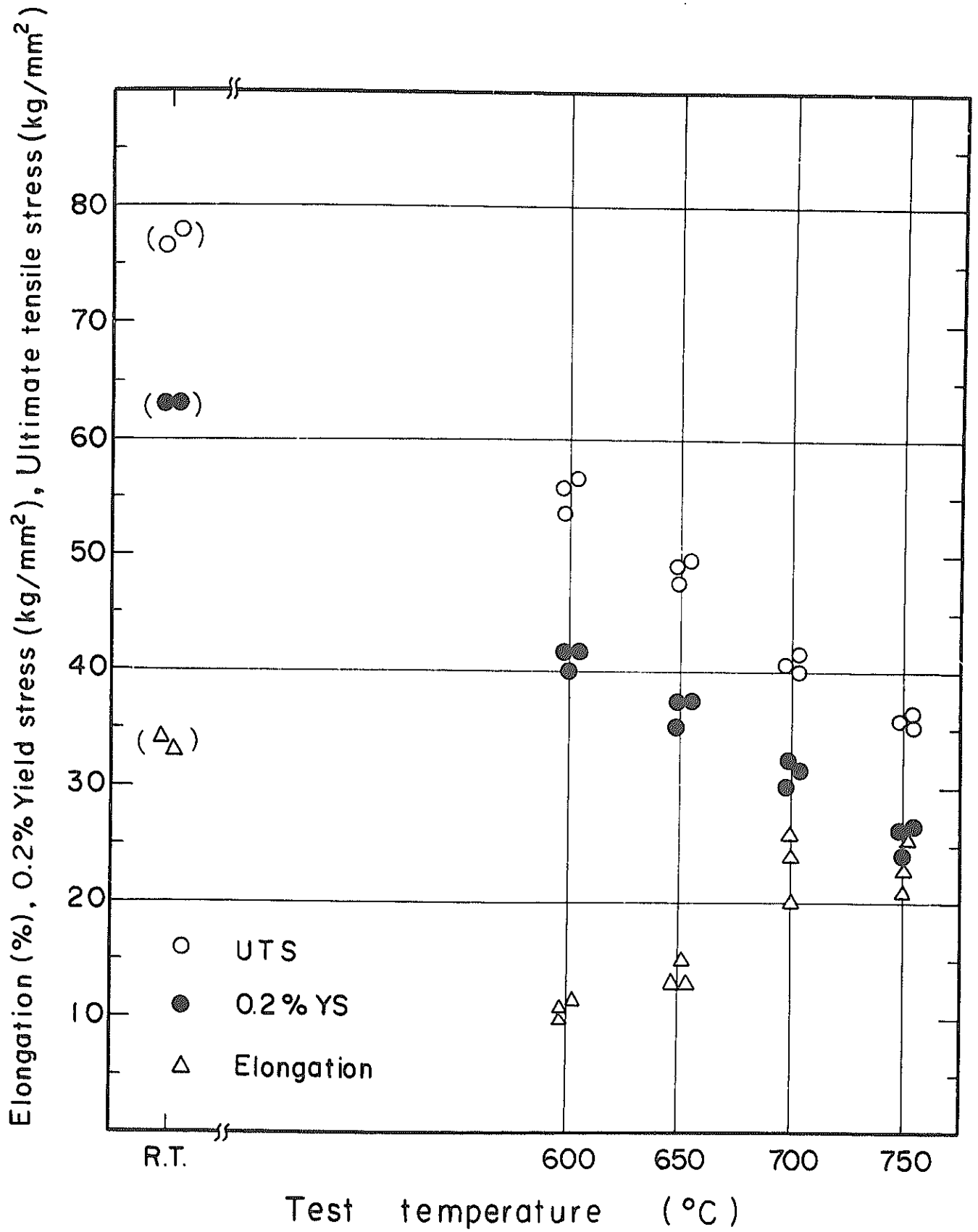
Fig. 1   Tensile properties vs. test temperature.
(Tube A)
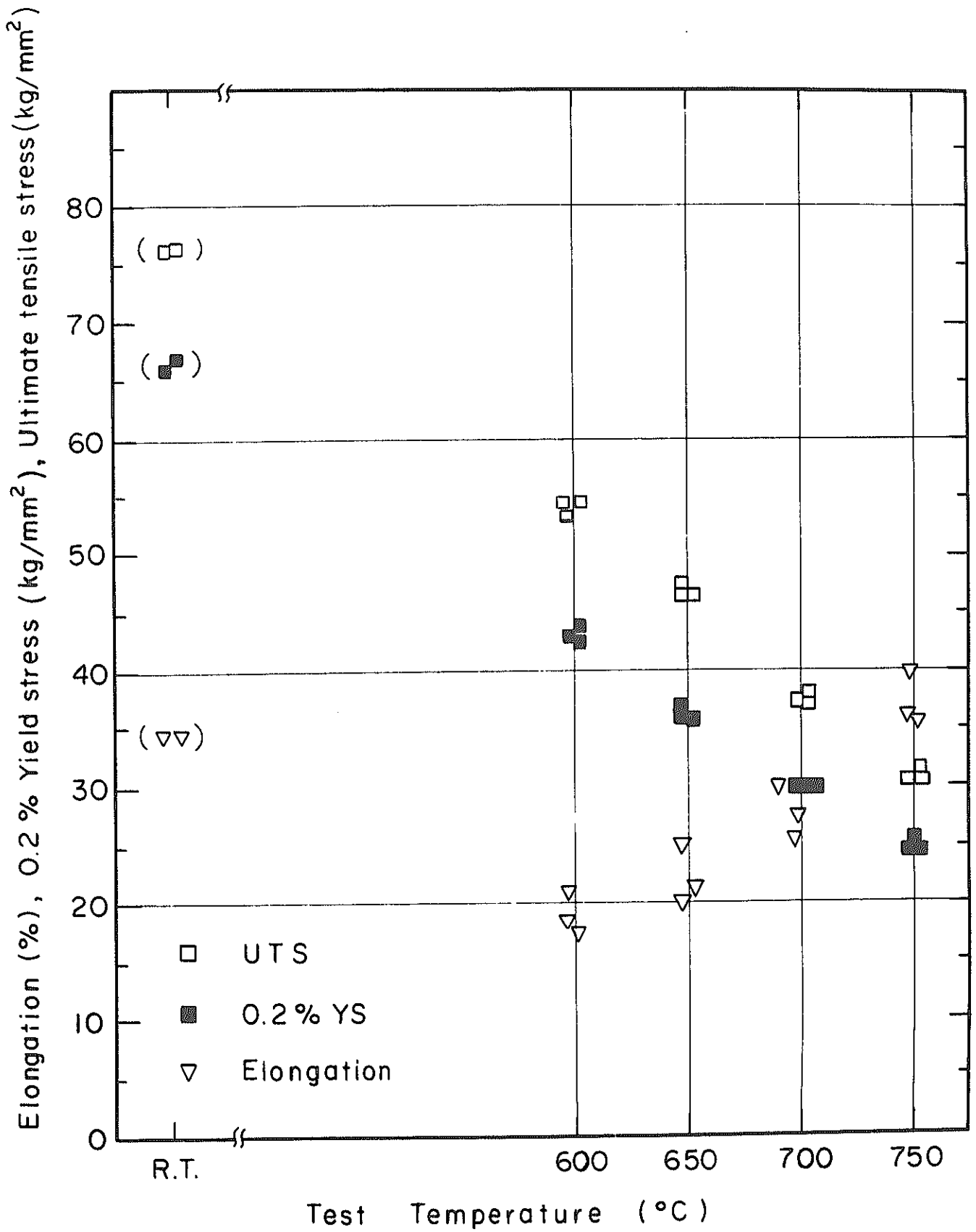
Fig. 2　　　Tensile properties vs. test temperature
(Tube B)
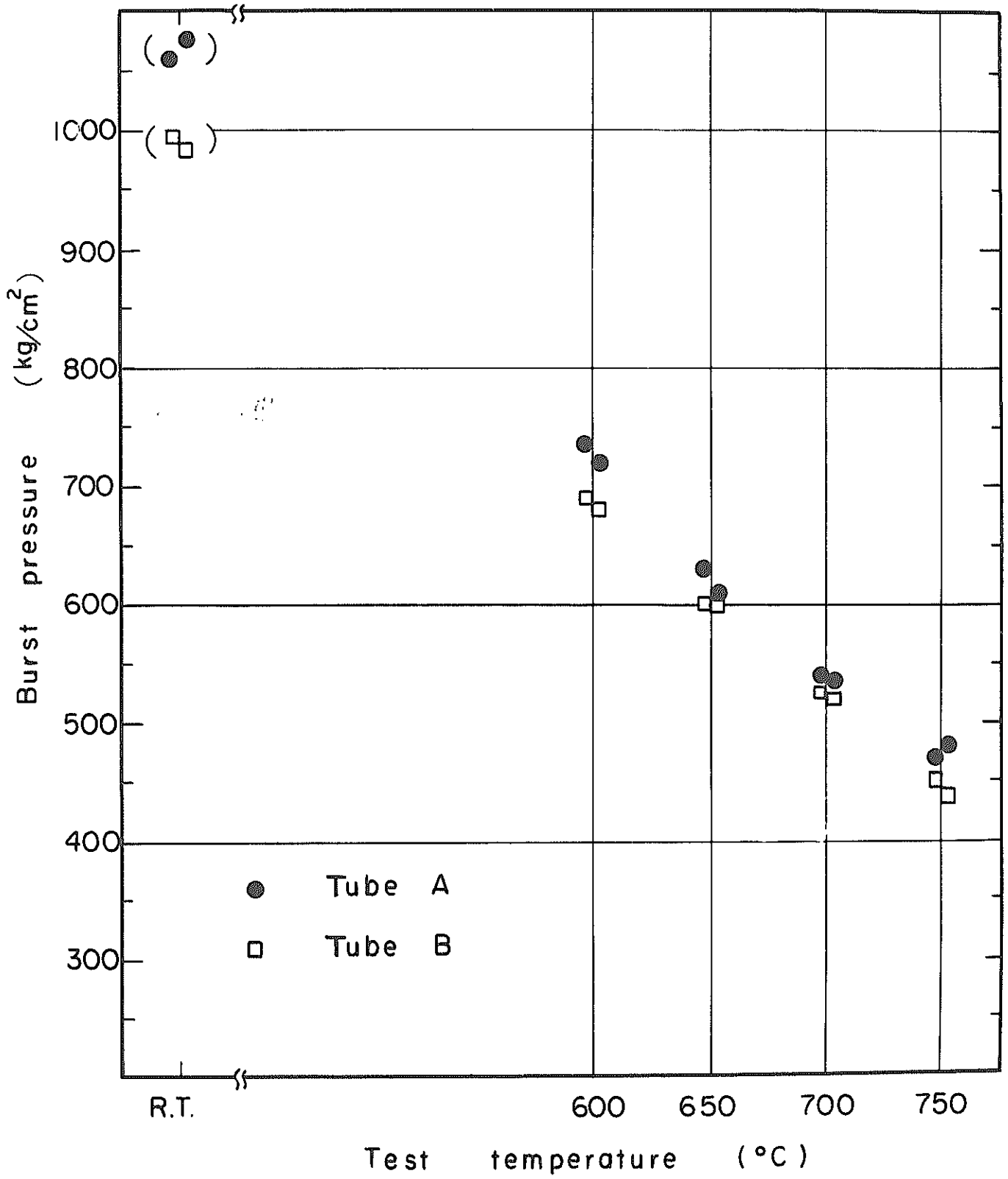
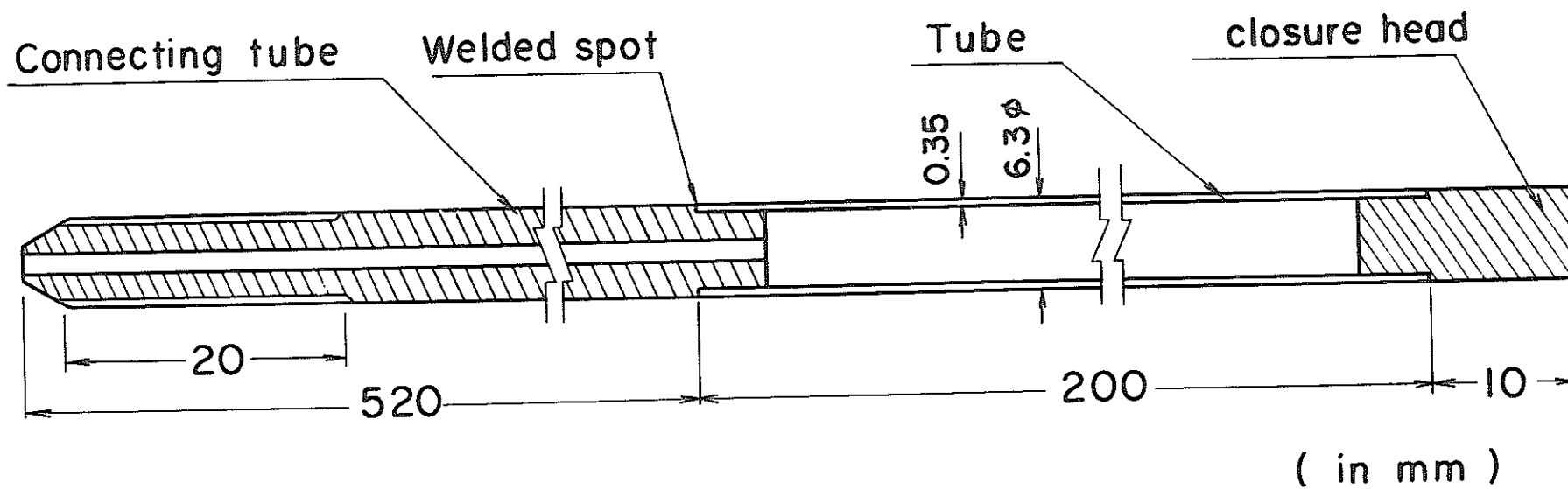Fig. 3   Burst pressure vs. test temperature

Connecting tube   Welded spot   Tube   closure head

0.35

6.3 ϕ

20

520   200   10

(in mm)

Fig. 4   Tubular creep−rupture specimen under internal pressure.

Screw coupling

Tube

Tight spot

Welded spot

0.35

6.3 ϕ

115

190

(in mm)
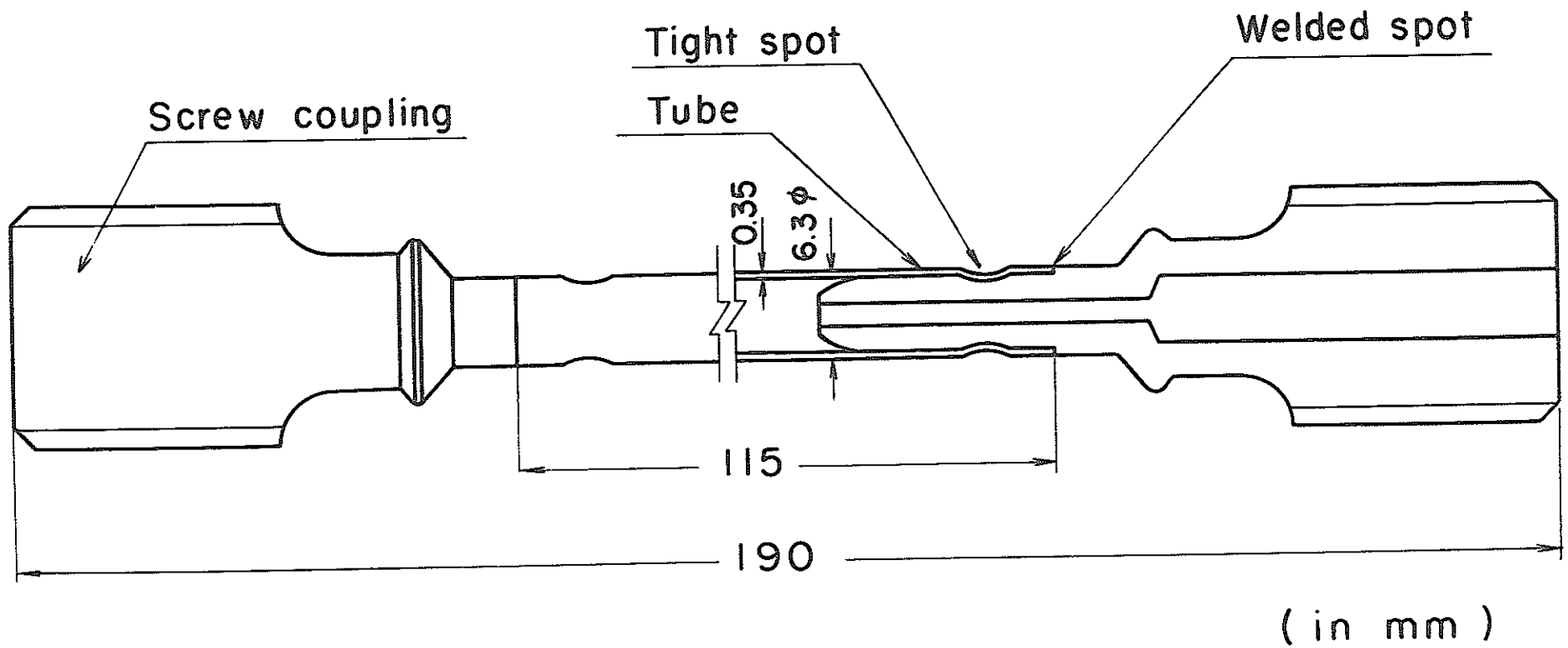
Fig. 5　　Tubular creep specimen under uniaxial tension.
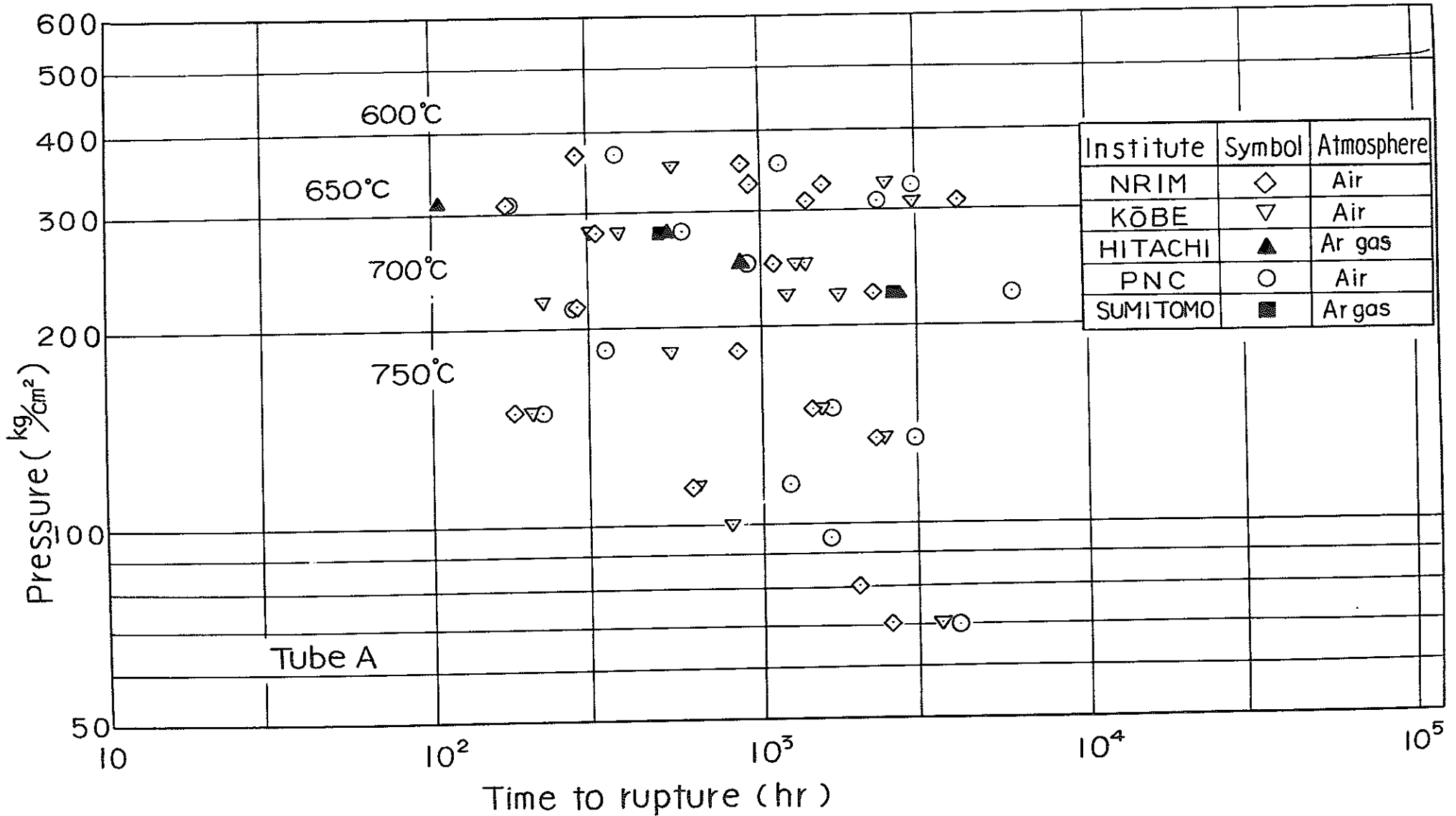
Fig. 6 Creep-rupture data under internal pressure for Tube A.
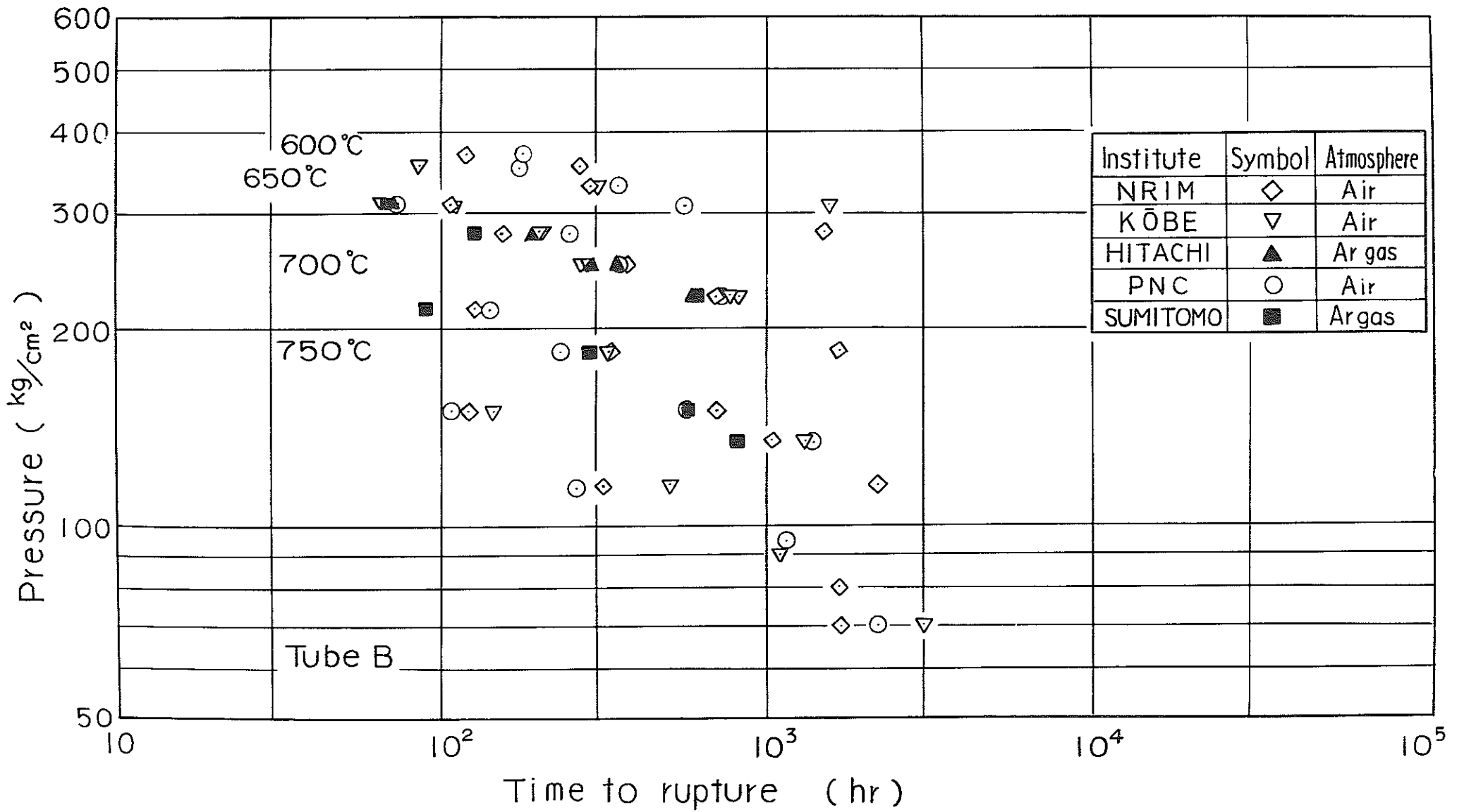
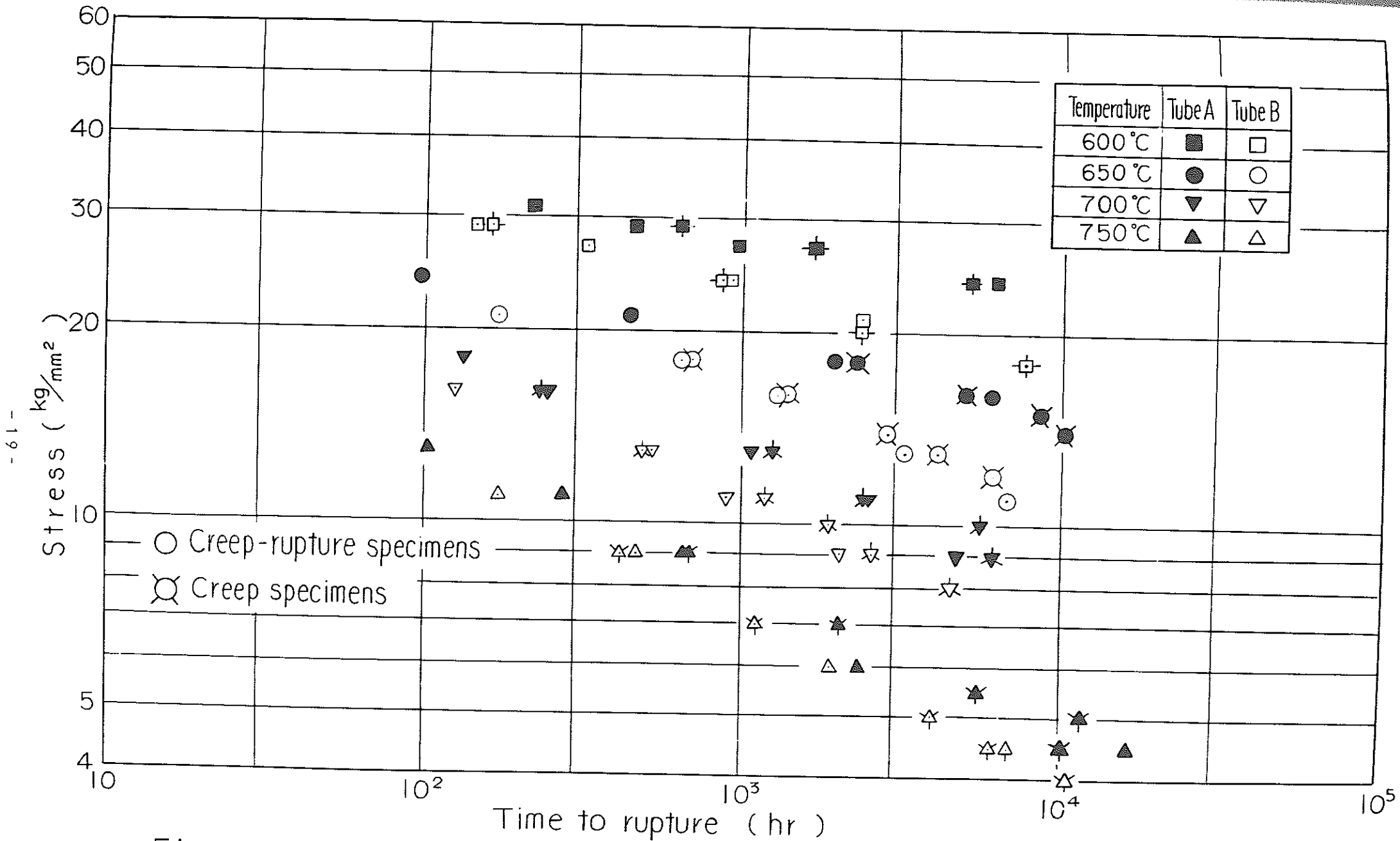Fig. 7 Creep-rupture data under internal pressure for Tube B.

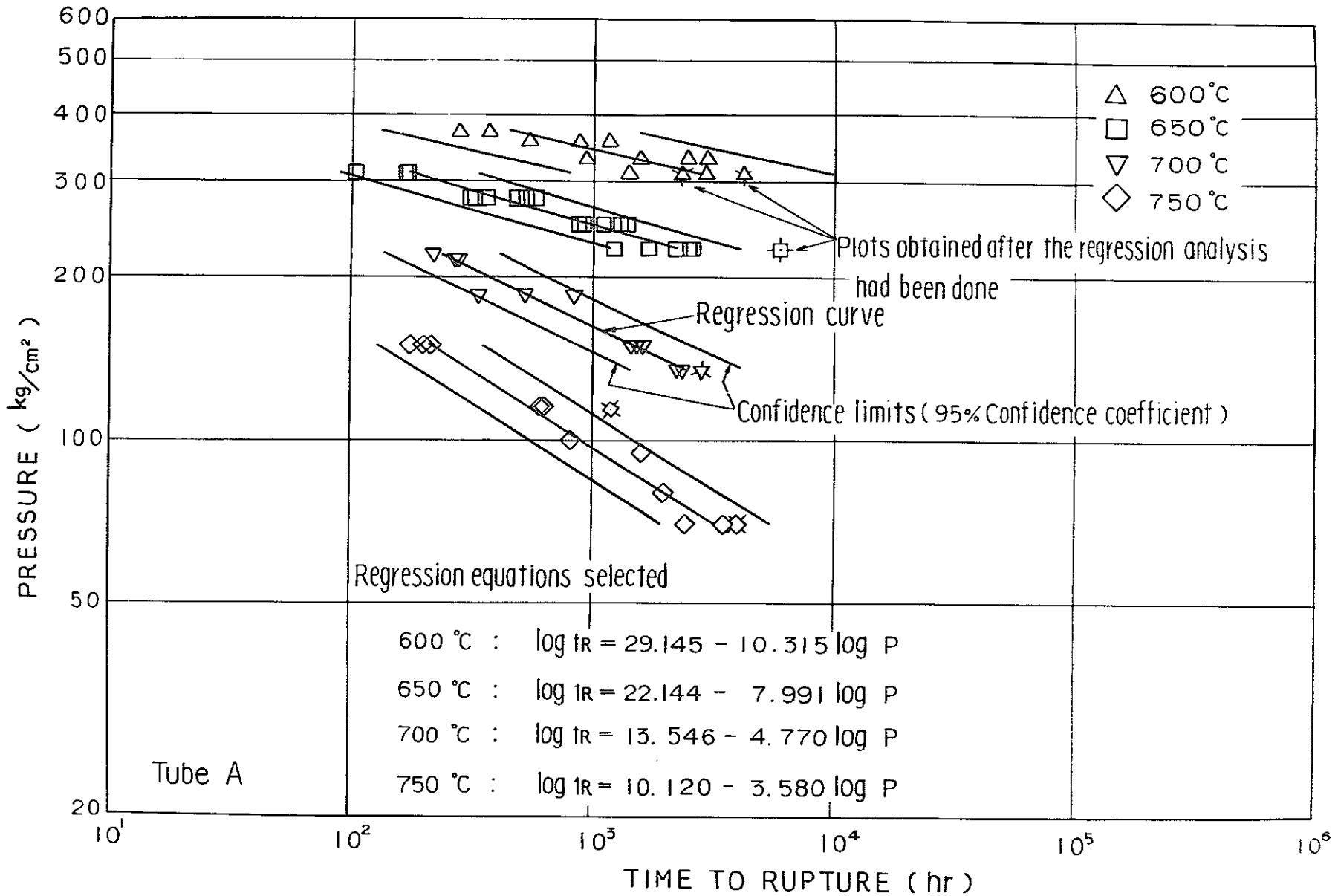Fig. 8 Creep-rupture data under uniaxial tension for Tubes A and B.

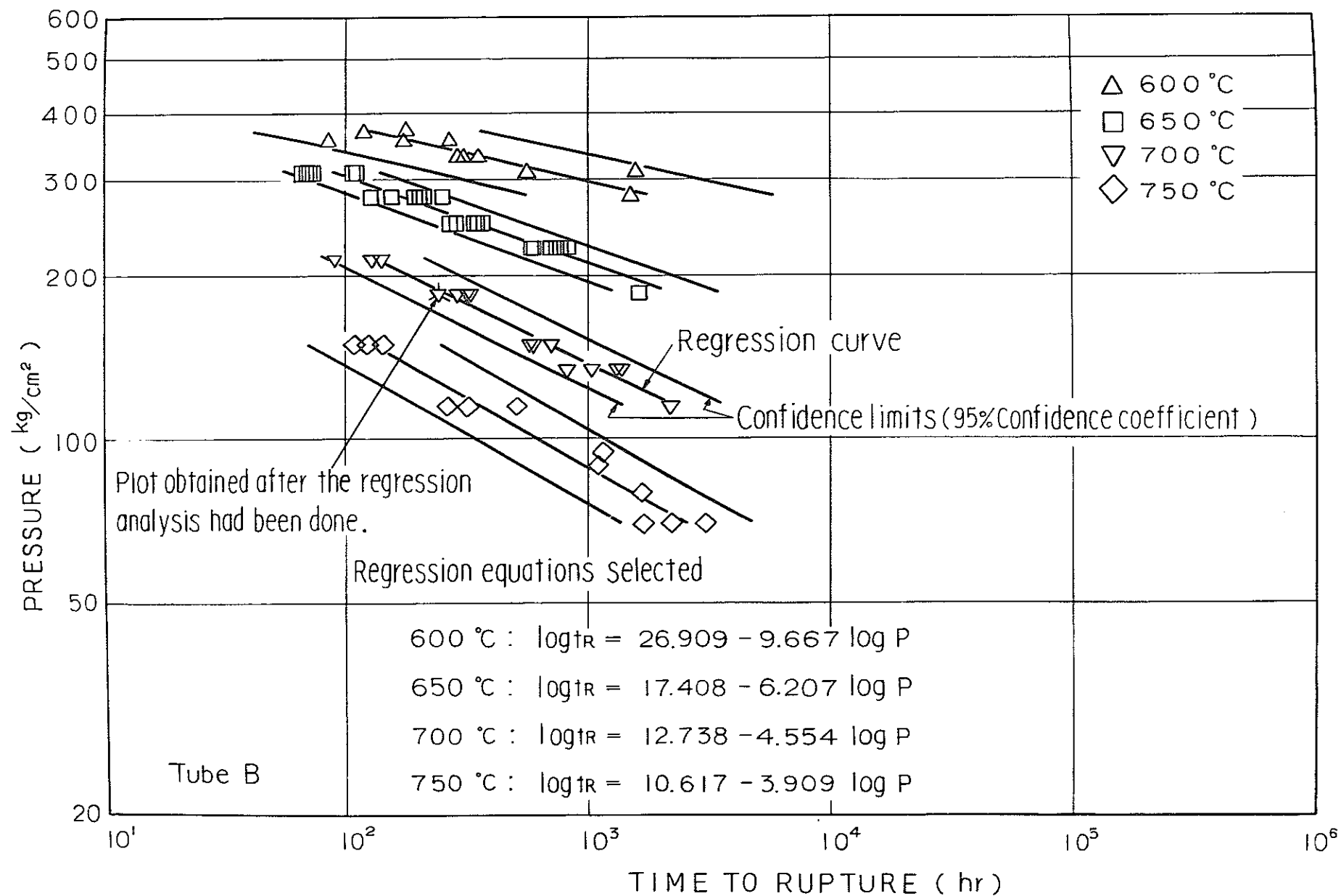Fig. 9 Regression curves and confidence intervals on creep-rupture data under internal pressure for Tube A.

F ig. 10 Regression curves and confidence intervals on creep - rupture data under internal
pressure for Tube B .

Δ 600 ℃
□ 650 ℃
▽ 700 ℃
◇ 750 ℃

Plots obtained after the regression analysis had been done.

Regression curve

Confidence limits (95% Confidence coefficient)

Regression equation selected

600 ℃ : $\log t_R = 25.329 - 8.924 \log P$

650 ℃ : $\log t_R = -107.081 + 97.974 \log P - 21.751 (\log P)^2$

700 ℃ : $\log t_R = 12.349 - 4.315 \log P$

750 ℃ : $\log t_R = 10.314 - 3.721 \log P$

PRESSURE ($^{kg}/cm^2$)
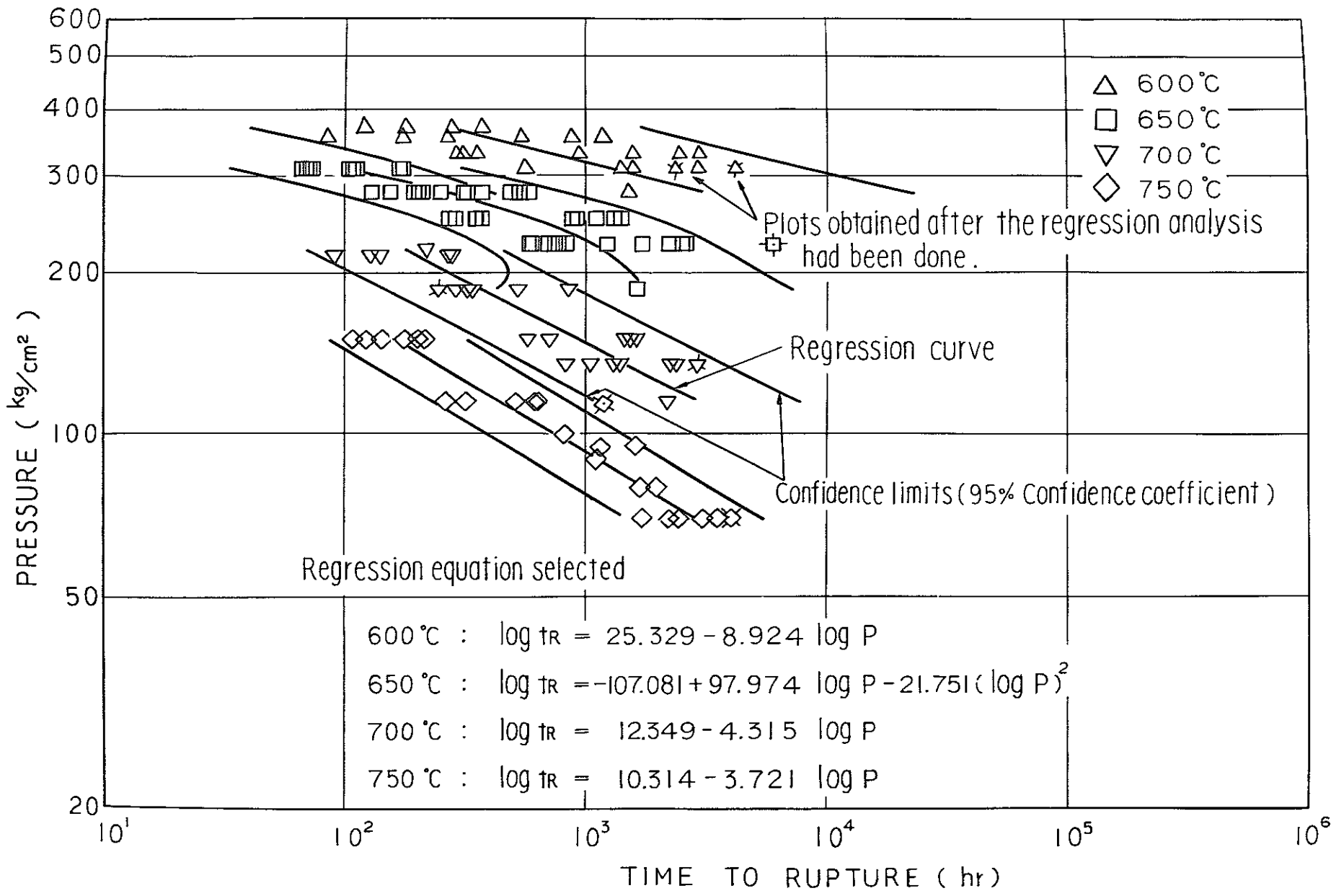
TIME TO RUPTURE (hr)

Fig.11 Regression curves and confidence intervals on creep-rupture data under internal pressure for Tubes A and B.
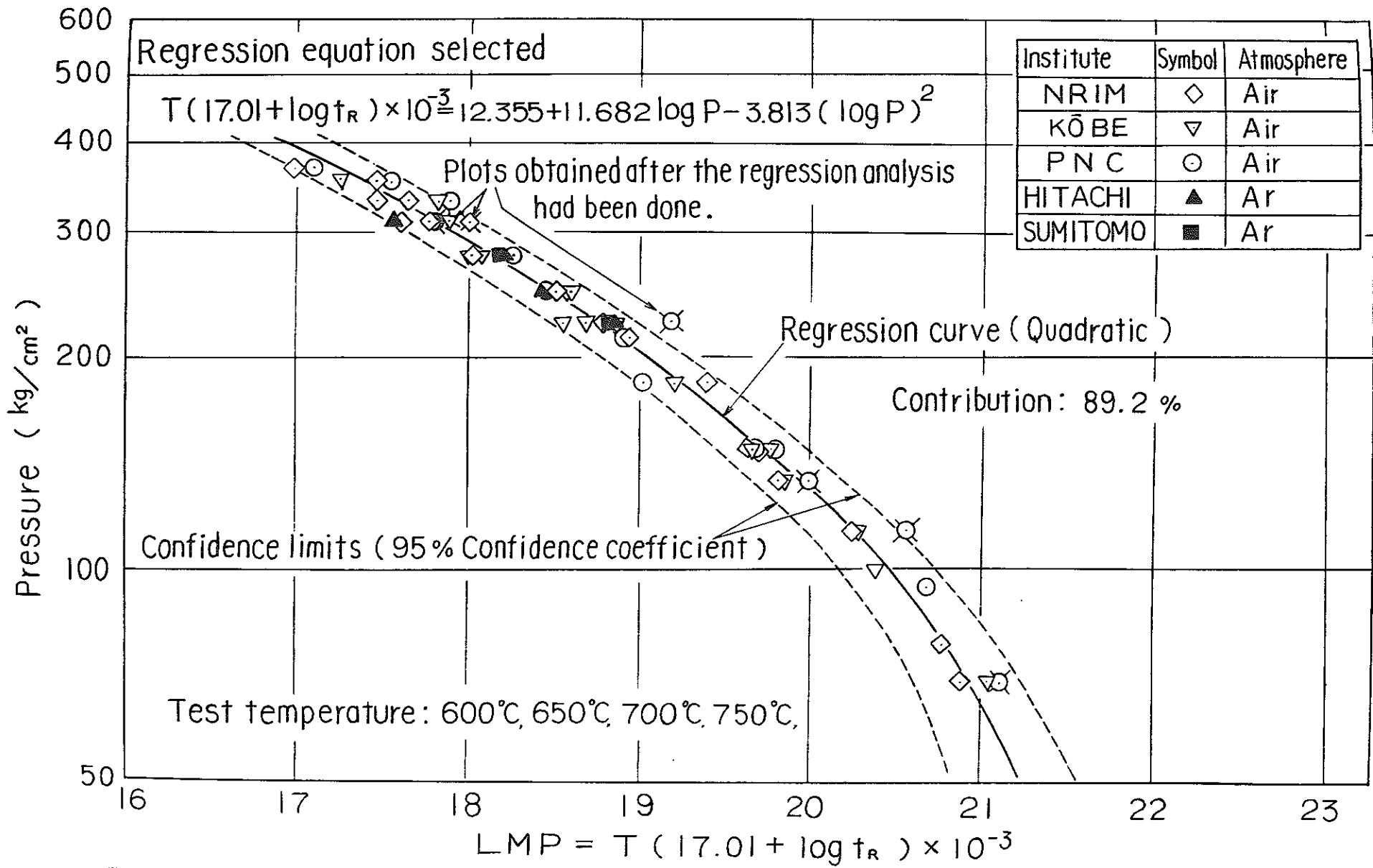
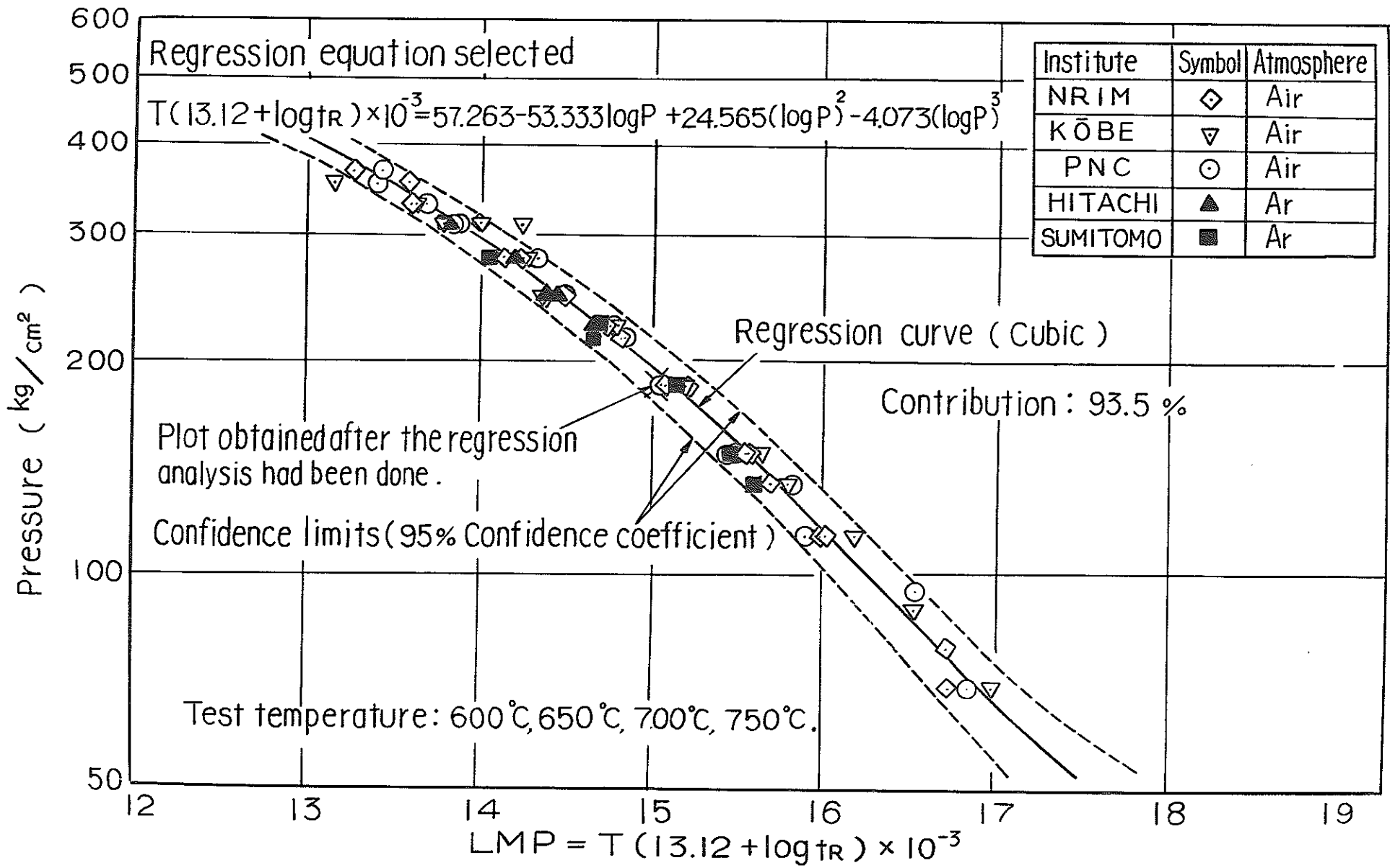Fig.12 Regression curve and confidence interval on master rupture data under internal pressure for Tube A.

Fig.13 Regression curve and confidence interval on master rupture data under internal pressure for Tube B.

The figure contains:

Axes: Pressure (kg/cm^2) on vertical axis (50 to 600), LMP = $T(13.12 + \log t_R) \times 10^{-3}$ on horizontal axis (12 to 19).

Regression equation selected:

$$T(13.12 + \log t_R) \times 10^{-3} = 57.263 - 53.333 \log P + 24.565(\log P)^2 - 4.073(\log P)^3$$

Institute	Symbol	Atmosphere
NRIM	◇	Air
KŌBE	▽	Air
PNC	⊙	Air
HITACHI	▲	Ar
SUMITOMO	■	Ar

Regression curve (Cubic)

Contribution : 93.5 %

Plot obtained after the regression analysis had been done.

Confidence limits (95% Confidence coefficient)

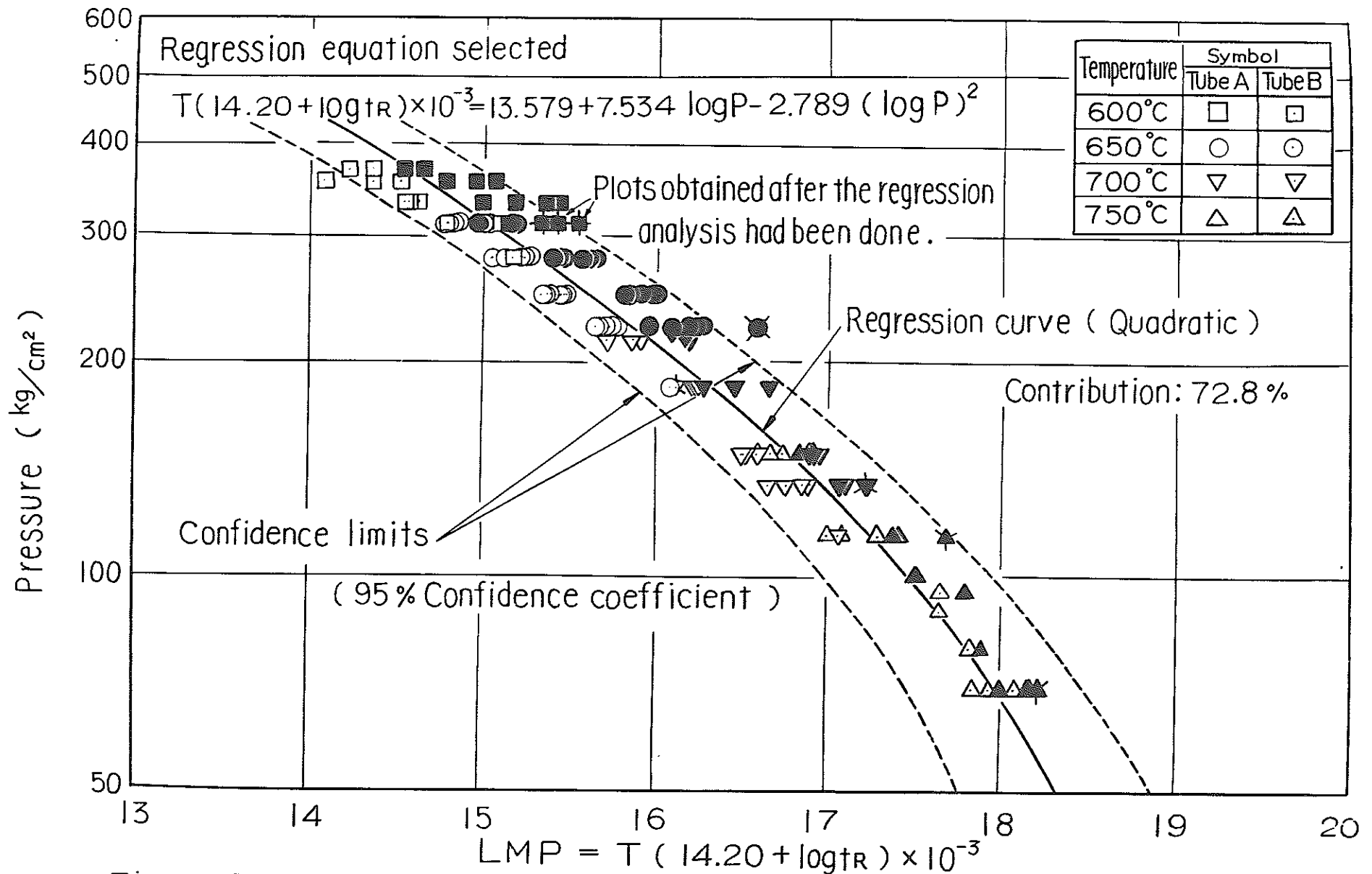Test temperature : 600°C, 650°C, 700°C, 750°C.

Fig. 14 Regression curve and confidence interval on master rupture data under internal pressure for Tubes A and B.
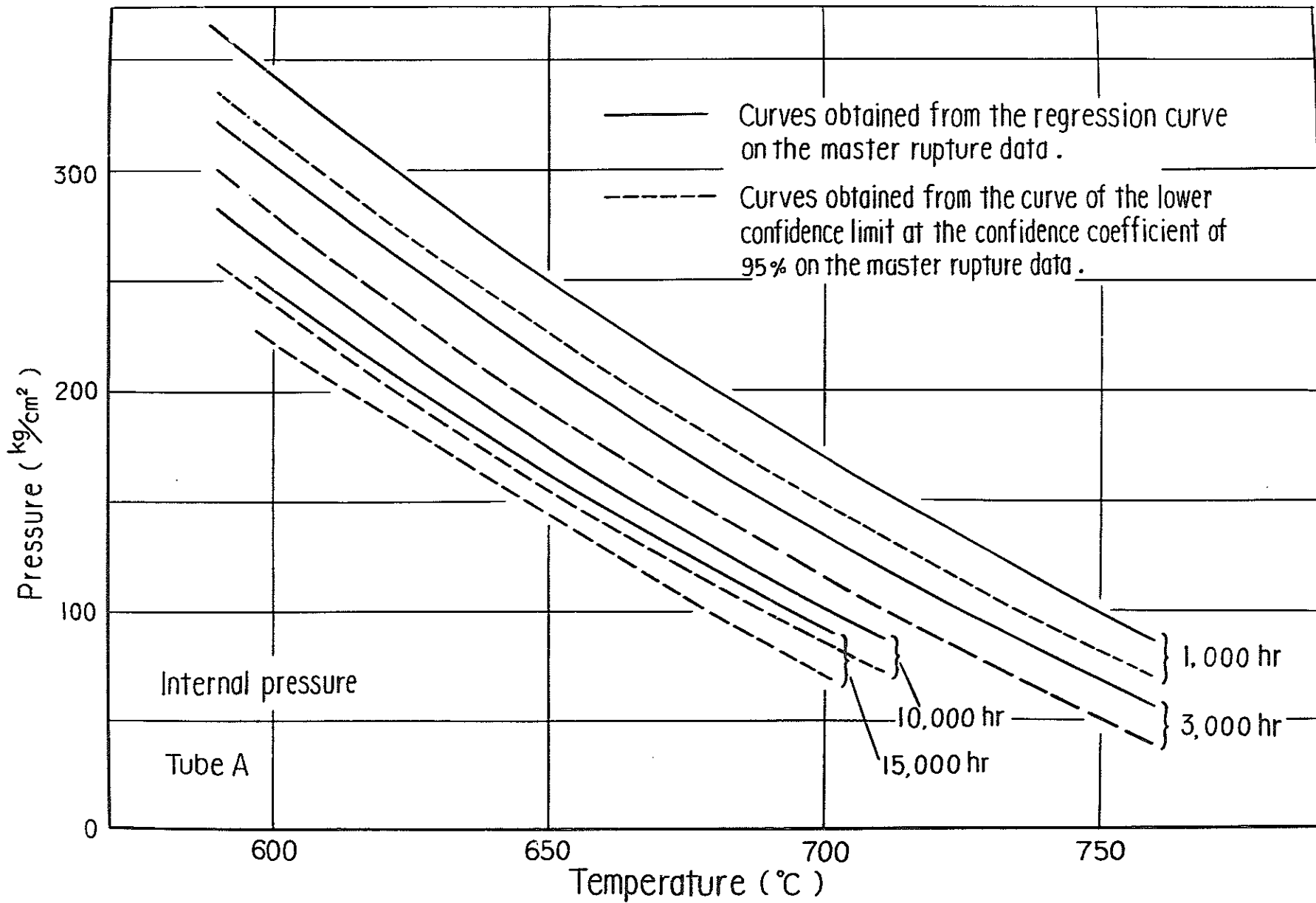
Fig. 15 Relations of temperature versus pressure estimated from the regression curve and the confidence interval on the master rupture data under internal pressure for Tube A.
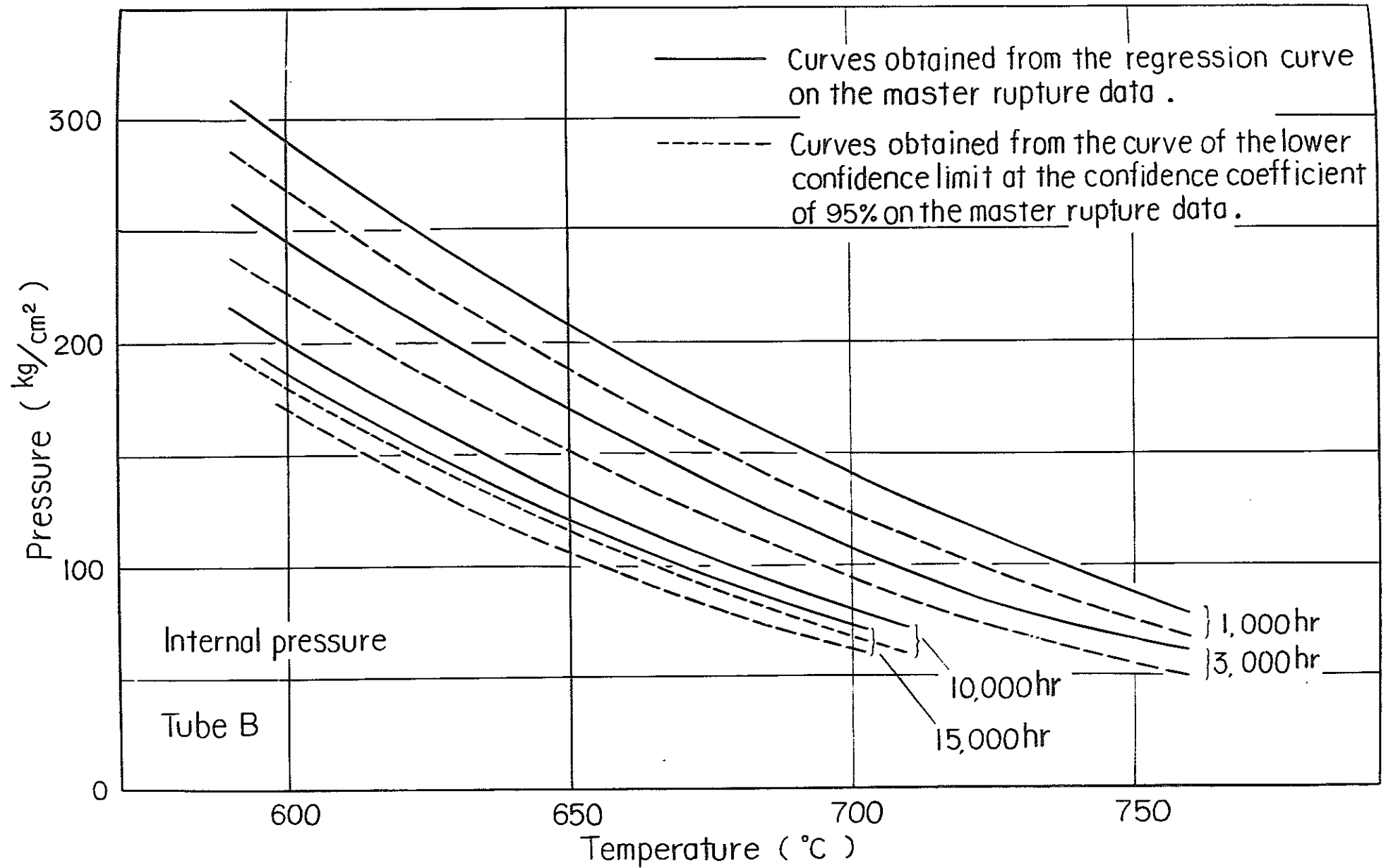
Fig.16 Relations of temperature versus pressure estimated from the regression curve and the confidence interval on the master rupture data under internal pressure for Tube B.
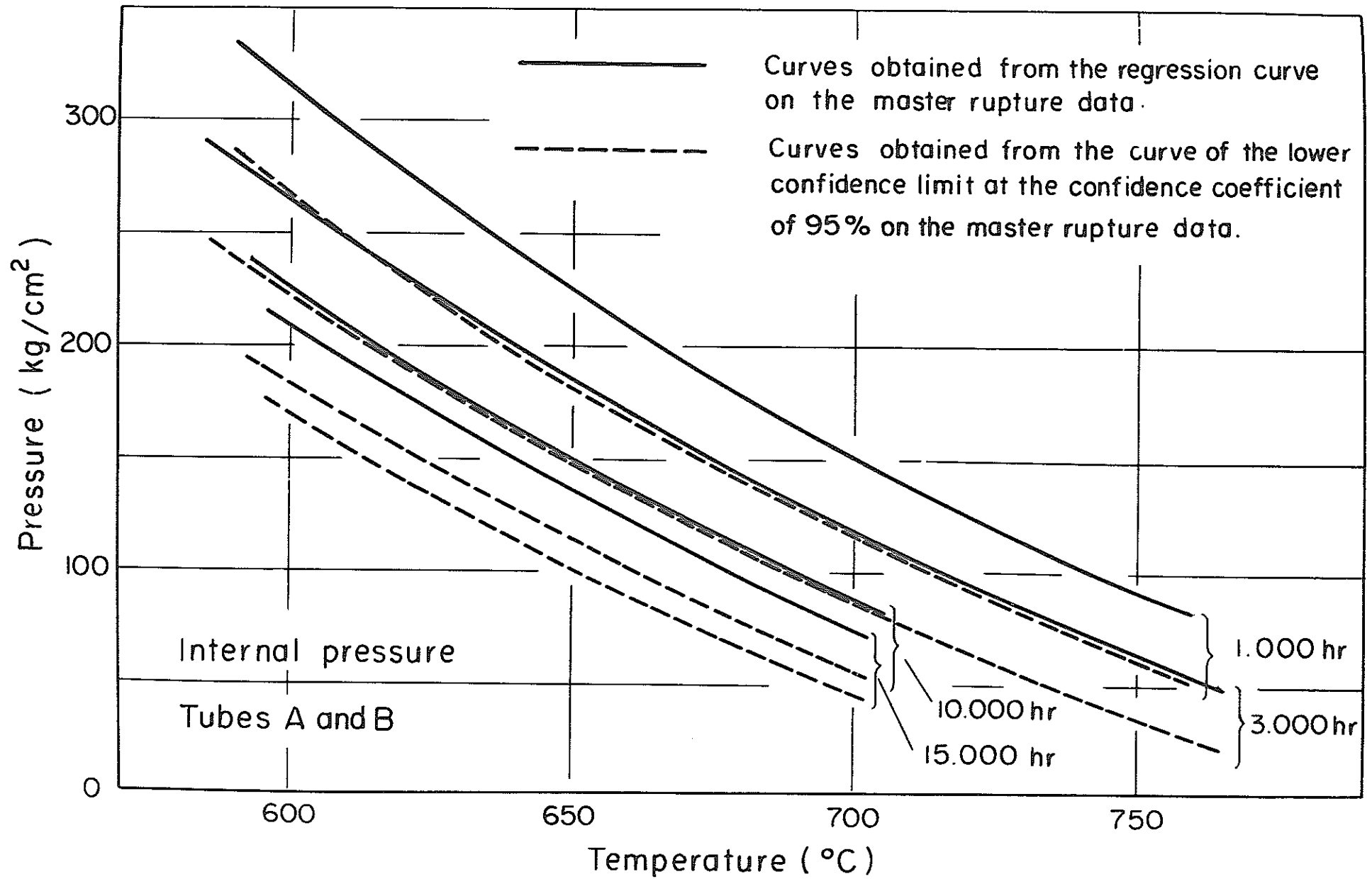
Curves obtained from the regression curve on the master rupture data.

Curves obtained from the curve of the lower confidence limit at the confidence coefficient of 95% on the master rupture data.

Pressure (kg/cm²)

Internal pressure

Tubes A and B

1.000 hr

10.000 hr

3.000 hr

15.000 hr

Temperature (°C)

Fig. 17 Relations of temperature versus pressure estimated from the regression curve and the confidence interval on the master rupture data under internal pressure for Tubes A and B.
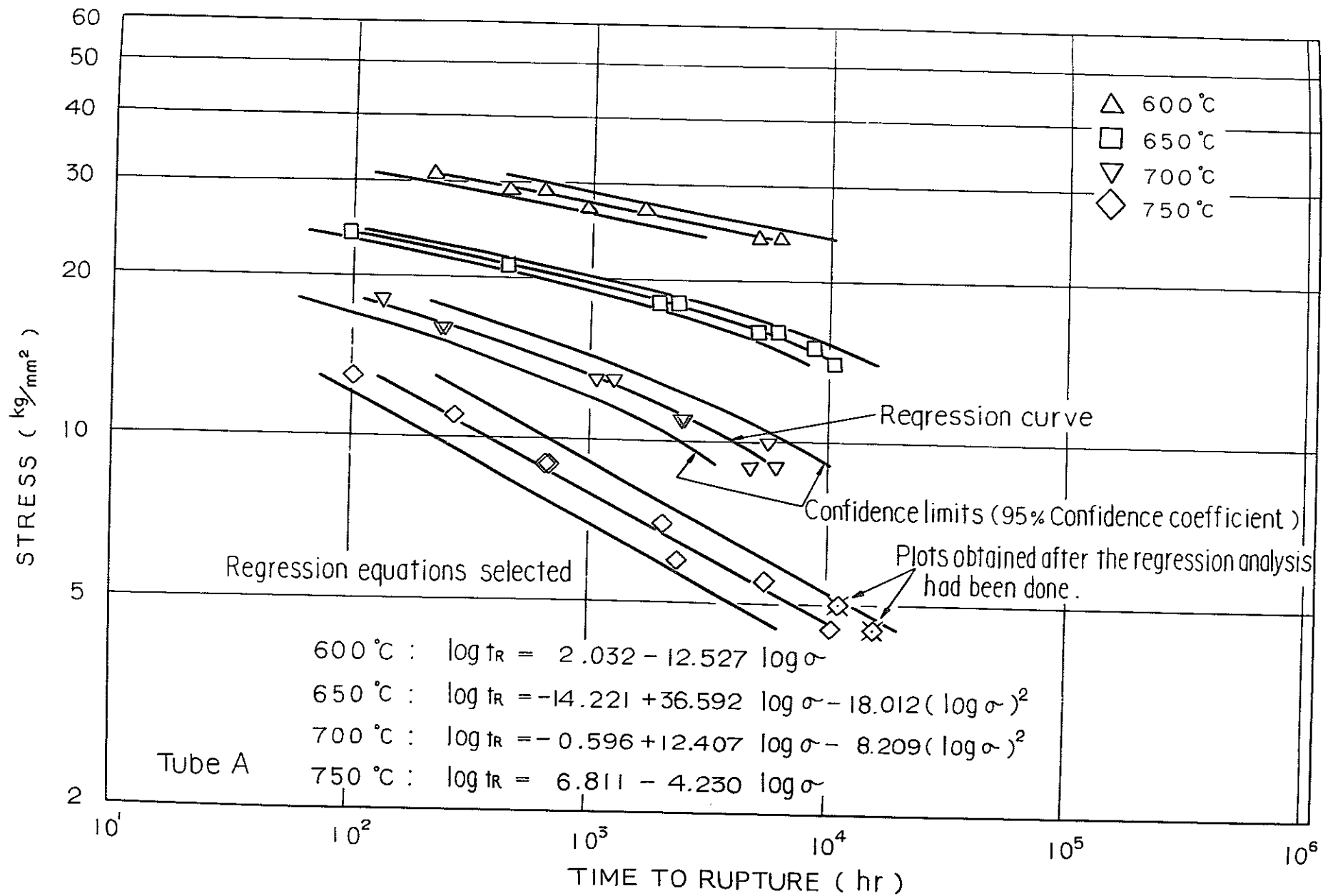
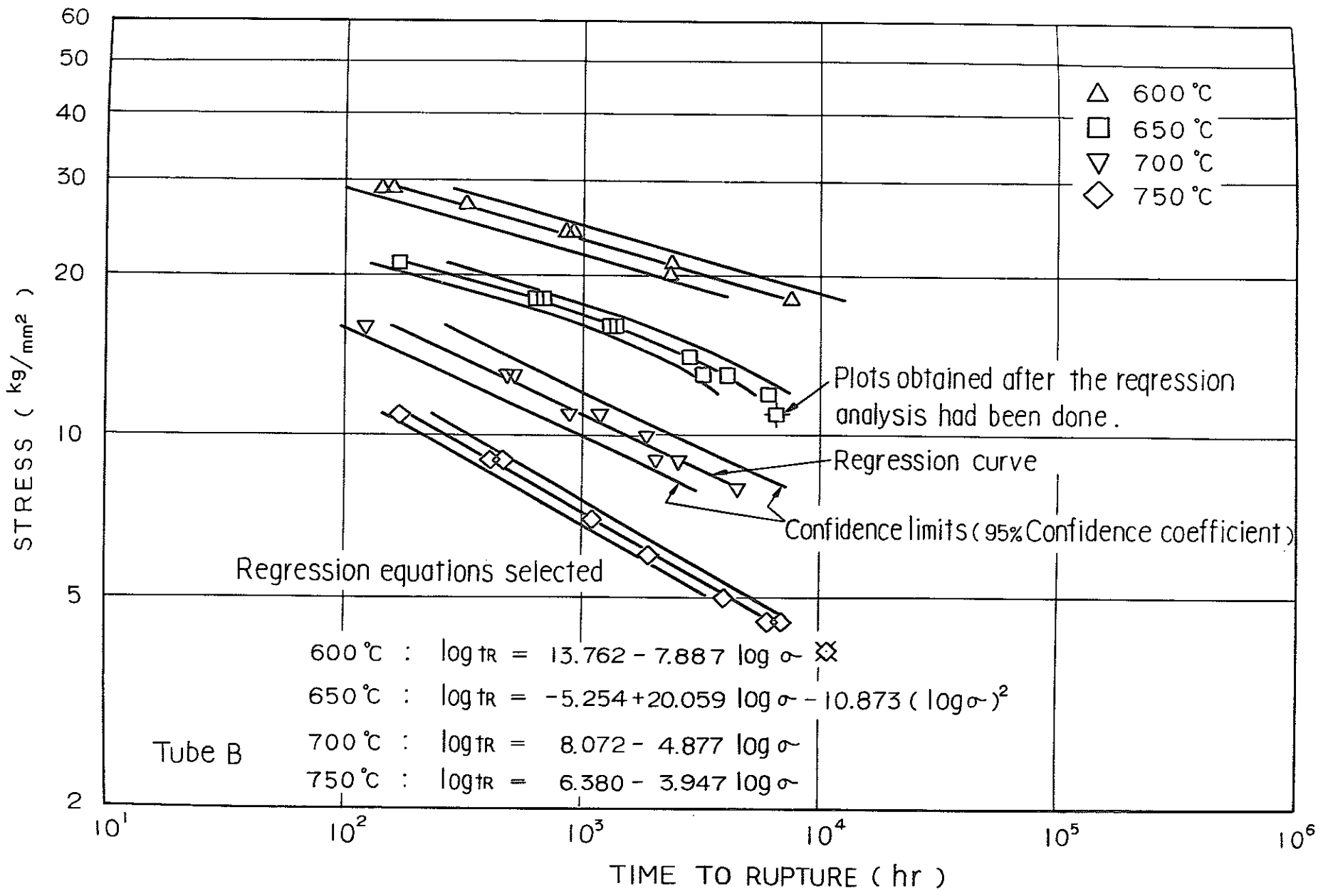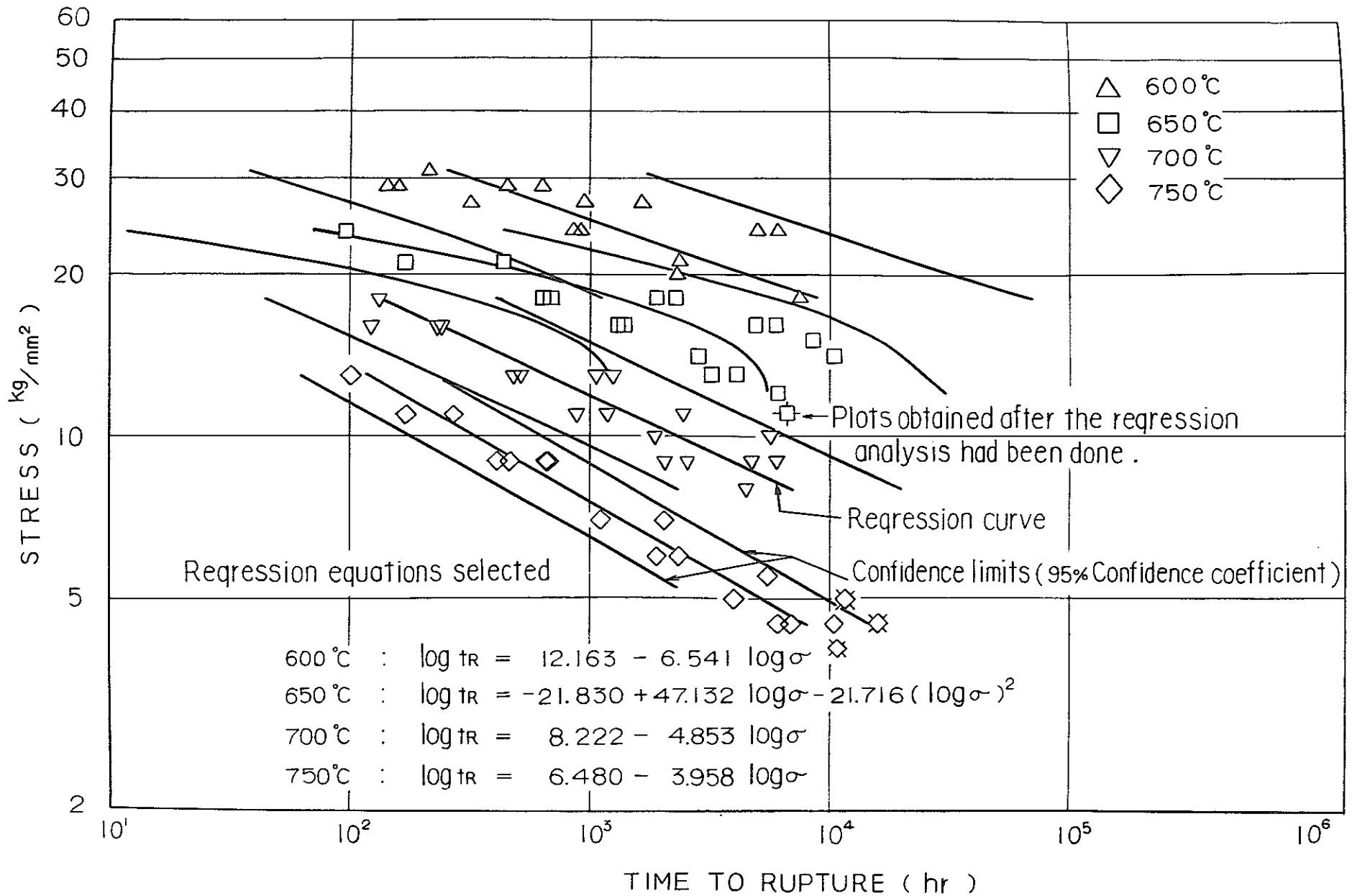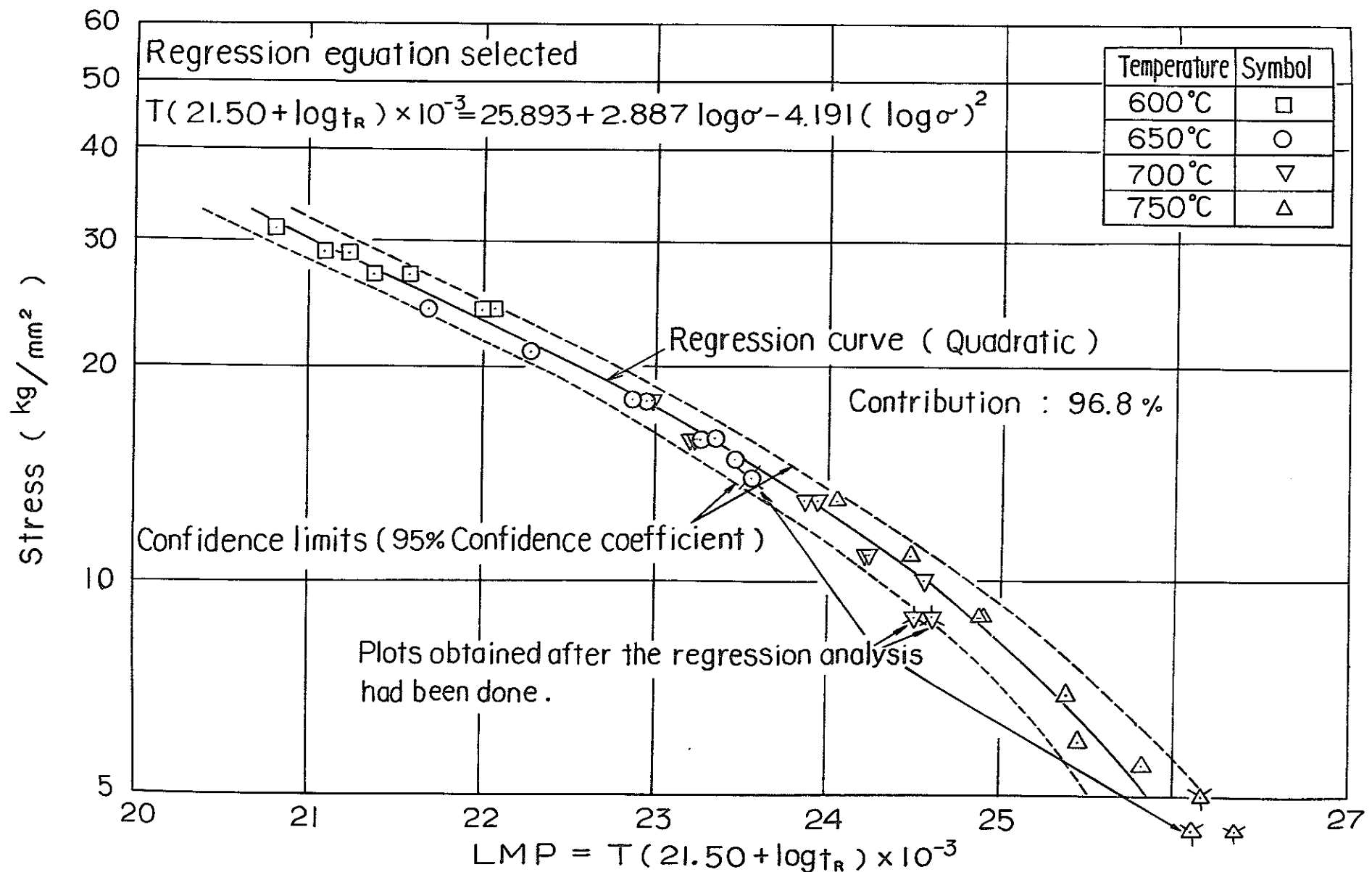Fig. 18 Regression curves and confidence intervals on creep-rupture data under uniaxial tension for Tube A.

Chart labels:

STRESS (kg/mm²)

TIME TO RUPTURE (hr)

△ 600 ℃
□ 650 ℃
▽ 700 ℃
◇ 750 ℃

Regression curve

Confidence limits (95% Confidence coefficient)

Plots obtained after the regression analysis had been done.

Regression equations selected

Tube A

$600\ ℃: \quad \log t_R = 2.032 - 12.527 \log \sigma$

$650\ ℃: \quad \log t_R = -14.221 + 36.592 \log \sigma - 18.012 (\log \sigma)^2$

$700\ ℃: \quad \log t_R = -0.596 + 12.407 \log \sigma - 8.209 (\log \sigma)^2$

$750\ ℃: \quad \log t_R = 6.811 - 4.230 \log \sigma$

Fig. 19 Regression curves and confidence intervals on creep-rupture data under uniaxial tension for Tube B.

60
50
40
30
20

STRESS ($^{kg}/_{mm^2}$)

10

5

2

△ 600°C
□ 650°C
▽ 700°C
◇ 750°C

⊕—Plots obtained after the regression
analysis had been done .

—Regression curve

—Confidence limits (95% Confidence coefficient)

Regression equations selected

600°C	:	$\log t_R = 12.163 - 6.541 \log \sigma$
650°C	:	$\log t_R = -21.830 + 47.132 \log \sigma - 21.716 (\log \sigma)^2$
700°C	:	$\log t_R = 8.222 - 4.853 \log \sigma$
750°C	:	$\log t_R = 6.480 - 3.958 \log \sigma$

10^1 10^2 10^3 10^4 10^5 10^6

TIME TO RUPTURE (hr)

Fig. 20 Regression curves and confidence intervals on creep-rupture data under uniaxial tension for
Tubes A and B .

Regression equation selected

$$T(21.50 + \log t_R) \times 10^{-3} = 25.893 + 2.887 \log \sigma - 4.191 (\log \sigma)^2$$

Temperature	Symbol
600°C	□
650°C	○
700°C	▽
750°C	△

Regression curve (Quadratic)

Contribution : 96.8 %

Confidence limits (95% Confidence coefficient)

Plots obtained after the regression analysis had been done.

Stress (kg/mm²)

$$LMP = T(21.50 + \log t_R) \times 10^{-3}$$

Fig. 21 Regression curve and confidence interval on master rupture data under uniaxial tension for Tube A.

Stress (kg/mm²)

Regression equation selected

$$T(14.07+\log t_R)\times10^{-3}=22.206-8.753\log\sigma+5.827(\log\sigma)^2-2.444(\log\sigma)^3$$

Temperature	Symbol
600 ℃	□
650 ℃	○
700 ℃	▽
750 ℃	△

Regression curve (Cubic)

Contribution : 98.5 %

Confidence limits

Plots obtained after the regression analysis had been done.

(95% Confidence coefficient)

$$LMP = T(14.07+\log t_R)\times10^{-3}$$

Fig. 22 Regression curve and confidence interval on master rupture data under uniaxial tension for Tube B.

Fig. 23 Regression curve and confidence interval on master rupture dada under uniaxial tension for Tubes A and B.
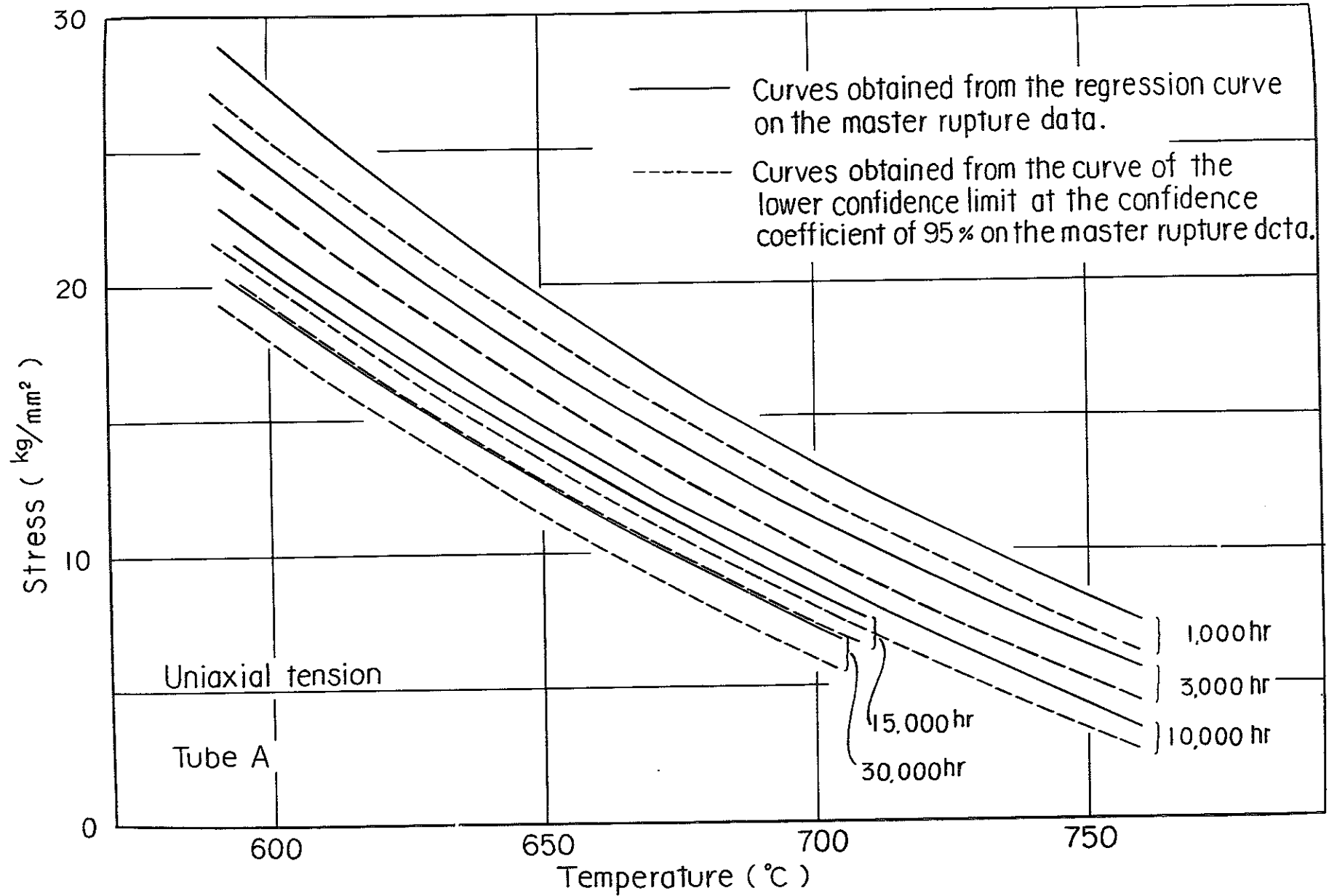
Fig. 24 Relations of temperatur versus stress estimated from the regression curve and the confidence interval on the master rupture data under uniaxial tension for Tube A.
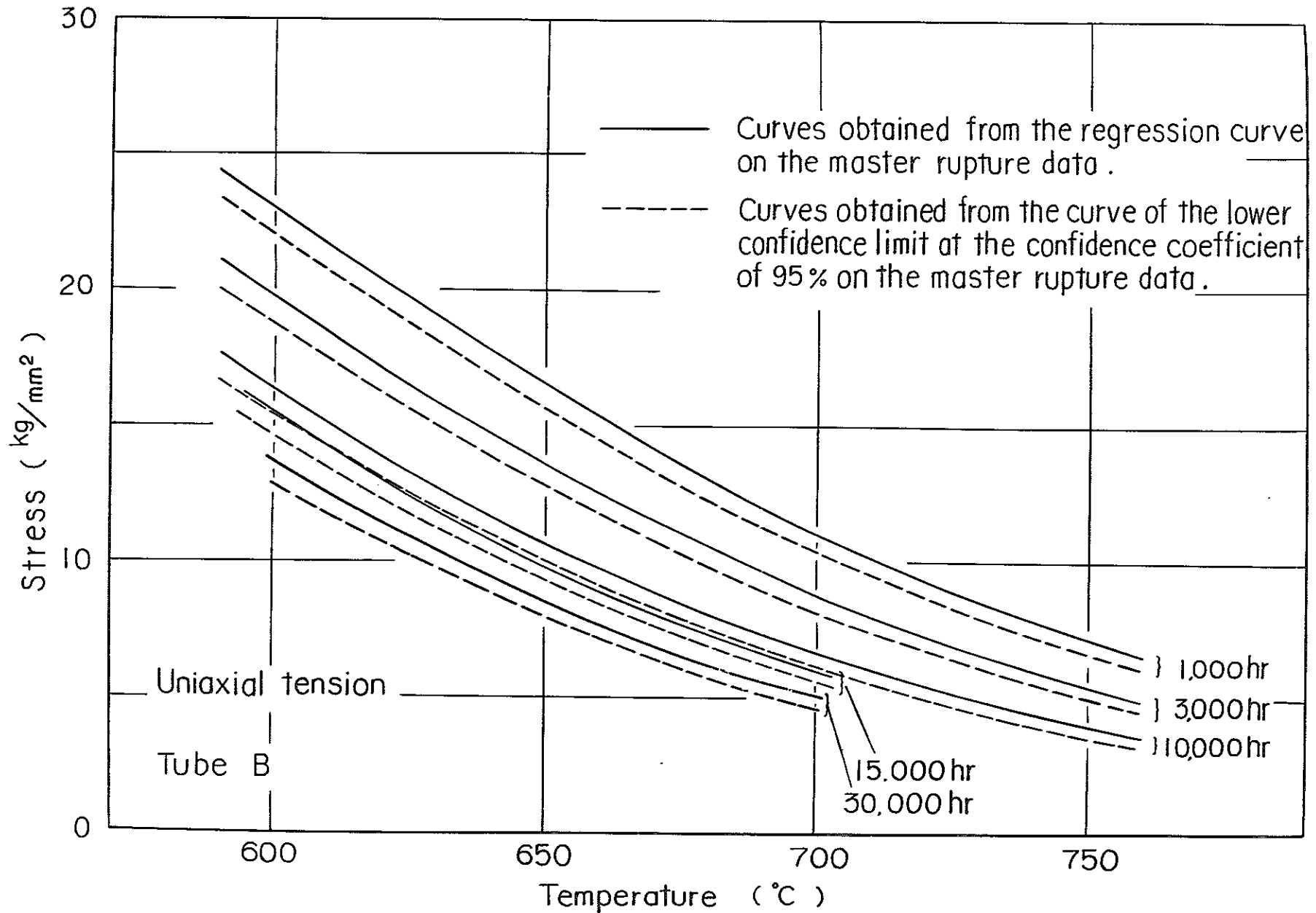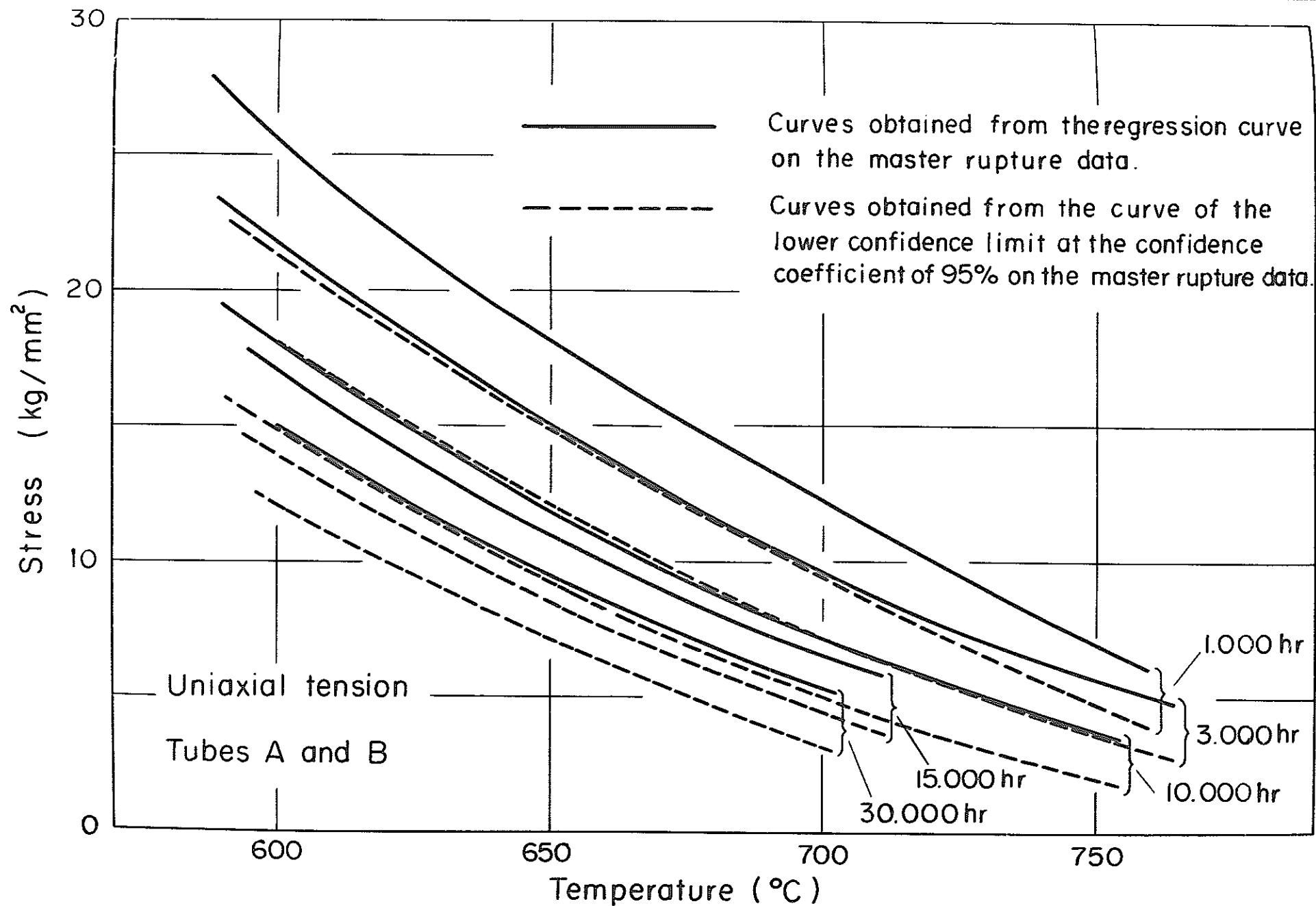
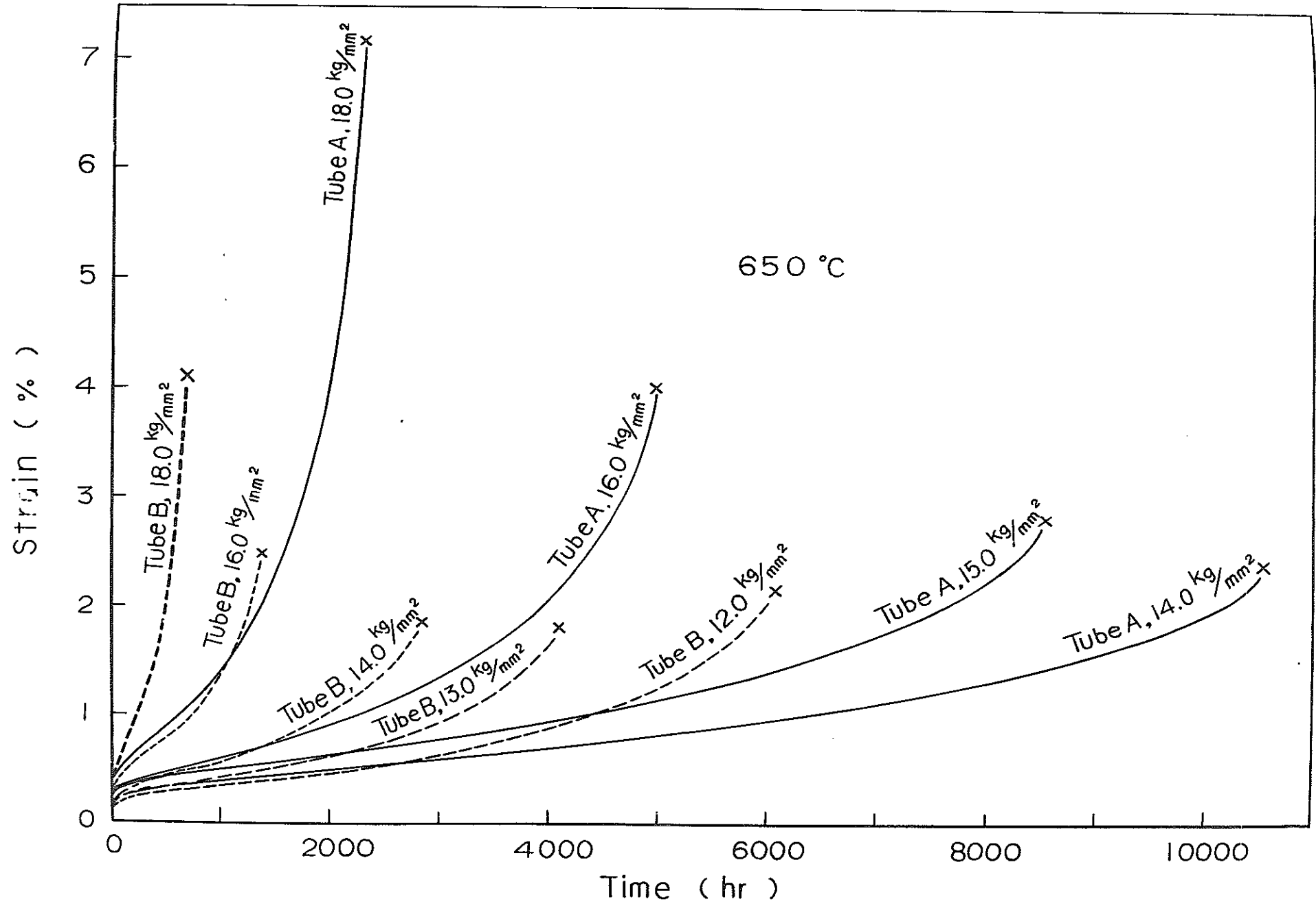Fig. 25 Relations of temperature versus stress estimated from the regression curve and the confidence interval on the master rupture data under uniaxial tension for Tube B.

Fig. 26 Relations of temperature versus stress estimated from the regression curve and the confidence interval on the master rupture data under uniaxial tension for Tubes A and B.

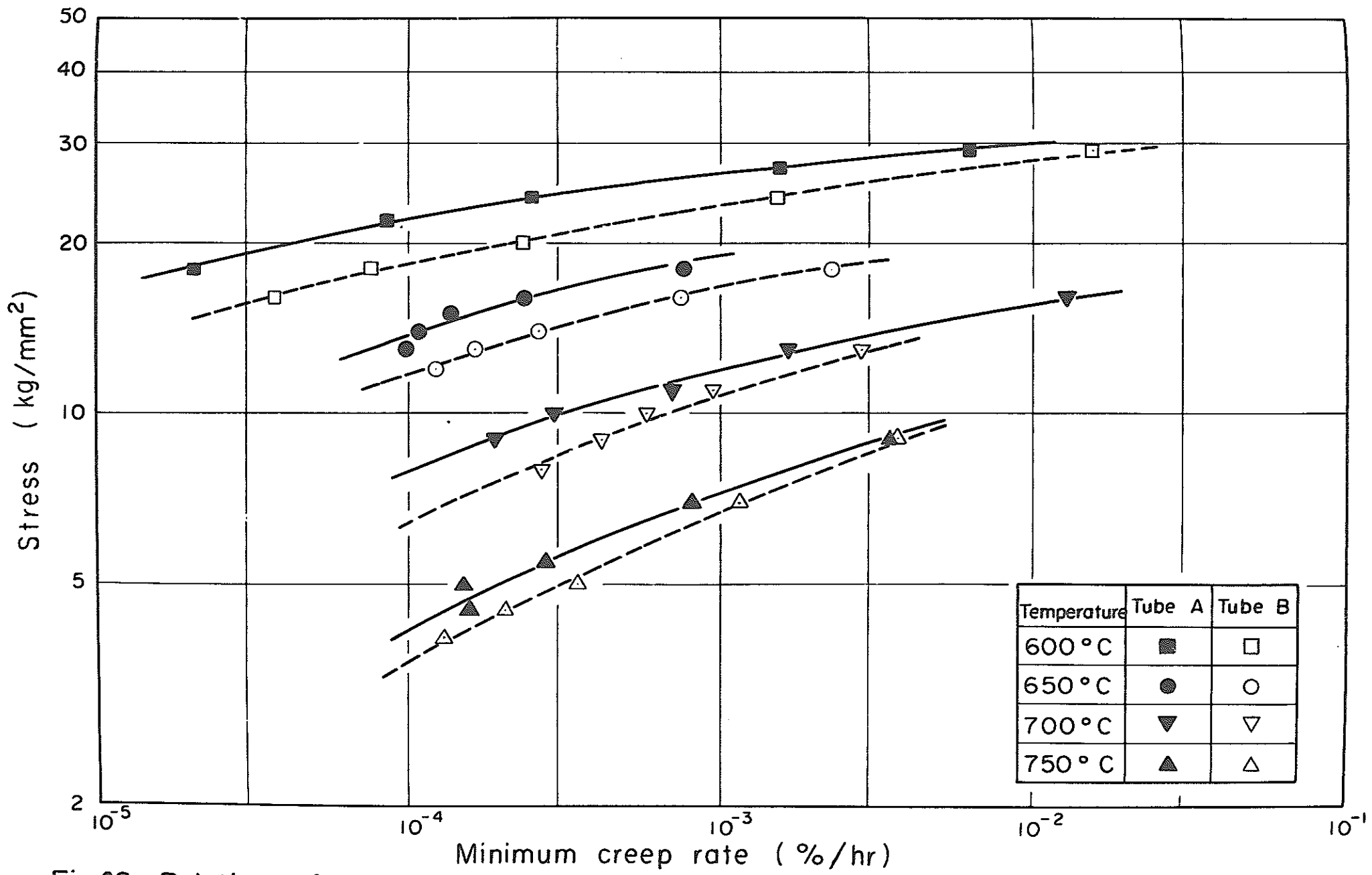Fig. 27 Creep curves under uniaxial tension for Tubes A and B at 650°C

Temperature	Tube A	Tube B
600 °C	■	□
650 °C	●	○
700 °C	▼	▽
750 °C	▲	△

Stress (kg/mm^2)

Minimum creep rate (% / hr)

Fig.28 Relations of stress versus minimum creep rate under uniaxial tension for Tubes A and B.
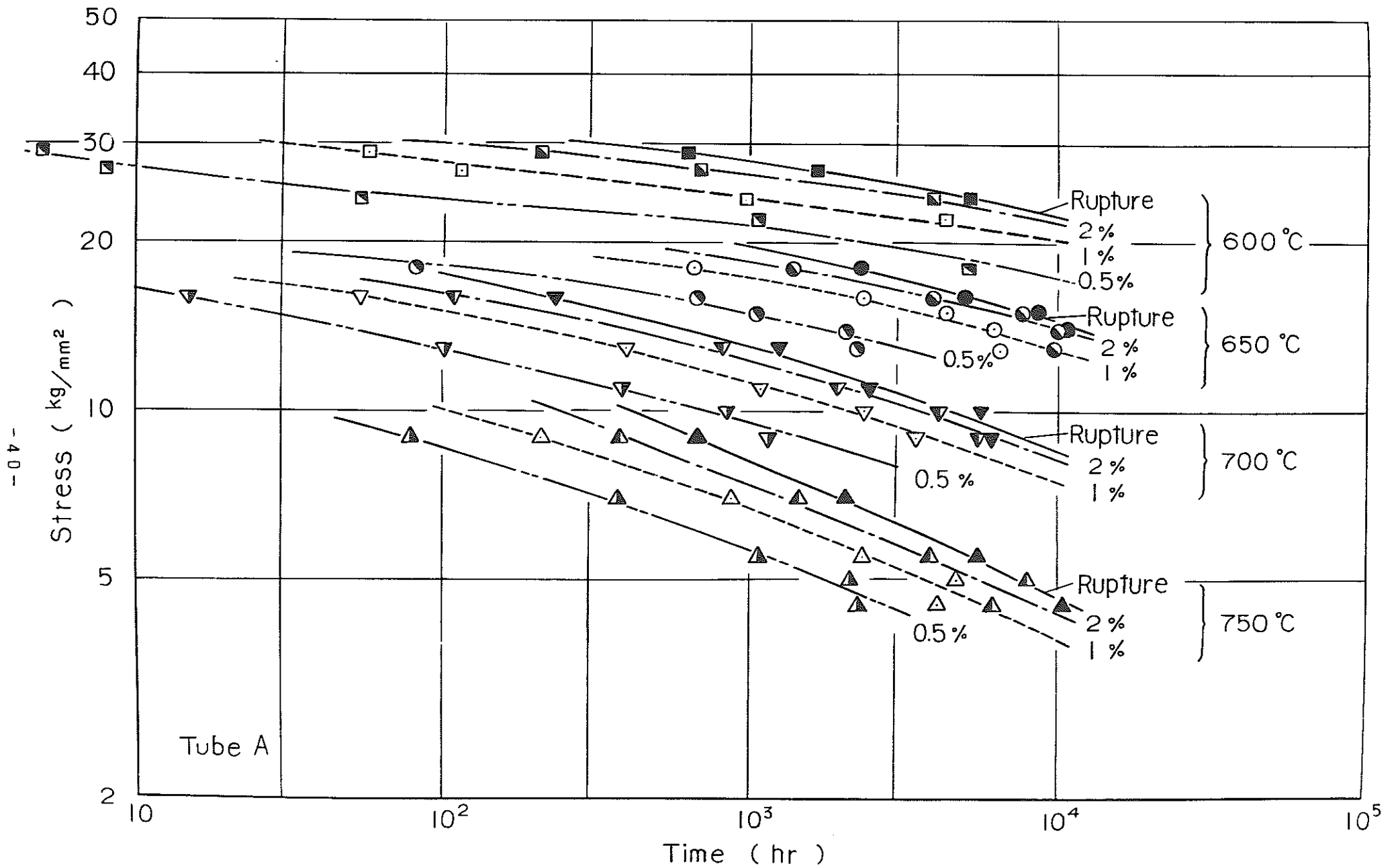
Fig.29 Relations of stress versus time for total strain of 0.5%, 1% and 2% under uniaxial tension for Tabe A.
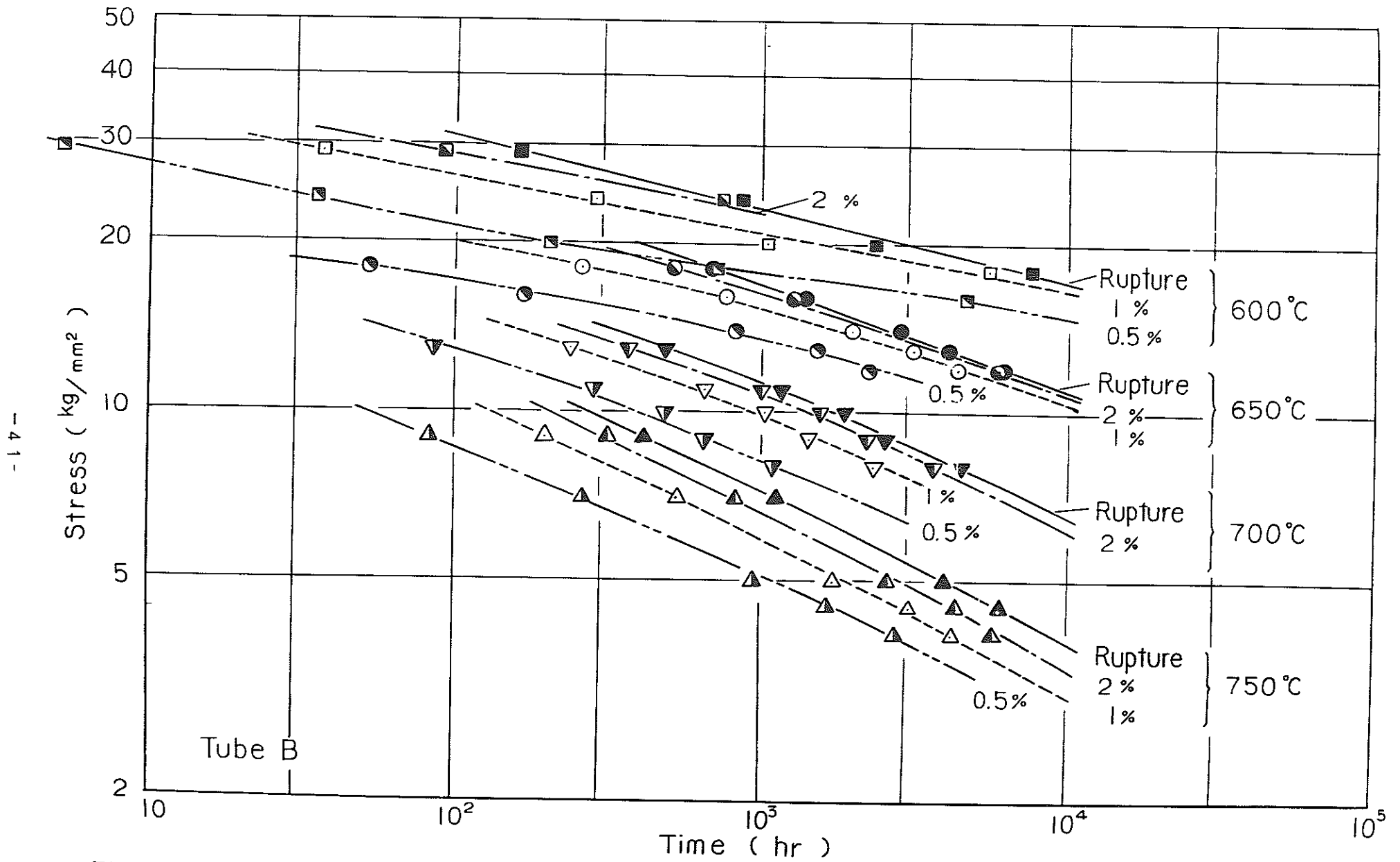
Fig.30 Relations of stress versus time for total strain of 0.5%, 1% and 2% under uniaxial tension for Tube B.
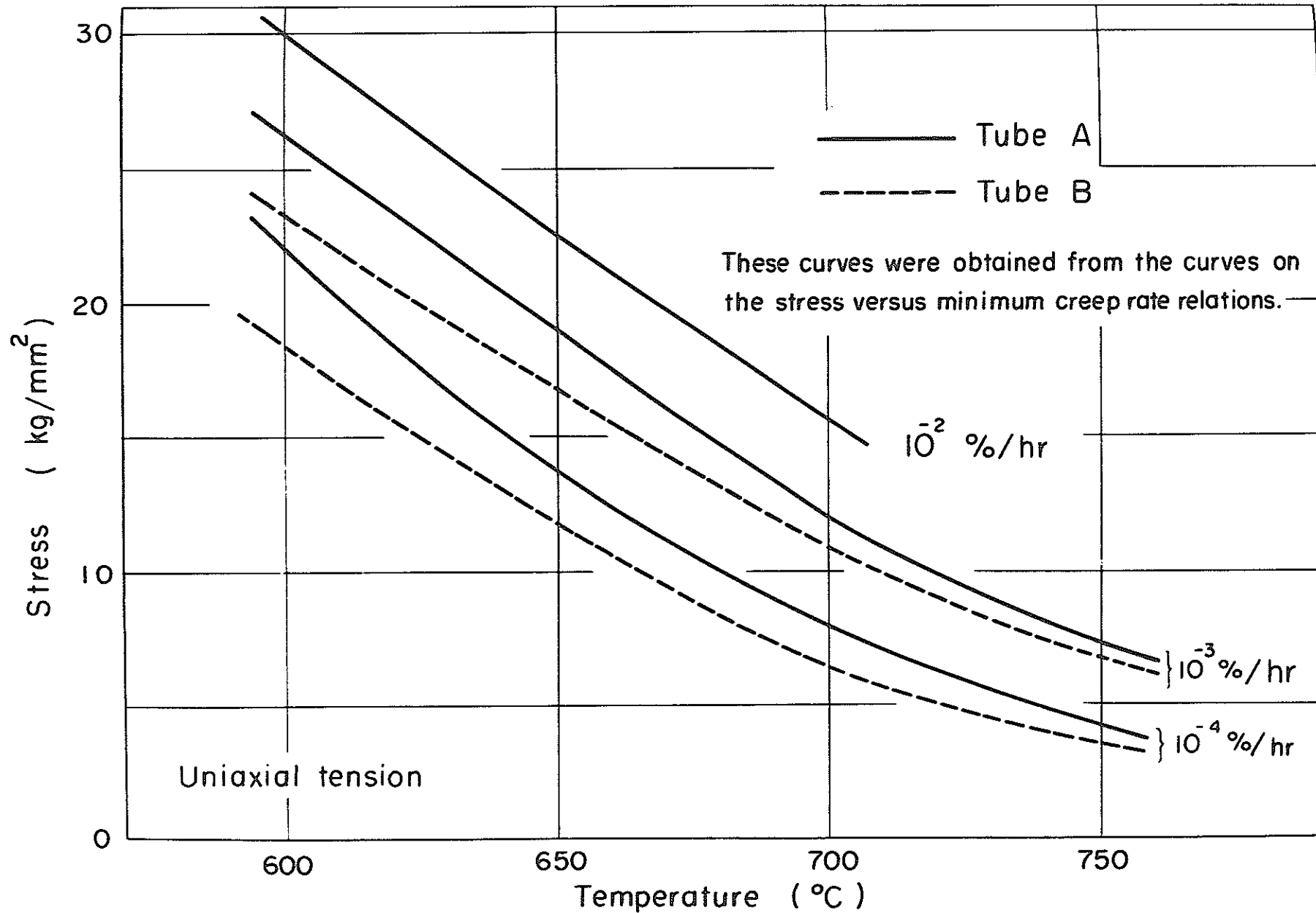
Fig.31   Relations of temperature versus stress at each minimum creep rate under
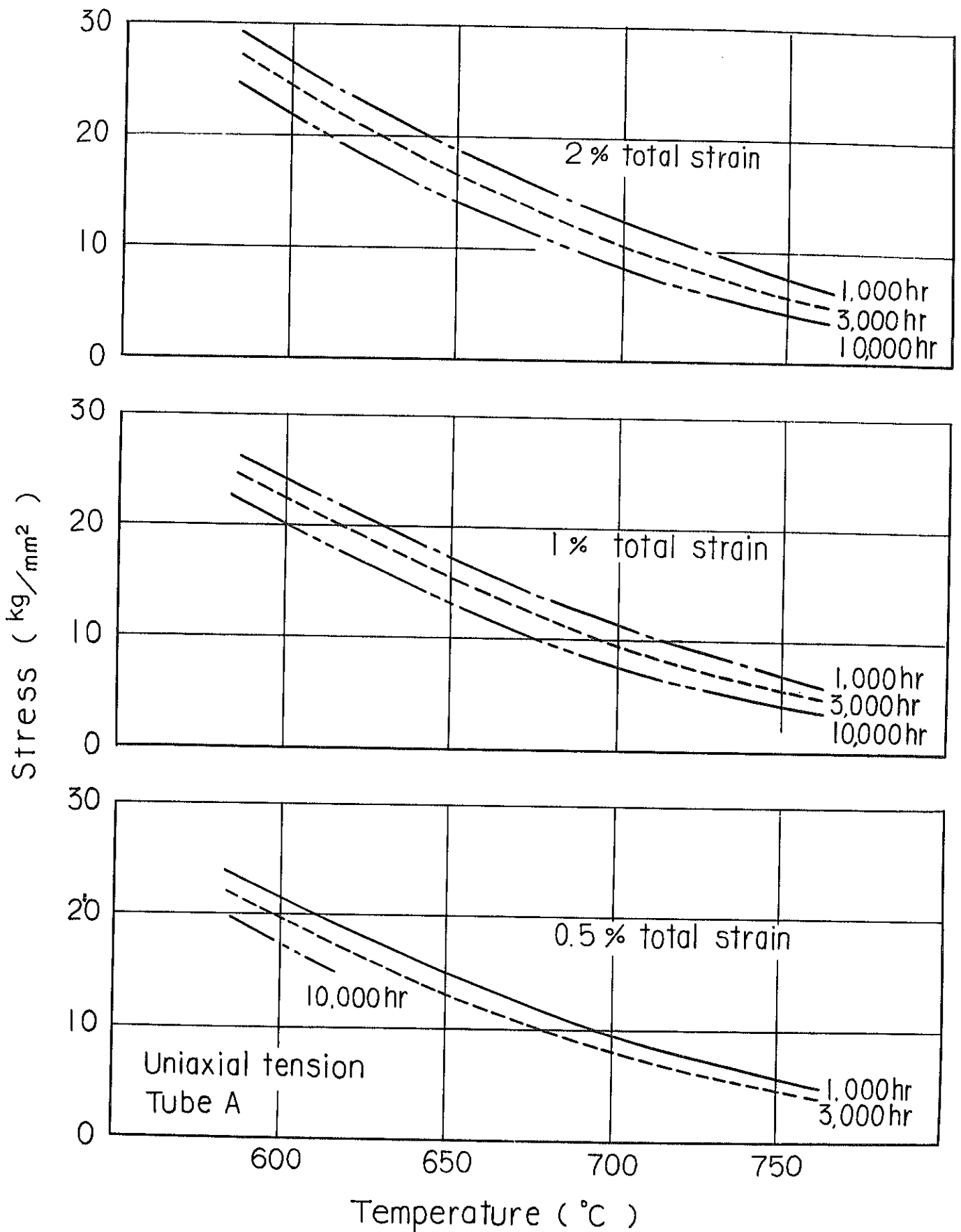uniaxial tension for Tubes A and B.

Fig. 32 Relations of temperature versus stress at each time
for total strain of 0.5 %, 1 % and 2 % under uniaxial
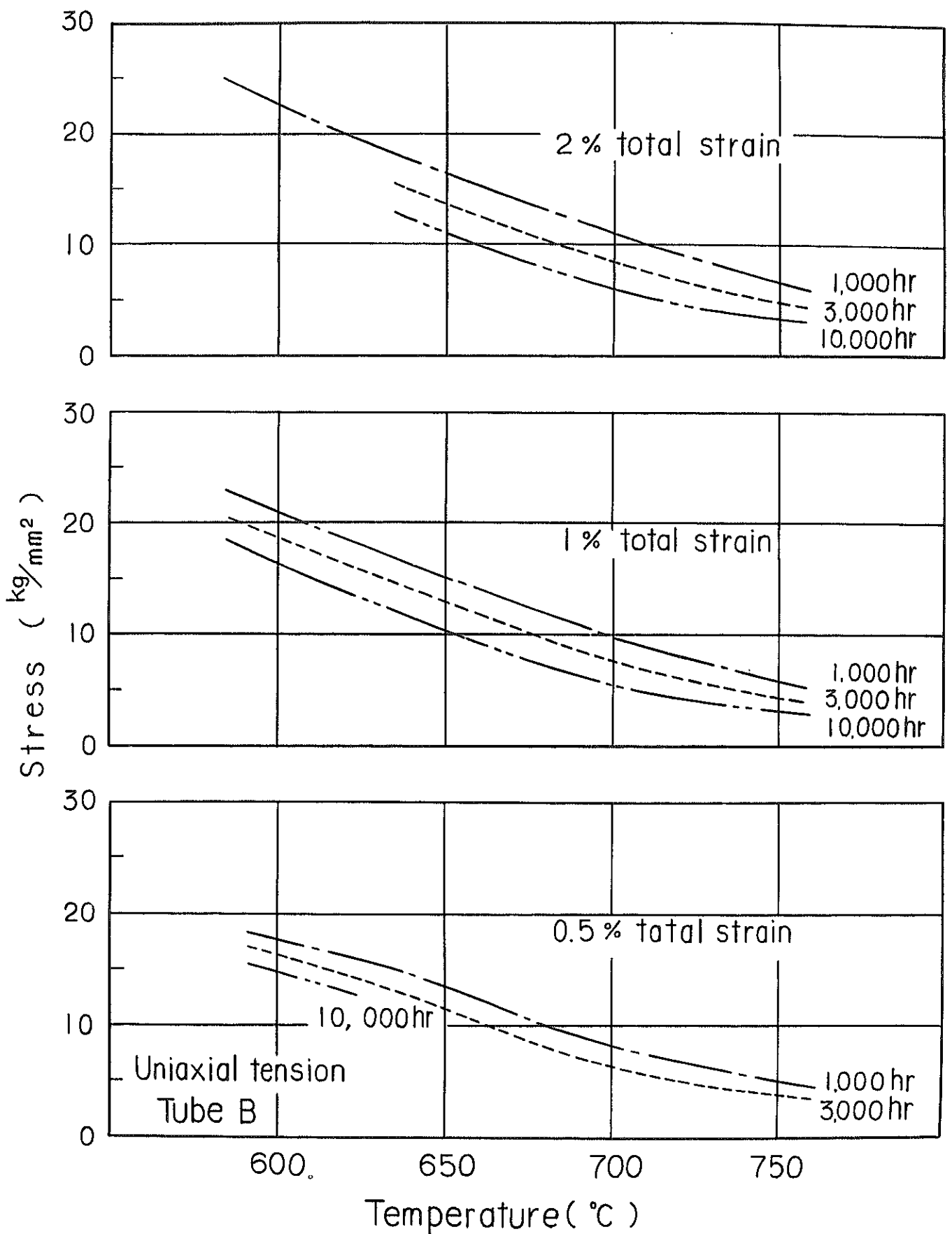tension for Tube A.

Fig. 33 Relations of temperature versus stress at each time
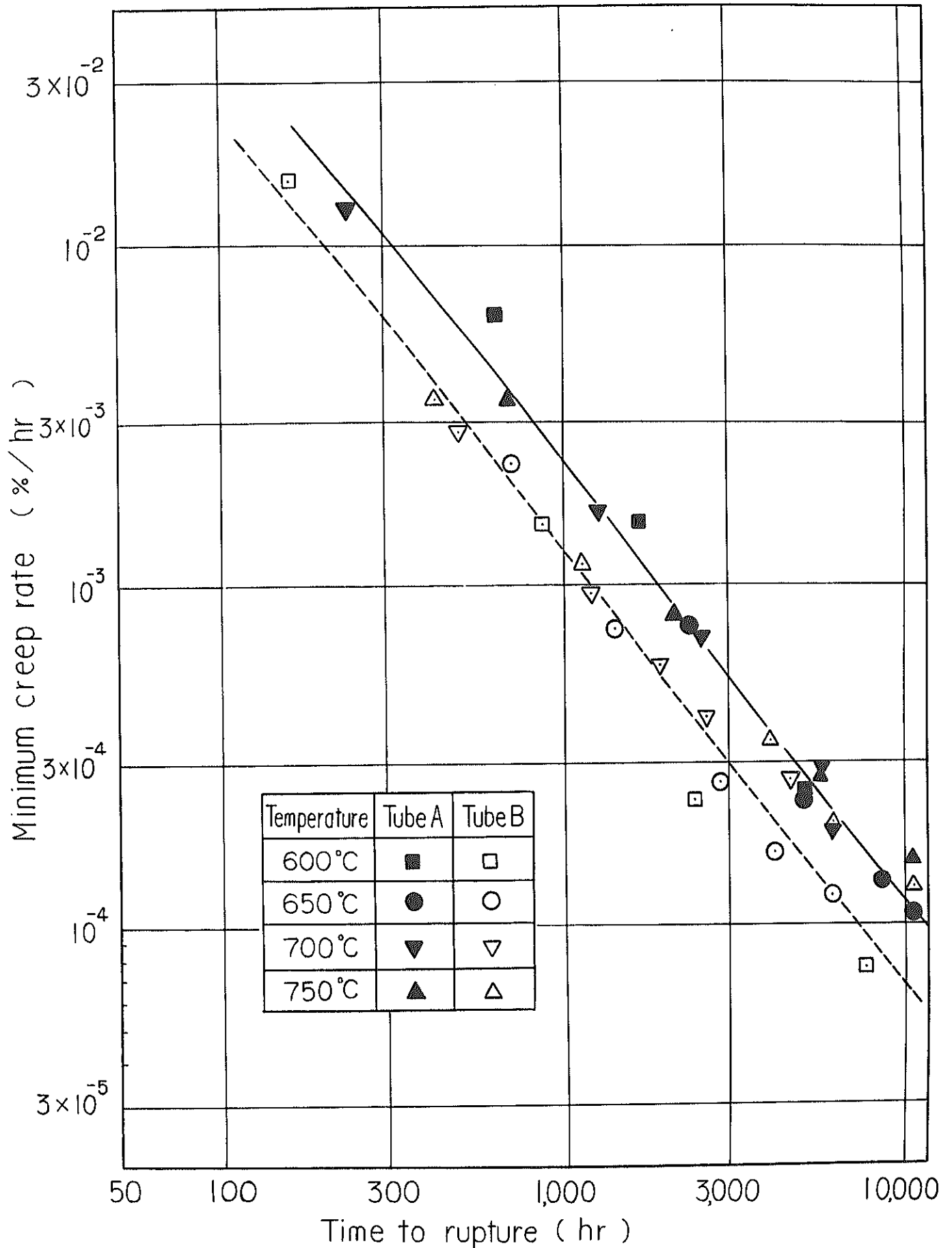for total strain of 0.5 %, 1 % and 2 % under uniaxial
tension for Tube B.

Fig.34 Relations of time to rupture versus minimum creep rate under uniaxial tension for Tubes A and B.

Fig. 35

Correlation between the tensile stress and hoop stress for the same rupture-time and at the same temperature, which were obtained by the uniaxial tention tests and by the internal pressure tests for Tube A, respectively. The hoop stresses were calculated by the inside diameter formula, mean diameter formula and outside diameter formula.
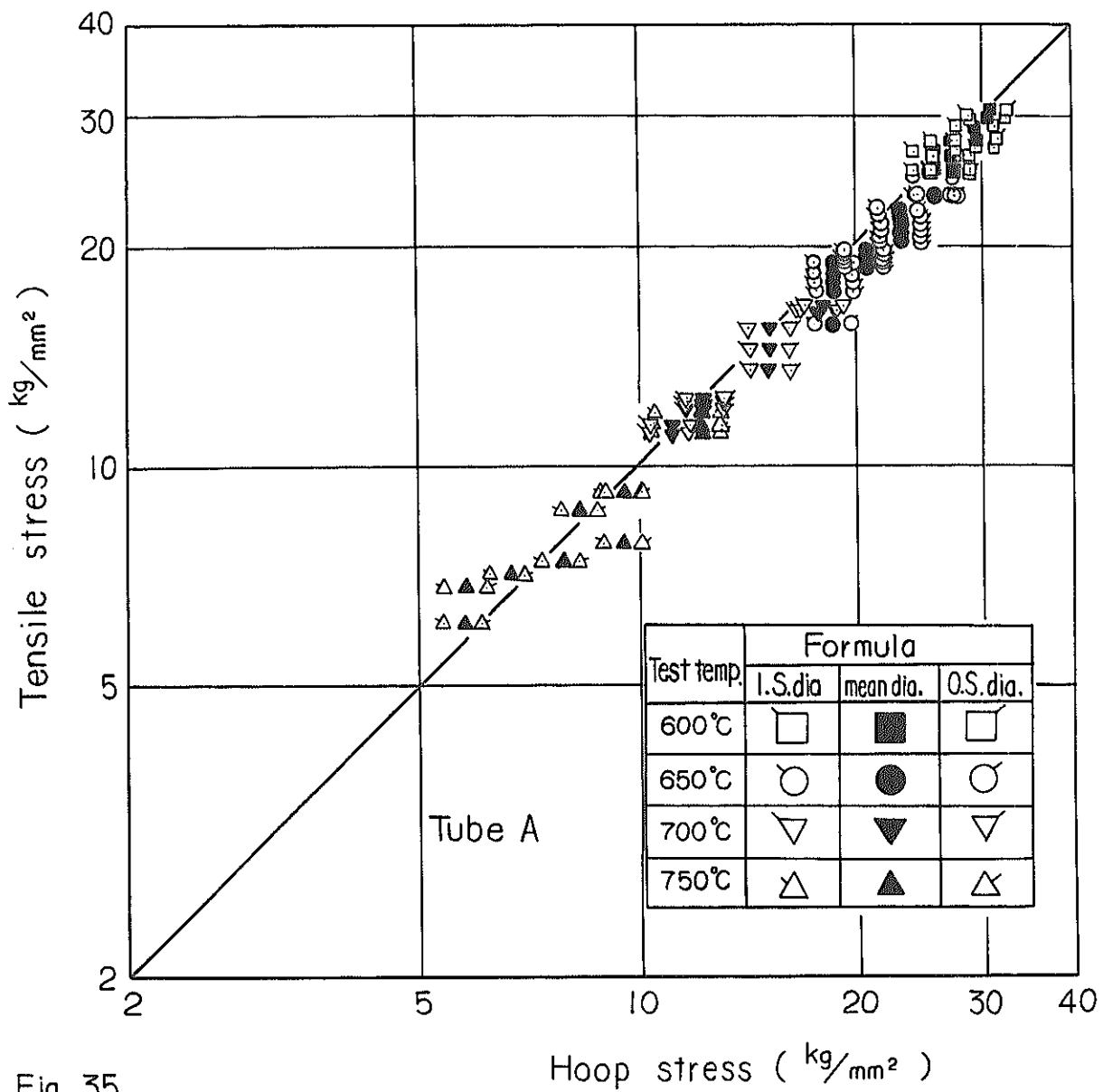
Fig. 36

Correlation between the tensile stress and hoop stress for the same rupture-time and at the same temperature, which were obtained by the uniaxial tension tests and by the internal pressure test for Tube B, respectively. The hoop stresses were calculated by the inside diameter formula, mean diameter formula and outside diameter formula.
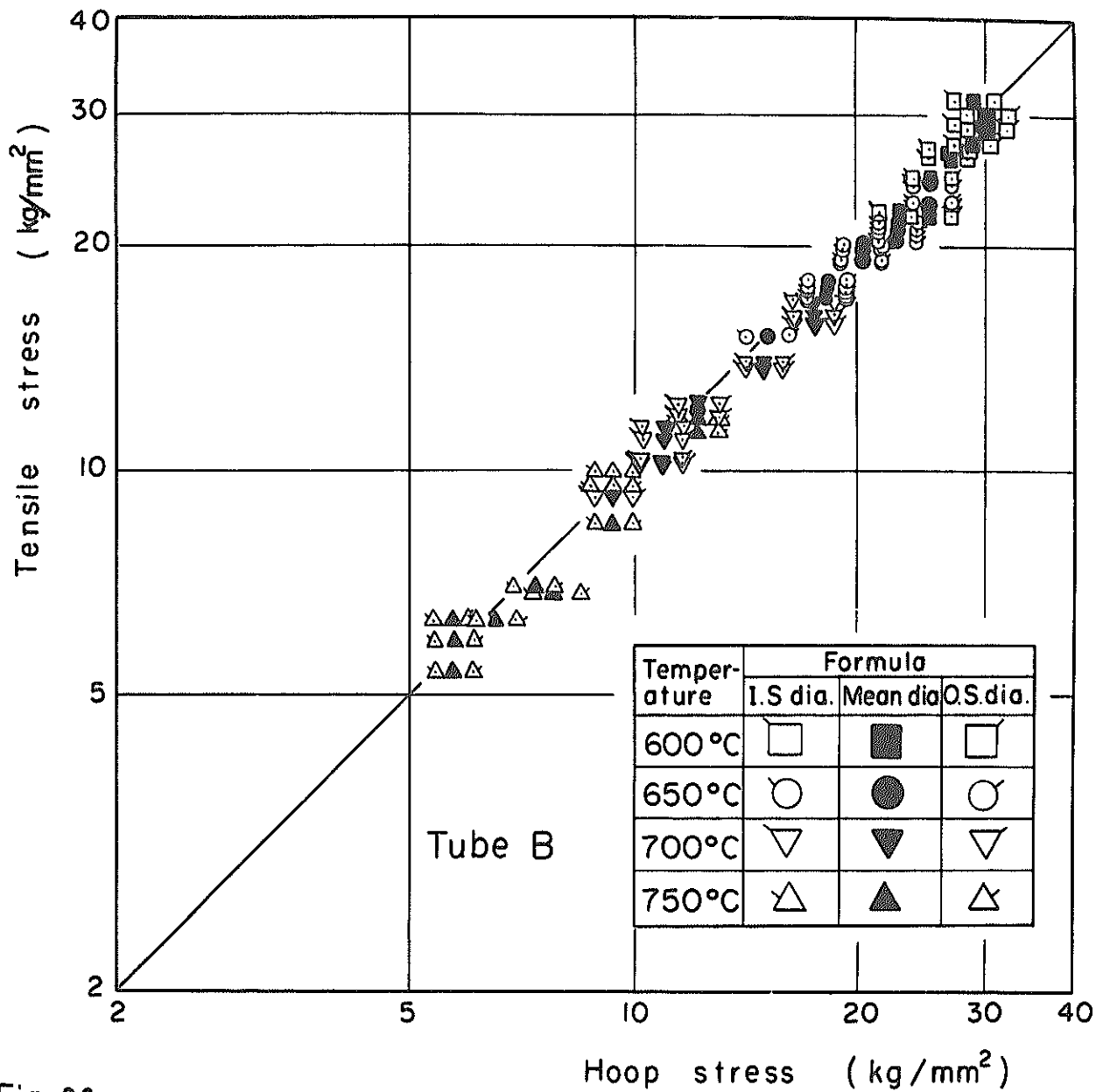
Fig 37 Comparison of the present data and ISO's data at 600 ℃ and 700 ℃.

The chart has the following axes and legend:

- Y-axis: Tensile stress or hoop stress (kg/mm^2)
- X-axis: Time to rupture (hr)

Annotation: Hoop stresses were calculated by the mean diameter formula.

Curve labels: 600 ℃, 700 ℃

Temp. °C	Tube A		Tube B	
	Internal pressure	Uniaxial tension	Internal pressure	Uniaxial tension
600	▦	■	⊞	□
700	▼	▼	▽	▽

— — — — — ISO's data under uniaxial tension
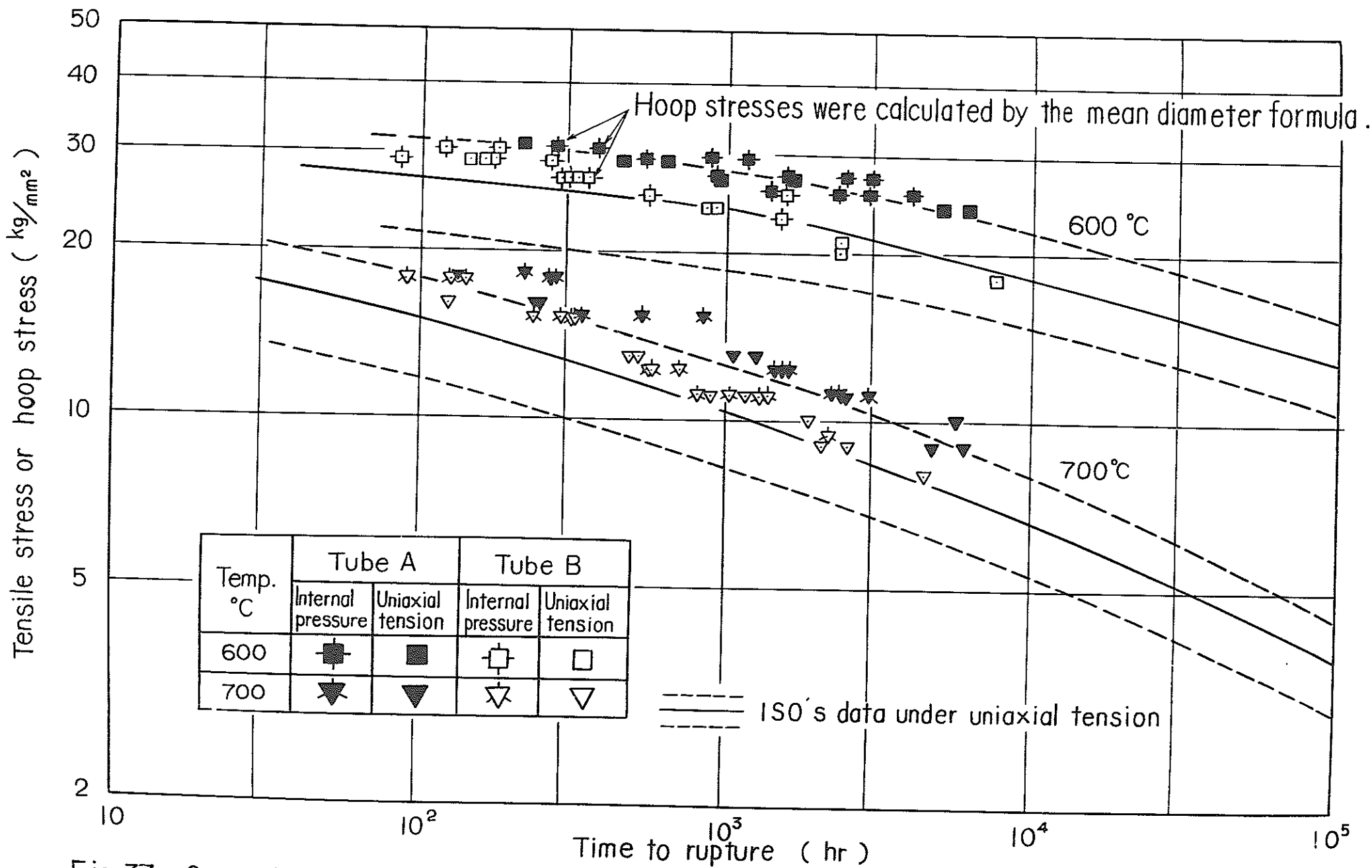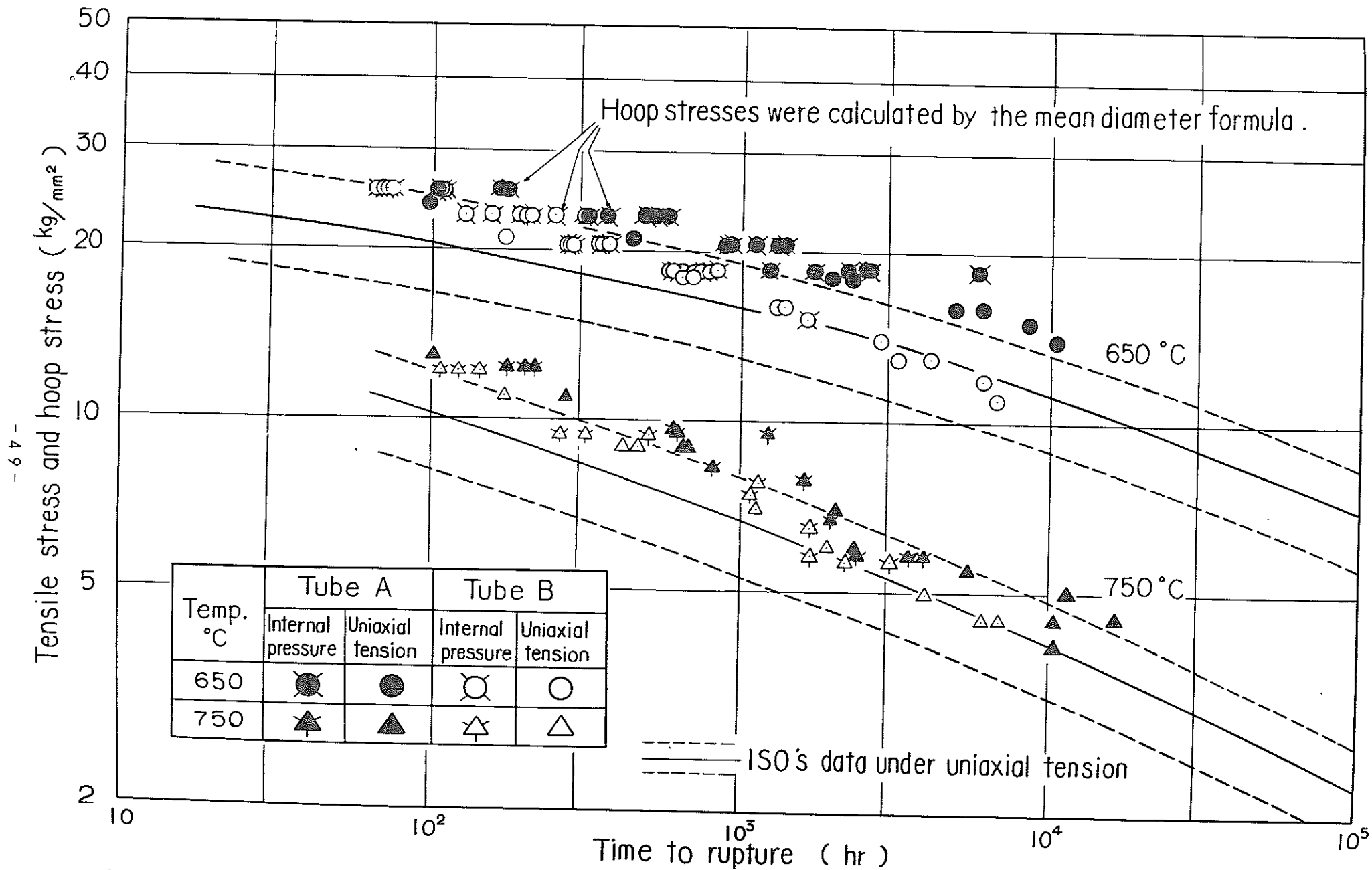
Fig. 38 Comparison of the present data and ISO's data at 650 °C and 750 °C
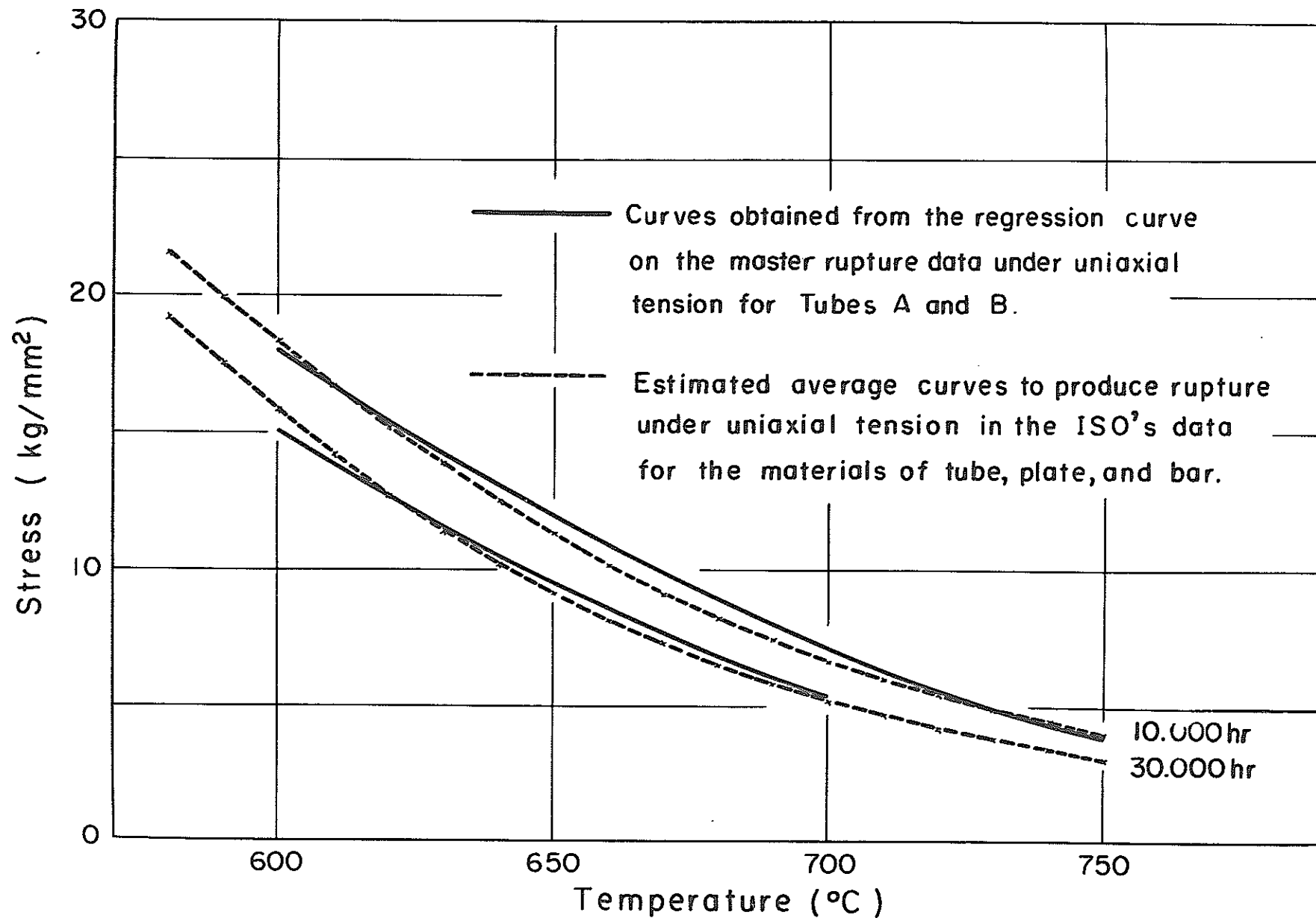
Fig.39   Comparison of the present data and ISO's data under uniaxial tension with regard to the rupture strength for 10,000 hr and 30,000 hr at each temperature.

Fig. 40 Increase of outside diameter versus position of longitudinal direction
of specimens ruptured under internal pressure .
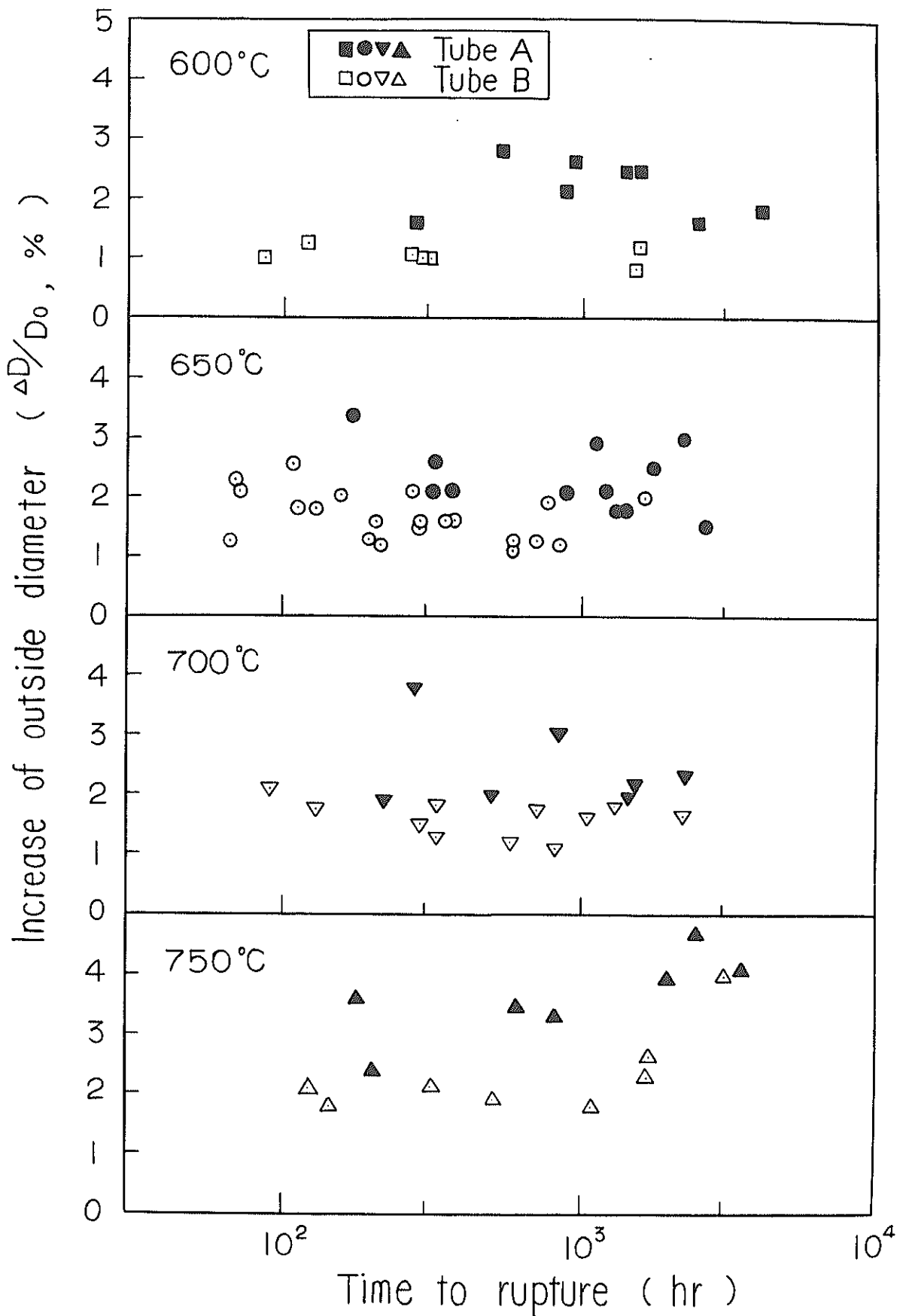
Fig. 41   Increase of outside diameter of specimens ruptured under internal pressure versus time to rupture.
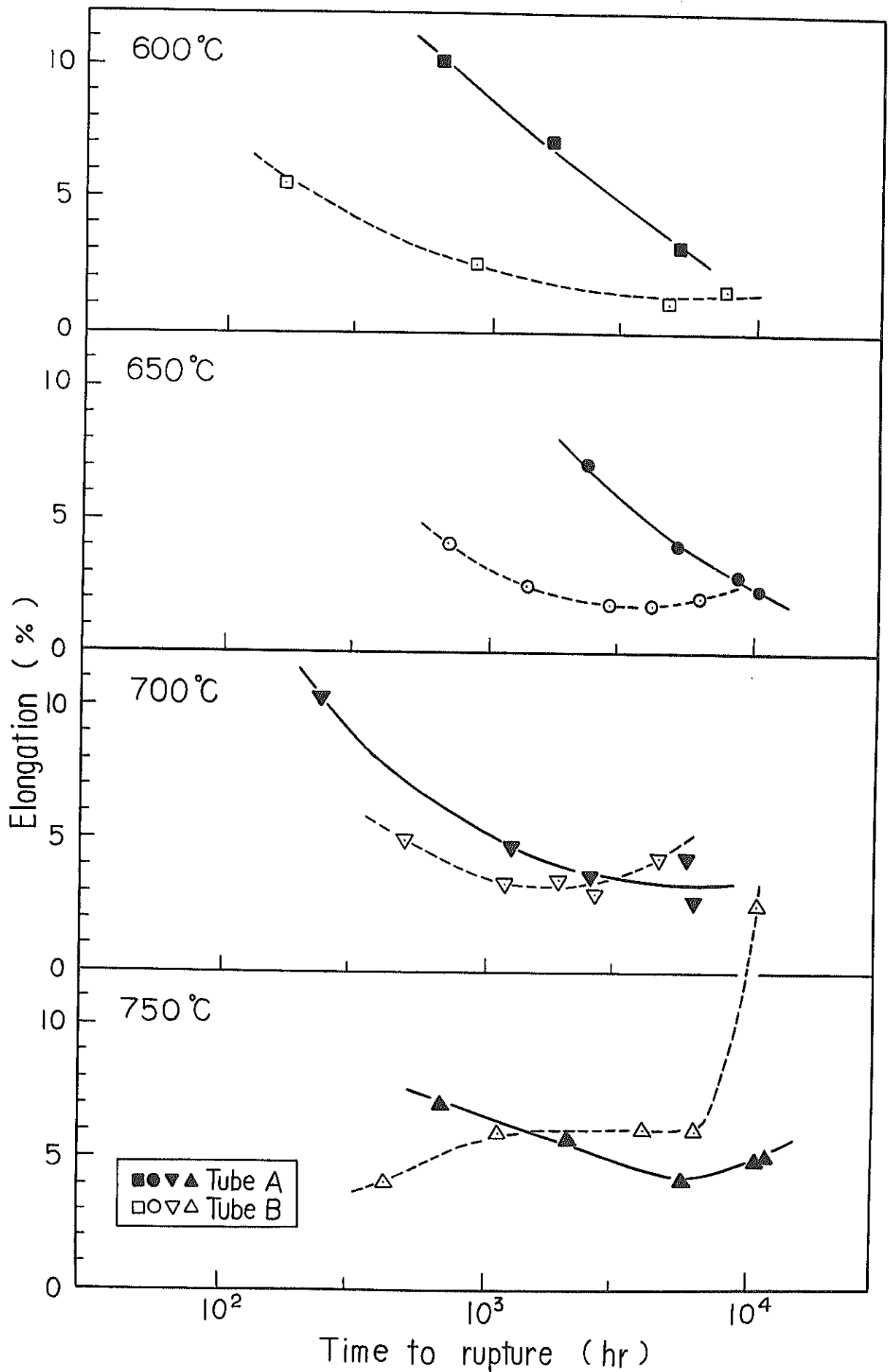
Fig. 42 Elongation of specimens ruptured under uniaxial
tension versus time to rupture.

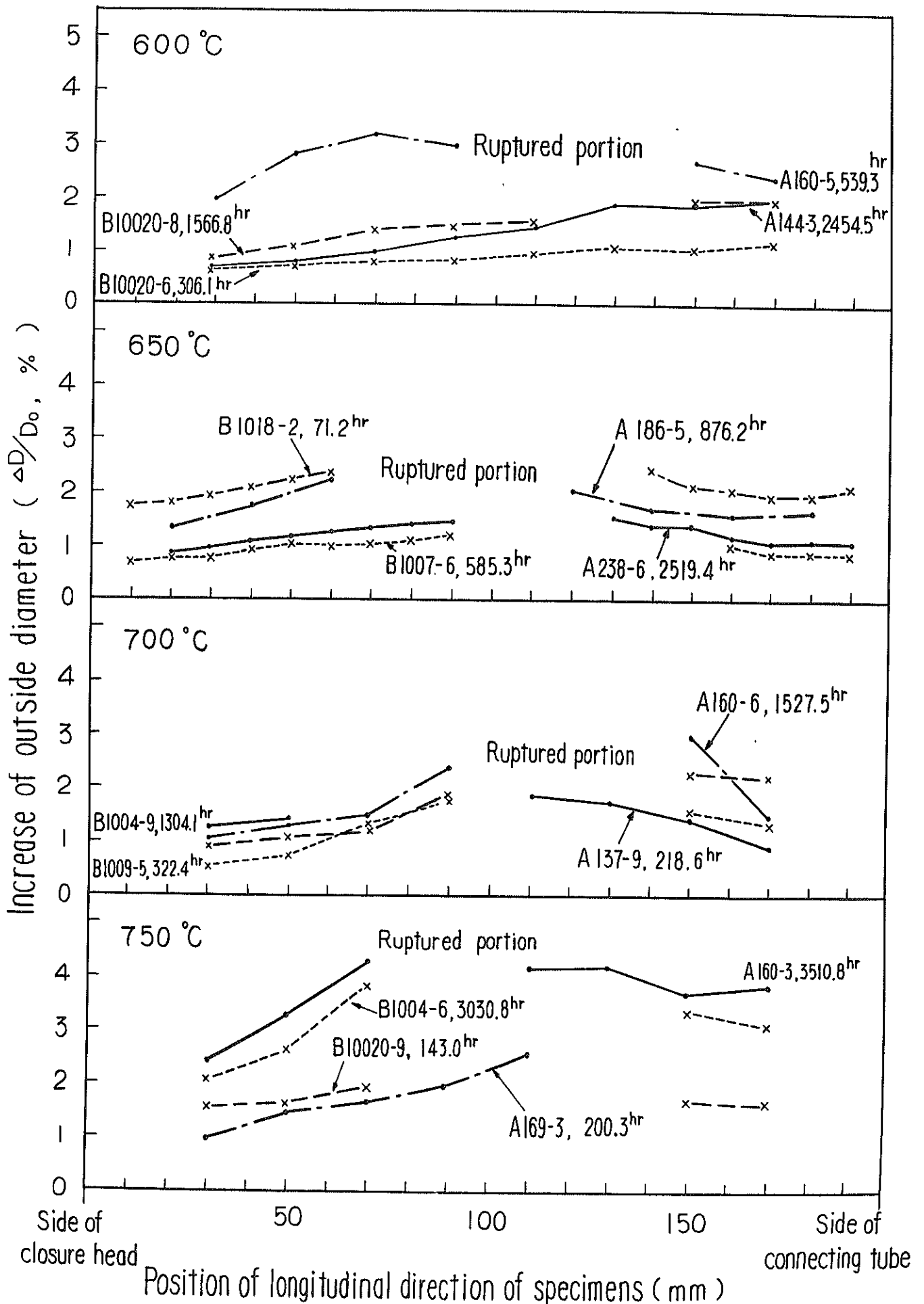| Symbol		No. of specimen	Time to rupture, hr	Hv, weight, g
Longitudinal	Transverse			
▲	✦	186-6	2601.1	500
■	✤	238-6	2519.4	100
◇	✪	155-8	2203.5	200
▽	⊽	109-4	1710.5	1000

Hardness (Hv 100g, 200g, 500g, 1kg)

300

250

200

Dotted line shows ruptured portion

Side of closure head

50

100

150

Side of connecting tube

Position of longitudinal direction of specimens (mm)

Fig. 43   Hardness versus position of longitudinal direction of specimens ruptured under internal pressure for Tube A at 650 °C.

| Symbol | | No. of specimen | Time to rupture, hr | Hv, weight, g |
Longitudinal	Transverse			
◇	⊗	1003-4	1634.0	200
▽	�	10022-8	826.1	1000
▪	✦	1007-6	595.3	100
▲	✹	1018-6	583.6	500

Hardness (Hv 100g , 200g , 500g , 1kg)

Position of longitudinal direction of specimens (mm)

Side of closure head

Side of connecting tube

Fig. 44   Hardness versus position of longitudinal direction of specimens ruptured under internal pressure for Tube B at 650°C.

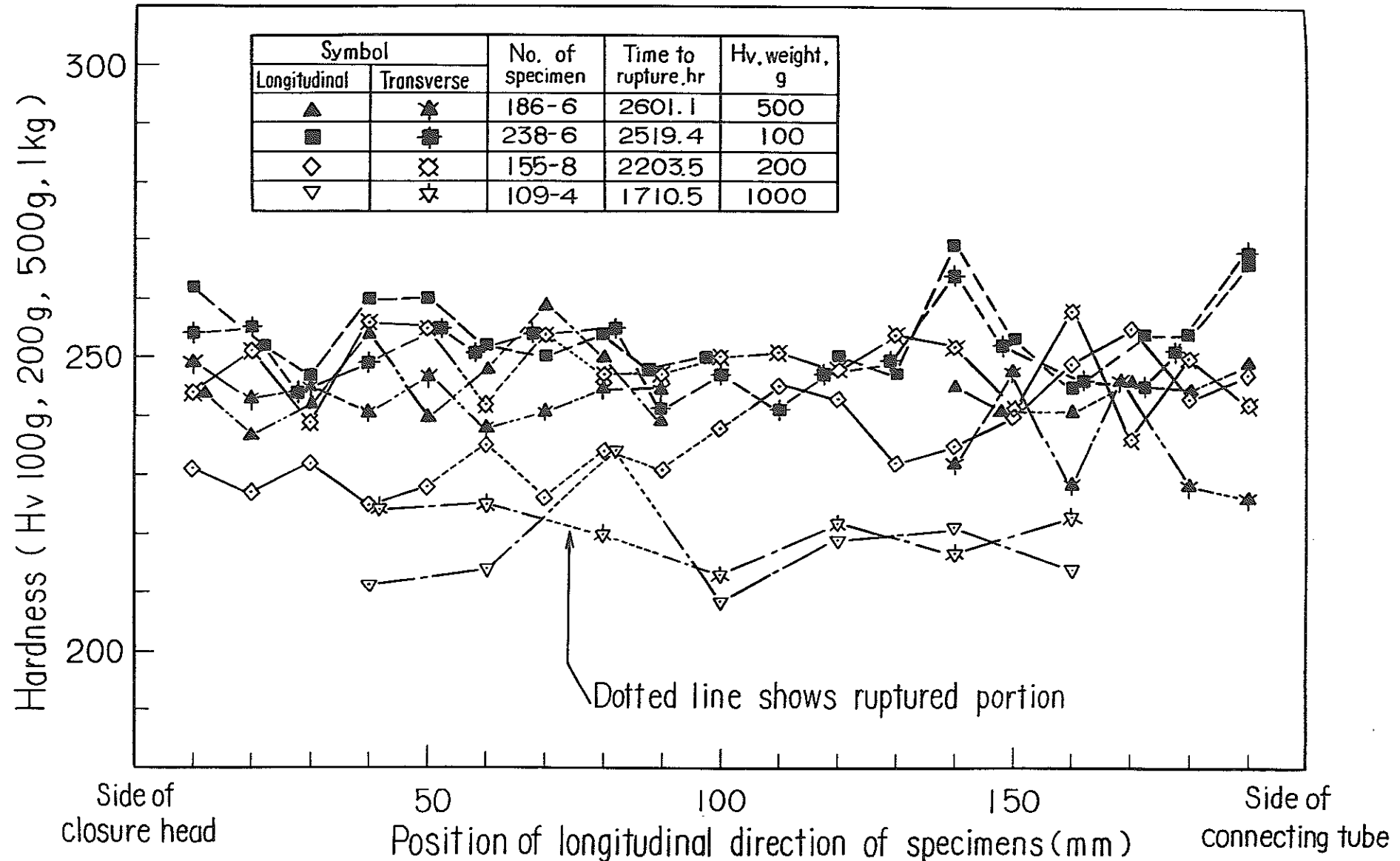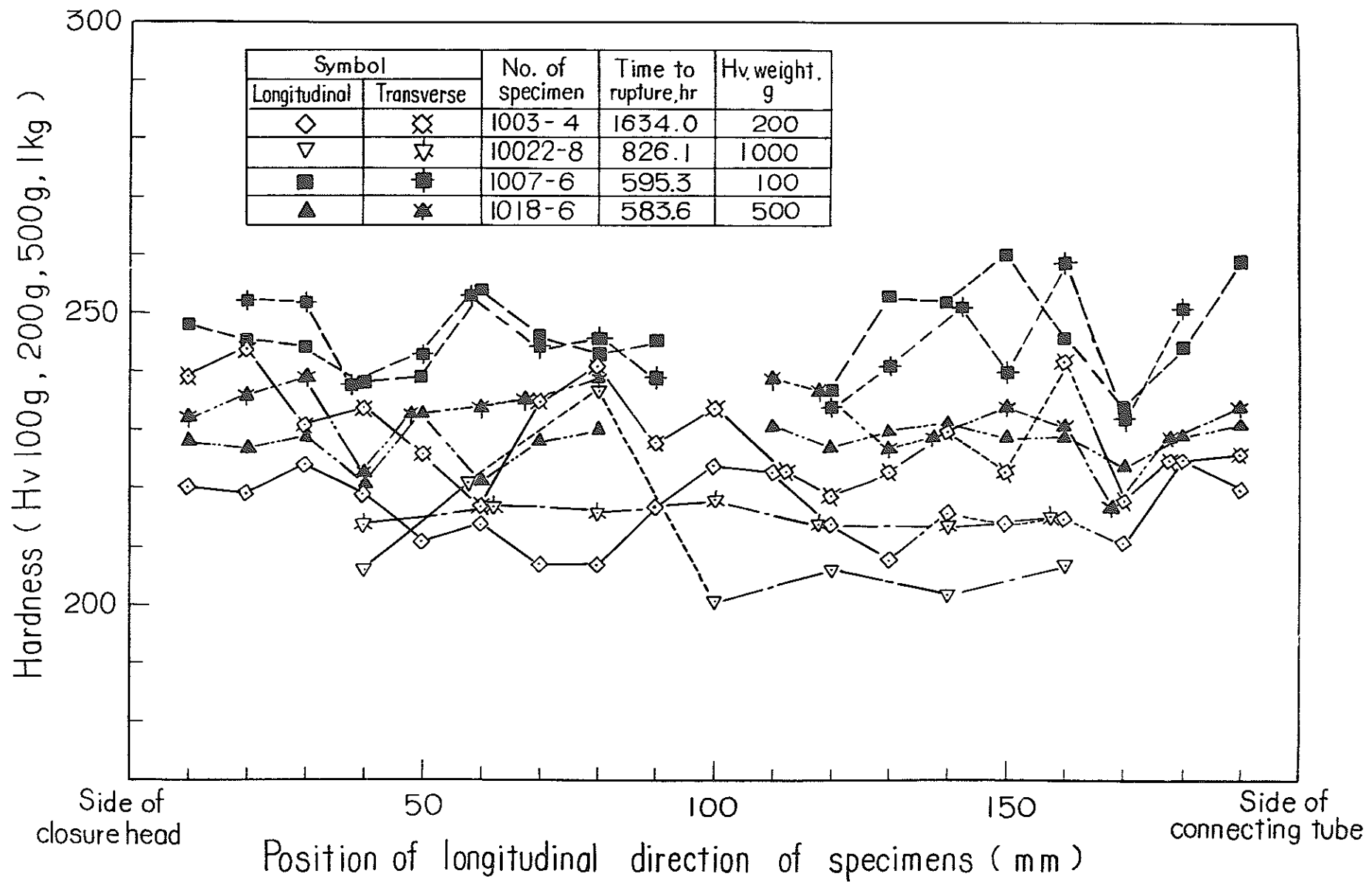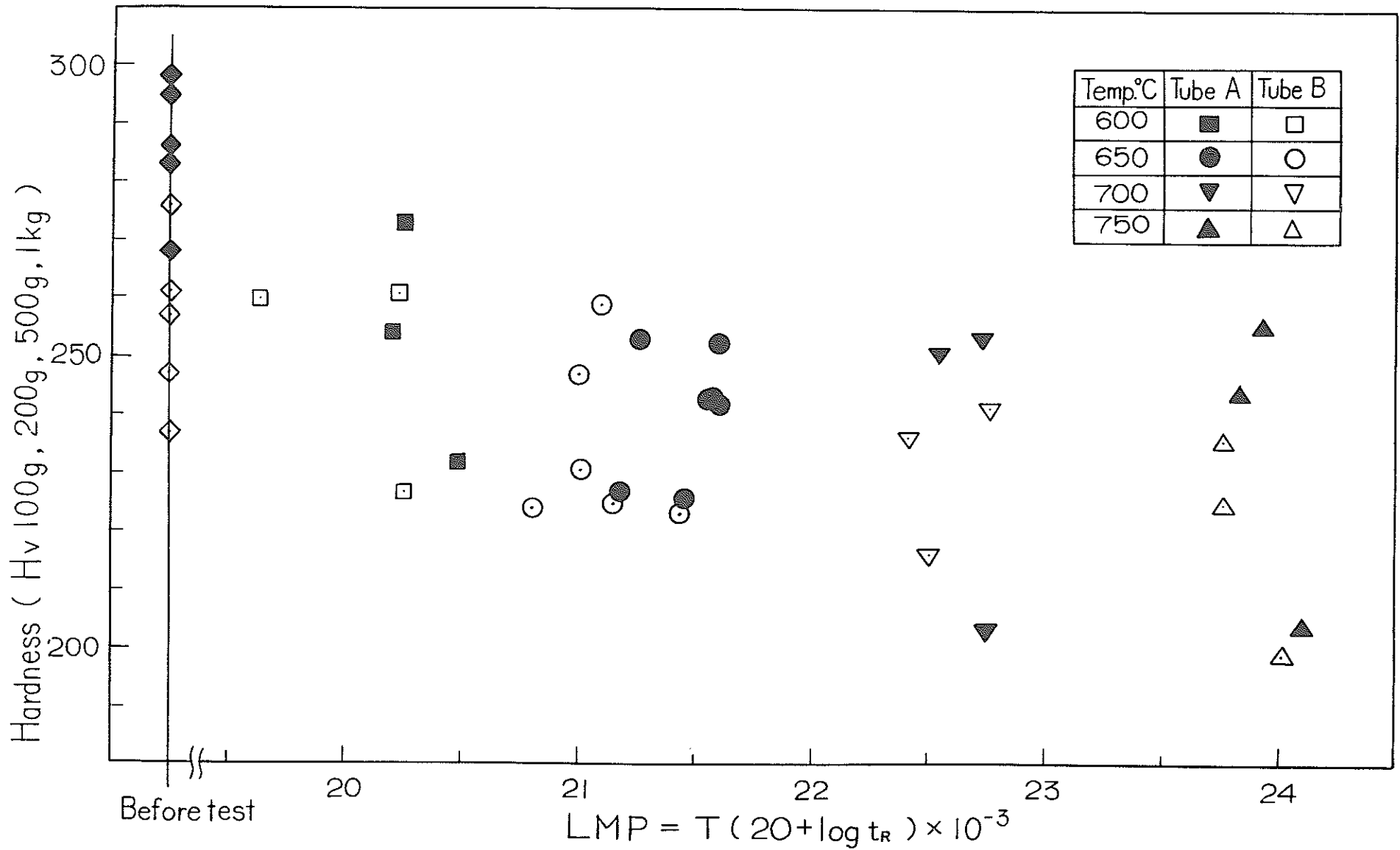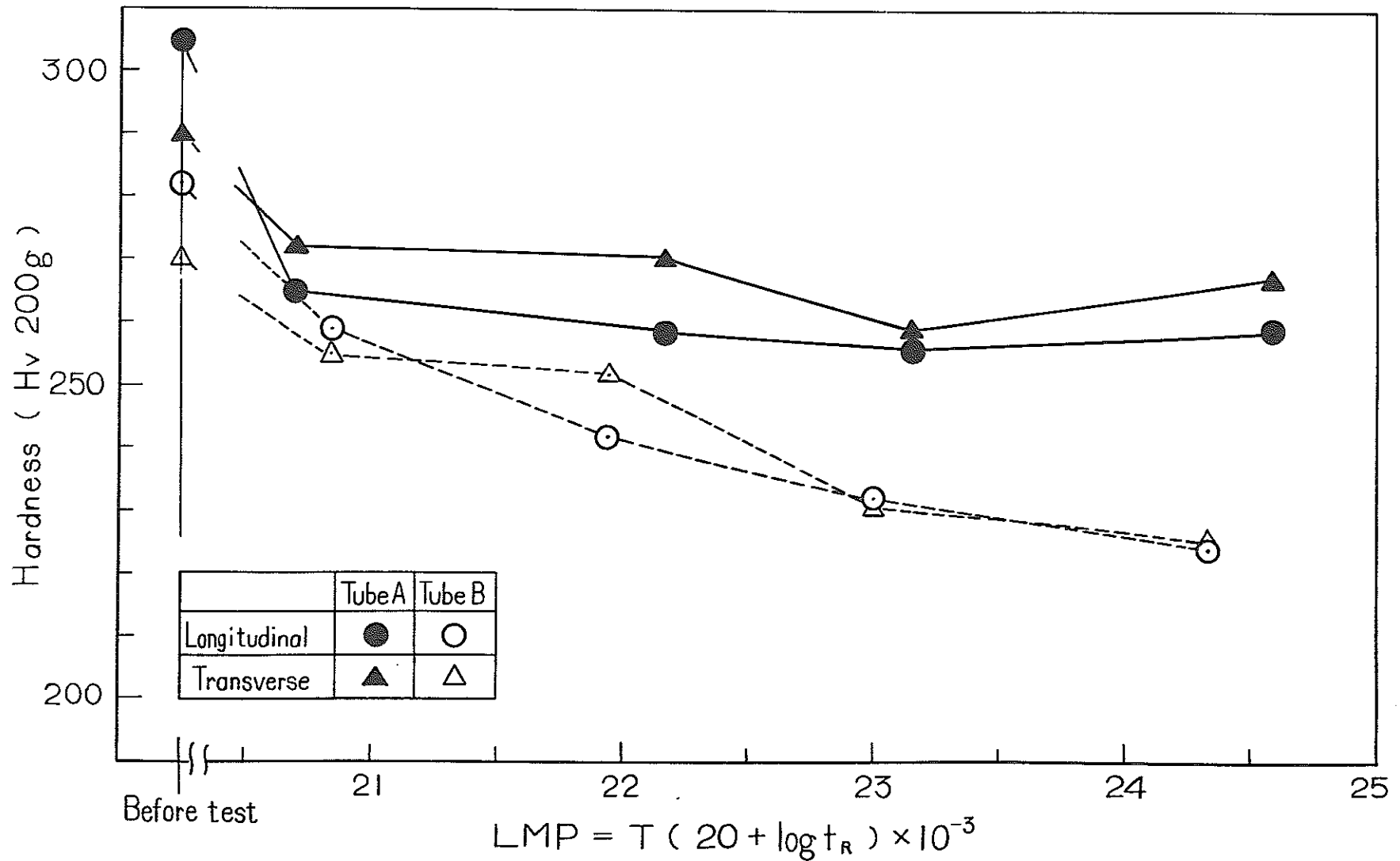Fig. 45 Hardness of specimens ruptured under internal pressure versus Larson - Miller parameter.

Fig. 46   Hardness of specimens ruptured under uniaxial tension versus Larson-Miller parameter.

Table 1.　Chemical composition of tubes

		Composition, wt %											
		Fe	C	Si	Mn	P	S	Ni	Cr	Mo	Co	B	N
Tube A	Ladle	Bal.	0.072	0.58	1.67	0.014	0.013	12.47	17.13	2.54	0.04		
	Check	Bal.	0.066	0.62	1.65	0.017	0.013	12.43	16.70	2.48	0.043	0.001	0.034
			0.067	0.62	1.69	0.020	0.015	12.40	16.72	2.45	0.043	0.001	0.035
Tube B	Ladle	Bal.	0.079	0.60	1.60	0.003	0.016	13.25	16.75	2.45	0.03	0.0003	0.0162
	Check	Bal.	0.079	0.60	1.60	0.002	0.011	13.23	16.80	2.58	0.01	0.0002	0.0164
			0.077	0.60	1.61	0.002	0.012	13.19	16.75	2.60	0.01	0.0002	0.0172

Table 2. Grain size, microstructure, hardness and surface roughness of tubes.
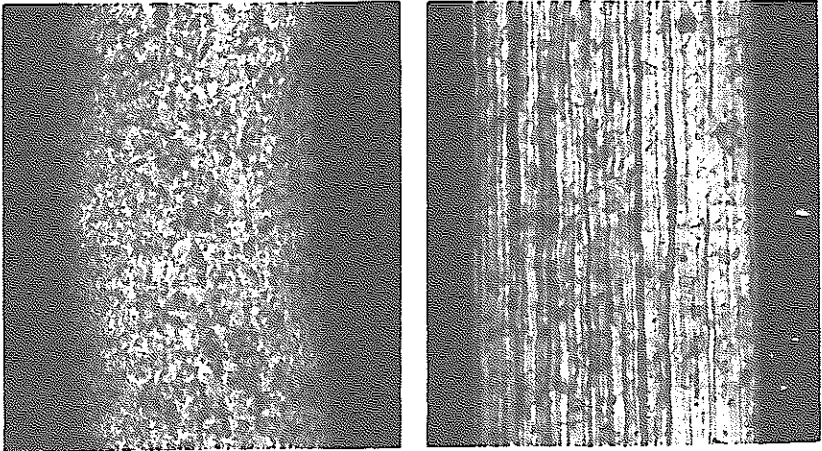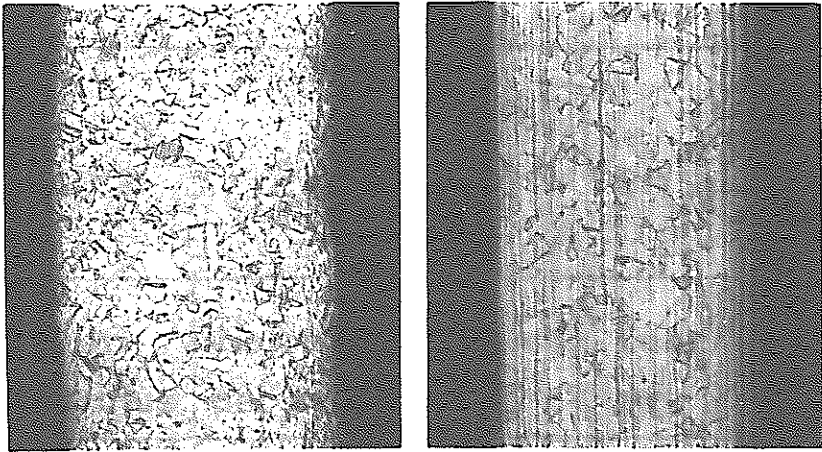
	Photomicrograph	Grain size (ASTM No.)	Surface roughness	Hardness (Hv)
Tube A	Transverse 0.1 mm Longitudinal	9.0	Inside surface 1. 0 S Outside surface 1. 6 S	Longitudinal 289 Transverse 283
Tube B	Transverse 0.1 mm Longitudinal	7.0	Inside surface 0. 8 S Outside surface 1. 5 S	Longitudinal 260 Transverse 254

Table 3-1　List of internal pressure creep testing apparatus

Institute	No. of apparatus	No. of specimen per apparatus	max. Pressure (kg /cm^2)	max. Temperature (°C)	Pressurizing medium	Atmosphere
NRIM	5	2	500	800	Ar	Air
HITACHI	1	2	500	800	〃	Ar
KŌBE	5	3	500	800	〃	Air
SUMITOMO	5	1	500	800	〃	Ar
PNC	10	1	500	750	〃	Air

Table 3-2　List of tensile creep testing machine

Institute	No. of apparatus	No. of specimen per apparatus	max. Load (kg)	max. Temperature (°C)	Atmosphere
NRIM	28	1	750 ~1,500	800	Air

Table 4   Test Condition

Test	Temperature (°C)	Pressure or Stress Level (Rupture Time or Testing Time)
Internal Pressure Creep-Rupture	600, 650 700, 750	4 Level (100 , 300, 1000 , 3000 hr)
Uniaxial Tension Creep-Rupture and Creep	600, 650 700, 750	Creep – Rupture ; 4 Level (100, 300, 1000, 3000 hr) Creep ; 5 Level (max. 10,000 hr)

Table 5 Results of creep-rupture tests under internal pressure for Tube A.

Institute		NRIM		KŌBE		HITACHI		PNC		SUMITOMO	
Temp. °C	Pressure kg/cm²	No.of speci.	Time to rupture hr	No.of speci.	Time to rupture hr	No.of speci.	Time to rupture hr	No.of speci.	Time to rupture hr	No.of speci.	Time to rupture hr
600	370	190-7	277.7	109-8	(140.8)	—	—	146-3	371.5	—	—
	355	190-4	876.4	160-5	539.3	—	—	146-8	1159.	—	—
	330	155-7 / 160-9	939.0 / 1571.2	144-3	2454.5	—	—	146-6	2965.3	—	—
	310	190-6 / 160-4	1394.1 / 4038.8	109-5	2914.1	—	—	126-8	2308.	—	—
650	310	190-3	168.4	144-2	(103.8)	186-3	103.7	146-9	172.	238-9 / 238-8	(66.1) / (72.3)
	280	186-9	316.6	109-2 / 169-2	311.4 / 364.8	186-4	526.0	146-5	578.	238-5	483.1
	250	155-5	1100.1	169-8 / 169-4	1300.0 / 1389.0	186-5	876.2	146-7	916.5	238-7	(901.0)
	225	155-8	2203.5	109-7 / 109-4	1218.5 / 1710.5	186-6	2601.1	126-4	5858.3	238-6	2519.4
700	220	—	—	137-9	218.6	—	—	—	—	—	—
	215	155-2	276.5	—	—	—	—	146-4	269.5	—	—
	185	160-8	840.1	169-7	523.0	—	—	146-2	337.	—	—
	150	160-2	1449.7	160-6	1527.5	—	—	126-7	1618.	—	—
	135	190-2	2243.4	109-9	2369.8	—	—	248-4	2902.5	—	—
750	150	190-9	176.6	169-3	200.3	—	—	144-8	214.	—	—
	115	190-8	612.0	137-7	630.1	—	—	126-2	1220.5	—	—
	100	—	—	169-9	812.5	—	—	—	—	—	—
	95	—	—	—	—	—	—	137-5	1604.	—	—
	80	190-5	1969.1	—	—	—	—	—	—	—	—
	70	155-4	2419.6	160-3	3510.8	—	—	126-5	3980.2	—	—

Parentheses show the reference values of specimen ruptured at welded spot.

Marks(●,○) show the values applied to statistical analysis of the relation between pressure and time to rupture.

Mark (●) shows the values applied to statistical analysis of the relation between pressure and Larson-Miller parameter.

Table 6 Results of creep-rupture tests under internal pressure for Tube B.

Institute		NRIM		KŌBE		HITACHI		P N C		SUMITOMO	
Temp. °C	Pressure kg/cm²	No.of speci.	Time to rupture hr	No.of speci.	Time to rupture hr	No.of speci.	Time to rupture hr	No.of speci.	Time to rupture hr	No.of speci.	Time to rupture hr
600	370	1012-5	119.2	—	—	—	—	1036-1	177.5	—	—
	355	1018-9	266.2	10020-2	85.0	—	—	1010-7	173.	—	—
	330	1004-1	288.6	10020-6	306.1	—	—	1036-8	351.	—	—
	310	1012-4 1004-3	(302.7) (309.0)	10020-8	1566.8	—	—	1029-4	556.	—	—
	280	1012-7	1499.4	—	—	—	—	—	—	—	—
650	310	1012-3	107.7	10020-4 1009-1	65.7 110.1	1018-2	71.2	1010-2	73.	1007-4	68.8
	280	1012-8	154.5	1004-8 1009-4	201.3 209.4	1018-3	192.2	1036-2	251.	1007-1	127.0
	250	1003-2	368.9	10022-1 10022-2	269.5 286.6	1018-4 1018-5	286.7 346.2	1036-9	348.	1007-8	(322.0)
	225	1012-9	699.7	1004-7 10022-8	770.1 826.1	1018-6	583.6	1011-9	739.	1007-6	595.3
	185	1003-4	1634.0	—	—	—	—	—	—	—	—
700	215	1012-2	127.8	10022-7 1009-3	(91.0) (130.0)	—	—	1036-7	141.	1007-3	89.9
	185	1003-5	323.8	1009-5	322.4	—	—	1011-2	231.3	1001-1	288.3
	155	—	—	1009-2	(477.5)	—	—	—	—	—	—
	150	1012-1	703.8	—	—	—	—	1022-4	572.	1007-9	576.6
	135	1004-2	1038.8	1004-9	1304.1	—	—	1011-8	1378.	1007-7	815.0
	115	1004-5	2181.0	—	—	—	—	—	—	—	—
750	150	1003-3	122.1	10020-9	143.0	—	—	1036-5	107.5	—	—
	115	1003-1	317.3	10022-6	509.3	—	—	1029-9	261.5	—	—
	95	—	—	—	—	—	—	1036-4	1142.	—	—
	90	—	—	10022-9	1095.3	—	—	—	—	—	—
	80	1003-7	1669.5	—	—	—	—	—	—	—	—
	70	1004-4	1692.9	1004-6	3030.8	—	—	1029-5	2201.5	—	—

Table 7 Results of creep and rupture tests under uniaxial tension for Tube A.

Temp. °C	Stress kg/mm²	No.of specimen	Instantaneous strain %	Time for total strain, hr			Minimum creep rate %/hr	Time to rupture hr	Elongation %
				0.5%	1.0%	2.0%			
600	31.0	127-5	—	—	—	—	—	216.2°	—
	29.0	156-4	—	—	—	—	—	452.4°	—
		220-8	0.35_0	5.0	57.5	210.0	$6.2_1 \times 10^{-3}$	630.6°	10.2
	27.0	153-1	—	—	—	—	—	946.7°	—
		220-2	0.30_6	8.0	114.0	689.0	1.54×10^{-3}	1644.0°	7.1
	24.0	110-4	—	—	—	—	—	6085.8°	—
		247-5	0.21_4	54.0	973.0	3842	$2.4_9 \times 10^{-4}$	5018.3°	3.3
	22.0	220-4	0.19_0	1070	4280	—	$8.5_0 \times 10^{-5}$	discontinue (7150.0)	—
	18.0	247-3	0.16_4	5020	—	—	2.05×10^{-5}	discontinue (6313.0)	—
650	24.0	127-2	—	—	—	—	—	96.8°	—
	21.0	117-5	—	—	—	—	—	441.8°	—
	18.0	117-3	—	—	—	—	—	1914.6°	—
		247-15	0.16_3	82.0	655.0	1373	7.64×10^{-4}	2290.4°	7.1
	16.0	117-4	—	—	—	—	—	6024.7°	—
		247-11	0.15_2	672.0	2335	3945	$2.3_4 \times 10^{-4}$	4971.9°	4.0
	15.0	247-4	0.13_0	1045	4330	7632	$1.3_7 \times 10^{-4}$	8528.3°	2.8
	14.0	247-8	0.12_0	2047	6215	10085	$1.0_9 \times 10^{-4}$	10535.3°	2.4
	13.0	220-6	0.12_9	2207	6580	9705	$9.8_3 \times 10^{-5}$	discontinue (10007.0)	—
700	18.0	110-6	—	—	—	—	—	132.0°	—
	16.0	127-6	—	—	—	—	—	243.0°	—
		247-9	0.16_1	14.8	53.9	109.6	$1.2_8 \times 10^{-2}$	234.9°	10.3
	13.0	110-2	—	—	—	—	—	1060.7°	—
		220-3	0.13_1	101.5	398.0	816.0	$1.6_4 \times 10^{-3}$	1248.5°	4.7
	11.0	153-3	—	—	—	—	—	2490.9°	—
		220-5	0.09_7	381.0	1086	1923	$6.9_9 \times 10^{-4}$	2457.6°	3.6
	10.0	247-16	0.09_8	840.0	2375	4109	$2.9_1 \times 10^{-4}$	5608.9°	4.3
	9.0	110-3	—	—	—	—	—	4753.8°	—
		247-12	0.08_3	1152	3422	5545	$1.9_0 \times 10^{-4}$	6028.2°	2.6
750	13.0	112-6	—	—	—	—	—	102.0°	—
	11.0	156-5	—	—	—	—	—	271.6°	—
	9.0	153-4	—	—	—	—	—	658.3°	—
		220-7	0.10_0	79.0	210.8	577.0	$3.4_9 \times 10^{-3}$	674.5°	7.0
	7.0	247-10	0.07_1	370.0	874.0	1431	$8.1_6 \times 10^{-4}$	2049.5°	5.7
	6.0	156-2	—	—	—	—	—	2562.2°	—
	5.5	247-13	0.05_1	1073	2327	3814	$2.7_3 \times 10^{-4}$	5503.8°	4.2
	5.0	247-7	0.04_1	2110	4630	7912	$1.5_0 \times 10^{-4}$	11625.9°	5.1
	4.5	117-2	—	—	—	—	—	16518.8	—
		247-14	0.03_2	2225	4047	6078	$1.5_7 \times 10^{-4}$	10539.4°	4.9

Marks (•, ○) show the values applied to statistical analysis of the relation between stress and time to rupture.

Mark (•) shows the values applied to statistical analysis of the relation between stress and Larson-Miller parameter.

Table 8 Results of creep and rupture tests under uniaxial tension for Tube B.

Temp. °C	Stress kg/mm²	No. of specimen	Instantaneous strain %	Time for total strain, hr			Minimum creep rate %/hr	Time to rupture hr	Elongation %
				0.5 %	1.0 %	2.0 %			
600	29.0	1049-1	—	—	—	—	—	143.2	—
		1005-1	0.31_1	5.2	36.9	91.0	$1.5_3 \times 10^{-2}$	160.3	5.6
	27.0	1015-4	—	—	—	—	—	321.9	—
	24.0	1015-2	—	—	—	—	—	919.0	—
		1051-5	0.22_8	35.6	284.0	740.5	$1.5_1 \times 10^{-3}$	856.5	2.6
	21.0	1050-3	—	—	—	—	—	2372.0	—
	20.0	1051-3	0.17_4	201.0	2049	—	$2.3_3 \times 10^{-4}$	2324.5	1.2
	18.0	1005-5	0.16_9	716.0	5443	—	$7.6_0 \times 10^{-5}$	7578.0	1.7
	16.0	1051-13	0.10_6	4679	—	—	$3.7_6 \times 10^{-5}$	discontinue [6313.0]	—
650	21.0	1048-3	—	—	—	—	—	170.5	—
	18.0	1042-2	—	—	—	—	—	639.8	—
		1005-9	0.16_6	52.0	257.0	517.0	$2.2_8 \times 10^{-3}$	691.2	4.1
	16.0	1050-1	—	—	—	—	—	1298.8	—
		1005-3	0.14_5	167.0	758.0	1274	7.50×10^{-4}	1387.8	2.5
	14.0	1051-15	0.12_7	817.0	1979	—	$2.6_4 \times 10^{-4}$	2853.0	1.9
	13.0	1049-2	—	—	—	—	—	3215.2	—
		1051-12	0.11_1	1510	3148	—	$1.6_5 \times 10^{-4}$	4091.7	1.8
	12.0	1005-12	0.08_5	2231	4343	5983	$1.2_2 \times 10^{-4}$	6080.6	2.2
	11.0	1049-3	—	—	—	—	—	6736.5	—
700	16.0	1049-5	—	—	—	—	—	123.9	—
	13.0	1042-5	—	—	—	—	—	518.4	—
		1005-13	0.12_6	85.6	238.5	367.0	$2.8_1 \times 10^{-3}$	485.8	5.0
	11.0	1048-1	—	—	—	—	—	890.1	—
		1051-11	0.09_4	283.2	655.0	1002	$9.4_4 \times 10^{-4}$	1177.2	3.4
	10.0	1005-2	0.08_5	479.0	1030	1567	$5.8_1 \times 10^{-4}$	1878.9	3.4
	9.0	1048-4	—	—	—	—	—	2069.5	—
		1051-9	0.07_9	652.5	1427	2206	$4.1_5 \times 10^{-4}$	2552.5	2.9
	8.0	1005-4	0.07_4	1096	2329	3618	$2.7_0 \times 10^{-4}$	4504.3	4.3
750	11.0	1015-3	—	—	—	—	—	171.8	—
	9.0	1042-1	—	—	—	—	—	465.4	—
		1051-4	0.08_8	85.0	196.5	316.5	$3.5_5 \times 10^{-3}$	415.0	4.0
	7.0	1051-14	0.08_1	262.0	533.8	824.5	$1.1_6 \times 10^{-3}$	1112.4	6.0
	6.0	1015-5	—	—	—	—	—	1911.5	—
	5.0	1051-2	0.05_5	944.0	1711	2597	$3.5_0 \times 10^{-4}$	3982.5	6.1
	4.5	1042-3	—	—	—	—	—	6950.5	—
		1051-1	0.03_6	1646	3072	4378	$2.0_4 \times 10^{-4}$	6091.1	6.1
	4.0	1005-6	0.03_9	2747	4276	5677	$1.3_0 \times 10^{-4}$	10541.7	14.5

Table 9 Regression analysis of the creep-rupture data under internal pressure represented by the relation between pressure and time to rupture.

Tube	Temp. °C	Degree of Polynomial	FO(RES) $\dfrac{\Sigma\{\hat{Y}_{ik}-\hat{Y}_{i(k-1)}\}^2}{\dfrac{\Sigma(Y_i-\hat{Y}_{ik})^2}{n-1-k}}$	F(0.05)	r^2 $\dfrac{\Sigma(\hat{Y}_{ik}-\bar{Y})^2}{\Sigma(Y_i-\bar{Y})^2}$	SD(RES) $\sqrt{\dfrac{\Sigma(Y_i-\hat{Y}_{ik})^2}{n}}$
A	600	①	18.409525	5.120	0.671647	0.190100
		2	3.947942	5.320	0.780144	0.155554
	650	①	187.035767	4.410	0.916681	0.117061
		2	4.141062	4.450	0.933812	0.104335
	700	①	160.859848	4.960	0.947015	0.087363
		2	0.045676	5.120	0.947316	0.087114
	750	①	258.422784	5.120	0.969973	0.078020
		2	3.269992	5.320	0.979533	0.064412
B	600	①	35.989340	4.960	0.799953	0.173013
		2	0.001982	5.120	0.800002	0.172992
	650	①	413.696265	4.260	0.947332	0.087047
		2	2.556391	4.280	0.952815	0.082392
	700	①	288.986303	4.670	0.960131	0.080685
		2	0.549646	4.750	0.962028	0.078742
	750	①	219.838639	4.840	0.956491	0.104213
		2	1.252361	4.960	0.961806	0.097641
A and B	600	①	13.095035	4.350	0.395680	0.348477
		2	1.258507	4.380	0.433222	0.337479
	650	②	4.692817	4.070	0.741418	0.225564
		3	0.000201	4.080	0.741420	0.225563
	700	①	93.043755	4.280	0.801799	0.180369
		2	0.958416	4.300	0.810073	0.176564
	750	①	271.475126	4.350	0.931384	0.125946
		2	2.040303	4.380	0.938037	0.119683

Y_i ; logarithms of observed value , $\bar{Y}$; mean of logarithms of observed value, $\hat{Y}_{ik}$; logarithms of estimated value at k-th degree of regression equation, n ; number of observed value , F(0.05) ; value in the F-Table at significance level of 5%, r^2 ; contribution, SD ; standard deviation, Round mark ; significant degree of regression equation.

Table 10 Regression analysis of the creep-rupture data under internal pressure represented by the relation between pressure and the Larson-Miller parameter.

Tube	Degree of Polynomial	FO(RES) $\dfrac{\sum\{\hat{Y}_{ik}-\hat{Y}_{i(k-1)}\}^2}{\dfrac{\sum(Y_i-\hat{Y}_{ik})^2}{n-1-k}}$	F(0.05)	r^2 $\dfrac{\sum(\hat{Y}_{ik}-\bar{Y})^2}{\sum(Y_i-\bar{Y})^2}$	SD(RES) $\sqrt{\dfrac{\sum(Y_i-\hat{Y}_{ik})^2}{n}}$
A	②	49.250843	4.045	0.89227	0.130528
A	3	1.318635	4.050	0.89564	0.128470
B	③	5.380995	4.008	0.93512	0.111418
B	4	3.721488	4.012	0.93901	0.108024
A and B	②	21.040552	3.929	0.72752	0.235072
A and B	3	1.528844	3.928	0.73162	0.233299

Yi ; values of LMP calculated from observed value, $\bar{Y}$; mean value of LMP calculated from observed value, $\hat{Y}_{ik}$; estimated values of LMP at k-th degree of regression equation, n ; number of observed value, F(0.05) ; value in the F-Table at significance level of 5 %, r^2 ; contribution, SD ; standard deviation, Round mark; significant degree of regression equation.

Table11 Regression analysis of the creep-rupture data under uniaxial tension represented by the relation between stress and time to rupture.

Tube	Temp. °C	Degree of Polynomial	FO(RES) $\dfrac{\Sigma\{\hat{Y}_{ik}-\hat{Y}_{i(k-1)}\}^2}{\dfrac{\Sigma(Y_i-\hat{Y}_{ik})^2}{n-1-k}}$	F(0.05)	r^2 $\dfrac{\Sigma(\hat{Y}_{ik}-\bar{Y})^2}{\Sigma(Y_i-\bar{Y})^2}$	SD(RES) $\sqrt{\dfrac{\Sigma(Y_i-\hat{Y}_{ik})^2}{n}}$
A	600	①	193.718773	5.990	0.974839	0.078696
		2	0.007570	6.610	0.974886	0.078621
	650	②	33.648239	6.610	0.997075	0.035549
		3	1.657270	7.710	0.997932	0.029891
	700	②	6.921388	5.990	0.985387	0.070419
		3	2.627653	6.610	0.989838	0.058724
	750	①	412.794942	5.990	0.985673	0.075233
		2	1.229049	6.610	0.988500	0.067404
B	600	①	405.502286	5.990	0.985419	0.068760
		2	1.155055	6.610	0.988155	0.061974
	650	②	11.925234	5.990	0.992047	0.040902
		3	3.692956	6.610	0.995425	0.031020
	700	①	275.310581	5.320	0.975205	0.069943
		2	3.507173	5.590	0.984352	0.055564
	750	①	2030.687664	5.590	0.997054	0.030116
		2	0.058811	5.990	0.997088	0.029942
A and B	600	①	22.561091	4.670	0.634432	0.327239
		2	1.529417	4.750	0.675757	0.308188
	650	②	5.302229	4.600	0.794952	0.256965
		3	0.624808	4.670	0.804355	0.251004
	700	①	103.969833	4.450	0.859469	0.196119
		2	1.768944	4.490	0.873459	0.186101
	750	①	387.130395	4.600	0.965099	0.110934
		2	0.626055	4.670	0.966702	0.108355

Y_i ; logarithms of observed value, $\bar{Y}$; mean of logarithms of observed value, $\hat{Y}_{ik}$; logarithms of estimated value at k-th degree of regression equation, n ; number of observed value, F(0.05) ; value in the F-Table at significance level of 5%, r^2 : contribution, SD : standard deviation, Round mark ; significant degree of regression equation.

Table 12 Regression analysis of the creep-rupture data under uniaxial tension represented by the relation between stress and the Larson-Miller parameter.

Tube	Degree of Polynomial	FO(RES) $\dfrac{\Sigma\left[\hat{Y}_{ik}-\hat{Y}_{i(k-1)}\right]^2}{\dfrac{\Sigma(Y_i-\hat{Y}_{ik})^2}{n-1-k}}$	F(0.05)	r^2 $\dfrac{\Sigma(\hat{Y}_{ik}-\bar{Y})^2}{\Sigma(Y_i-\bar{Y})^2}$	SD(RES) $\sqrt{\dfrac{\Sigma(Y_i-\hat{Y}_{ik})^2}{n}}$
A	②	85.414593	4.225	0.96832	0.102436
A	3	0.011957	4.240	0.96837	0.102359
B	③	6.684070	4.200	0.98547	0.059412
B	4	0.056541	4.215	0.98553	0.059281
A and B	②	12.174625	4.008	0.78895	0.245291
A and B	3	0.541474	4.012	0.79116	0.244004

Y_i ; values of LMP calculated from observed value, $\bar{Y}$; mean value of LMP calculated from observed value , $\hat{Y}_{ik}$; estimated values of LMP at k-th degree of regression equation, n ; number of observed value, F(0.05) ; value in the F-Table at significance level of 5%, r^2 ; contribution , SD ; standard deviation, Round mark ; significant degree of regression equation..

Table 13   Estimated values of stress obtained.   (kg/mm²)

Temperature	Rupture tests								Creep tests under uniaxial tension	
	Internal pressure ※1				Uniaxial tension ※2				Minimum creep rate of 10^{-4} %/hr ※5	1% total strain in 10.000 hr ※5
	10.000 hr		15.000 hr		10.000 hr		15.000 hr			
	※3	※4	※3	※4	※3	※4	※3	※4		
600°C	19.1	15.5	17.9	14.5	18.0	14.8	17.0	13.9	18.3	16.4
650°C	12.7	9.7	11.6	8.6	11.8	9.2	11.0	8.5	11.8	10.4
700°C	7.5	4.8	6.3	3.9	7.2	5.0	6.6	4.5	6.4	5.6
750°C	—	—	—	—	3.8	2.0	—	—	3.6	3.0

※1 :   The hoop stresses, being calculated by the mean diameter formula taking the dimension of the fuel cladding tubes as 6.3 mm in outside diameter and 0.35mm in wall-thickness, were obtained from the relations of temperature versus pressure for Tubes A and B (Fig. 17).

※2 :   The tensile stresses were obtained from the relations of temperature versus stress for Tubes A and B (Fig. 26).

※3 :   The values were obtained from the regression curves.

※4 :   The values were obtained from the curves of the lower confidence limit at the confidence coefficient of 95%.

※5 :   The estimated mean values were obtained for Tube B, the values of which were smaller than those of Tube A.
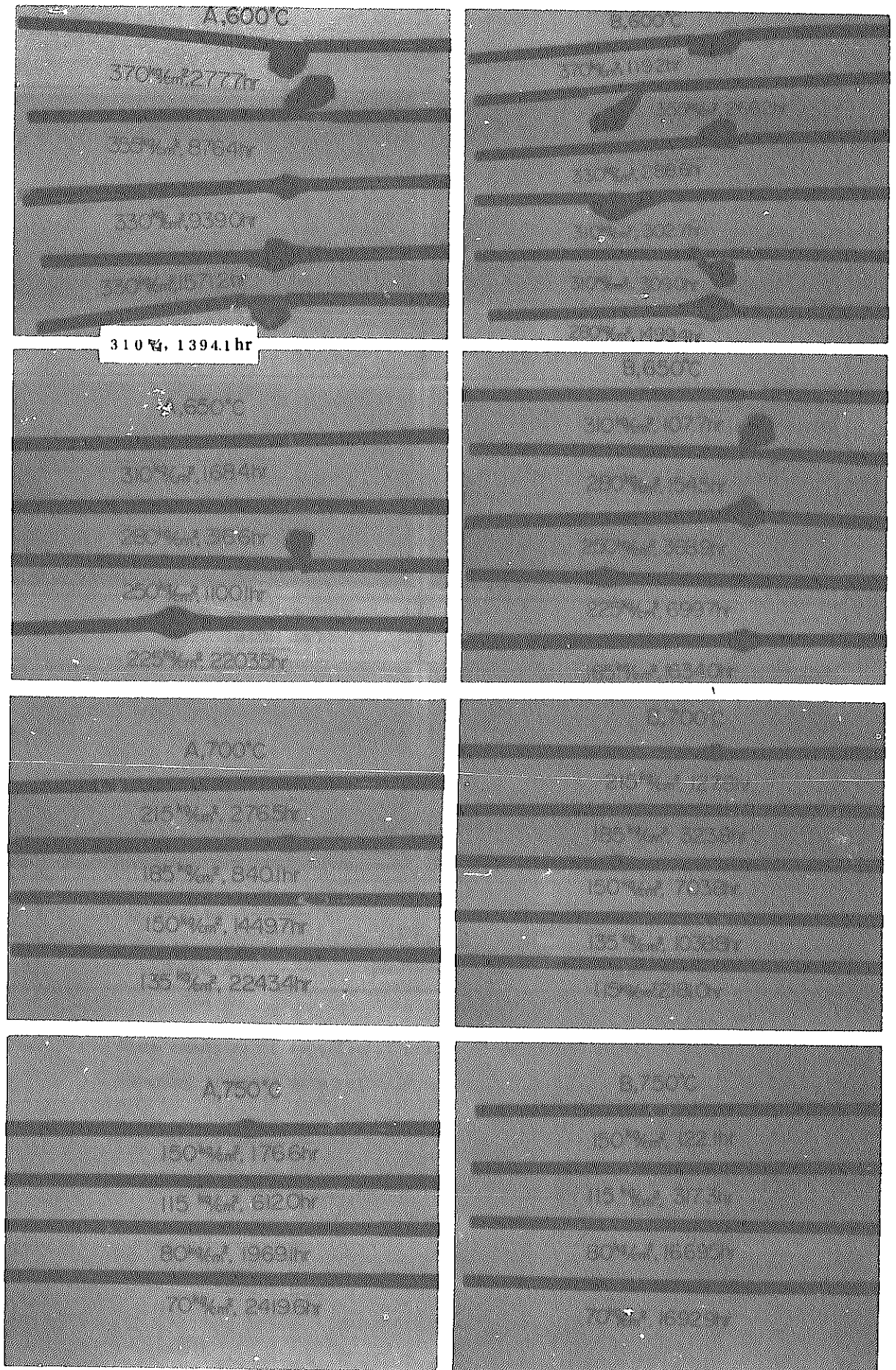
Photo. 1   Appearances of specimens after creep-rupture tests by internal pressure creep
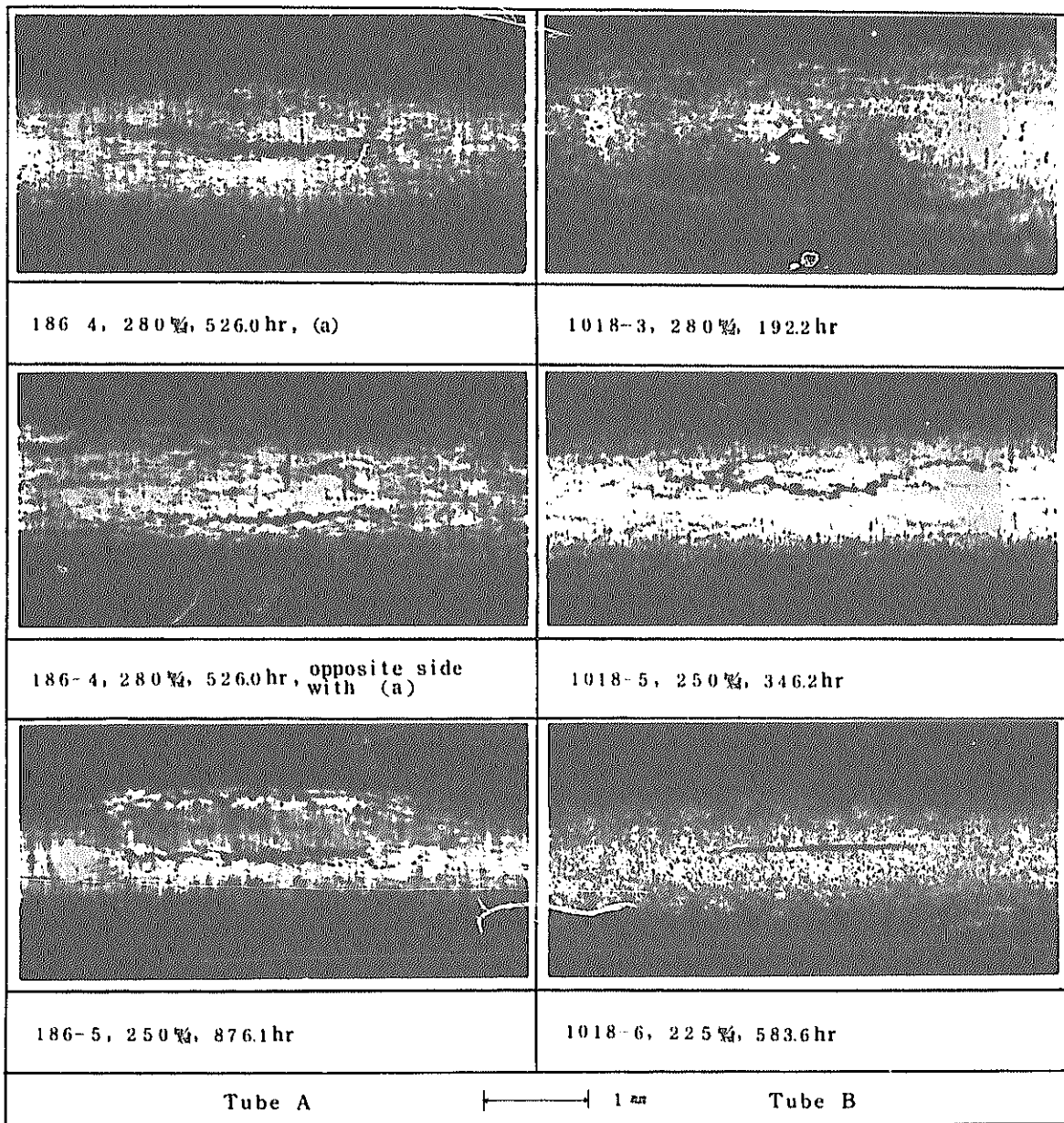testing apparatuses of the same institute.

186 4, 280℃, 526.0 hr, (a)	1018-3, 280℃, 192.2 hr
186-4, 280℃, 526.0 hr, opposite side with (a)	1018-5, 250℃, 346.2 hr
186-5, 250℃, 876.1 hr	1018-6, 225℃, 583.6 hr
Tube A	⊢———⊣ 1 ㎜ Tube B

Photo. 2　　Some examples of superficial cracks of specimens ruptured under
internal pressure at 650℃.
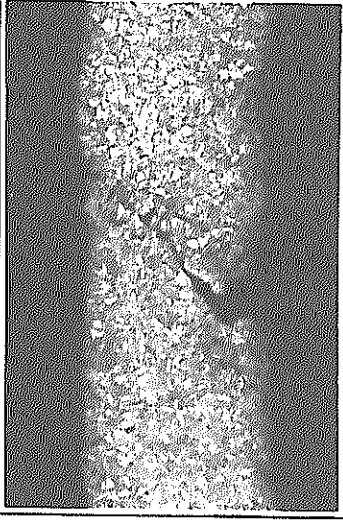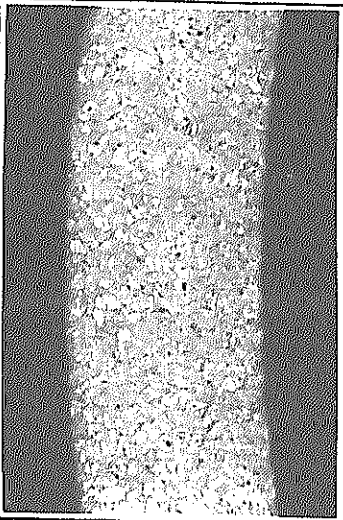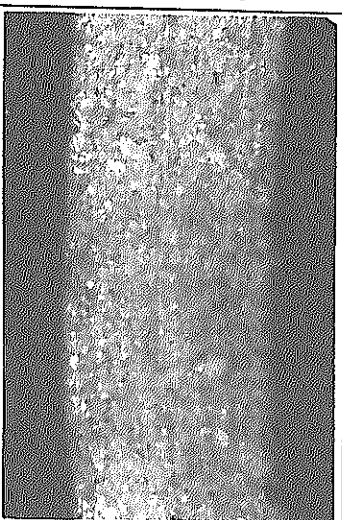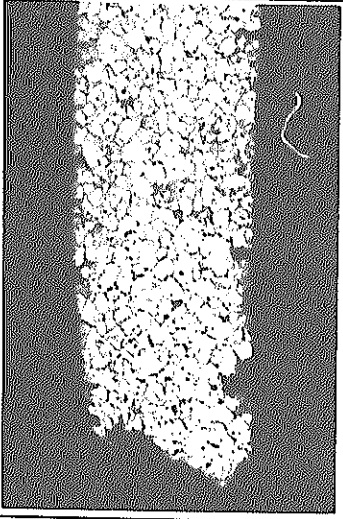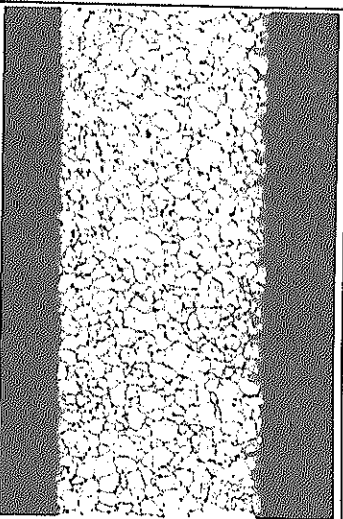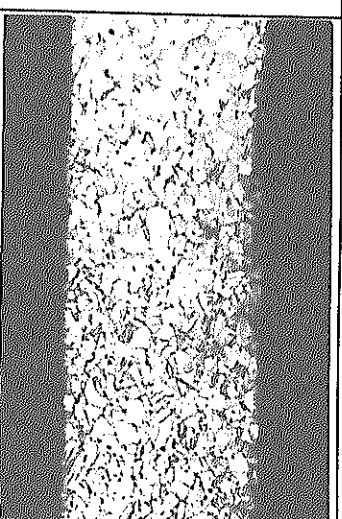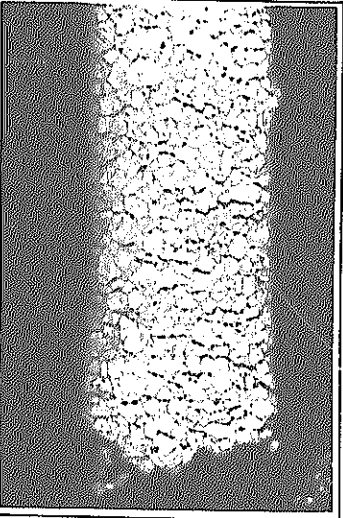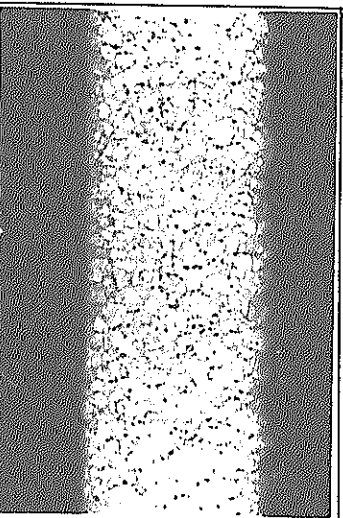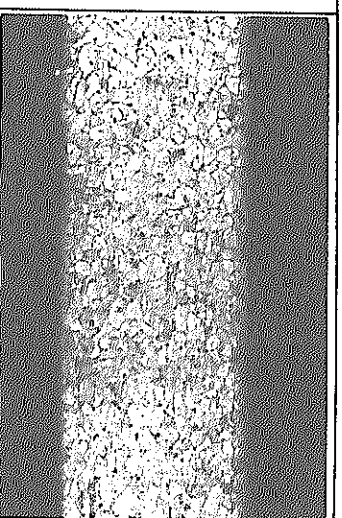
Fractured portion, Transverse	Vicinity of fractured portion	
	Transverse	Longitudinal

Tube A, 650℃, 238-6, 225 ㎏/㎟, 2519.4 hr

Tube B, 650℃, 1007 1, 280 ㎏/㎟, 127.0 hr

Tube B, 700℃, 1007 7, 135 ㎏/㎟, 815.0 hr

Photo. 3   Some examples of photomicrographs of specimens ;uptured under
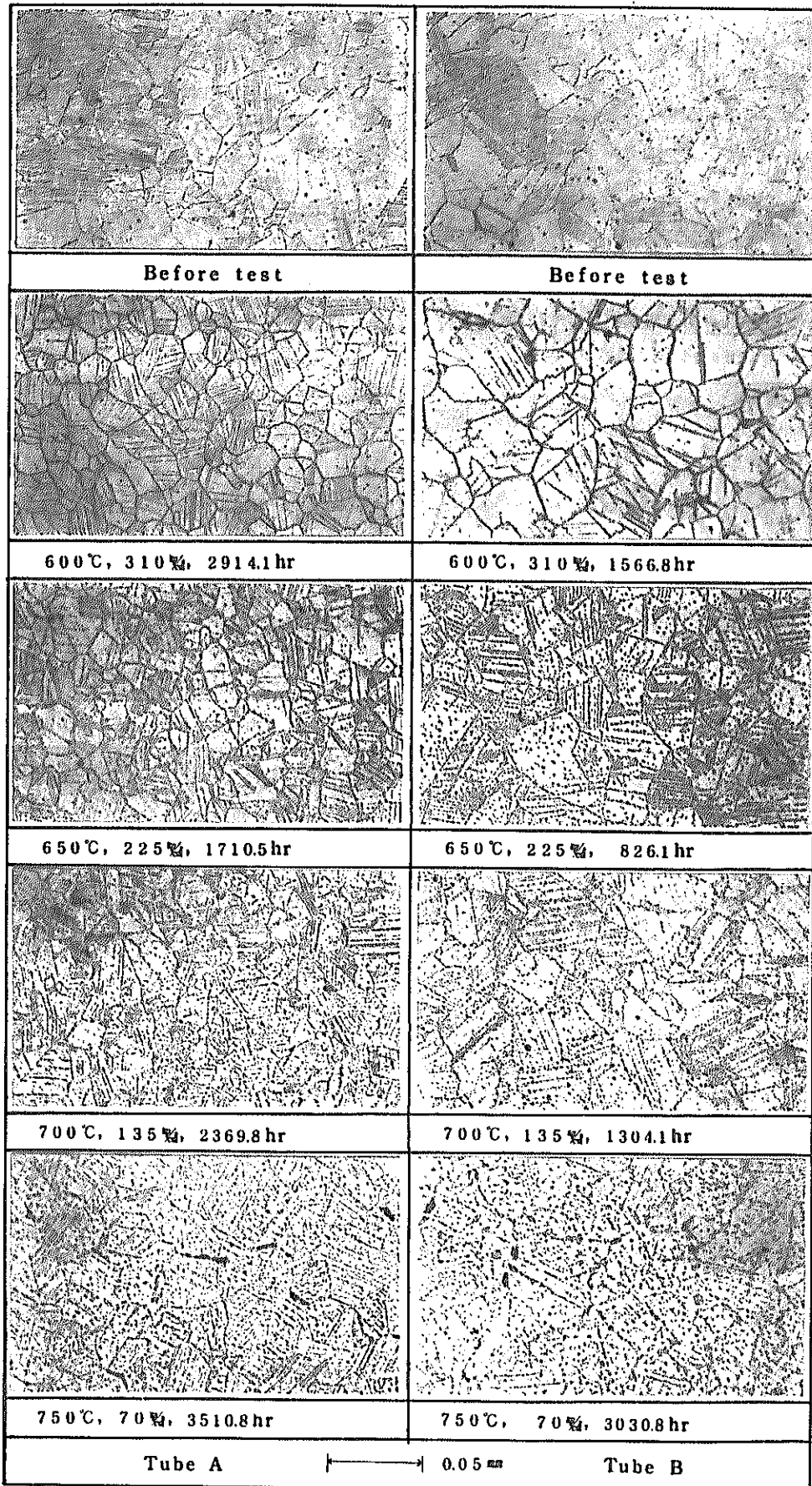internal pressure.

Before test	Before test
600℃, 310㎏, 2914.1hr	600℃, 310㎏, 1566.8hr
650℃, 225㎏, 1710.5hr	650℃, 225㎏, 826.1hr
700℃, 135㎏, 2369.8hr	700℃, 135㎏, 1304.1hr
750℃, 70㎏, 3510.8hr	750℃, 70㎏, 3030.8hr
Tube A	0.05㎜	Tube B

Photo. 4　Photomicrographs of specimens of long term ruptre at each temperature tested under internal pressure (transverse).

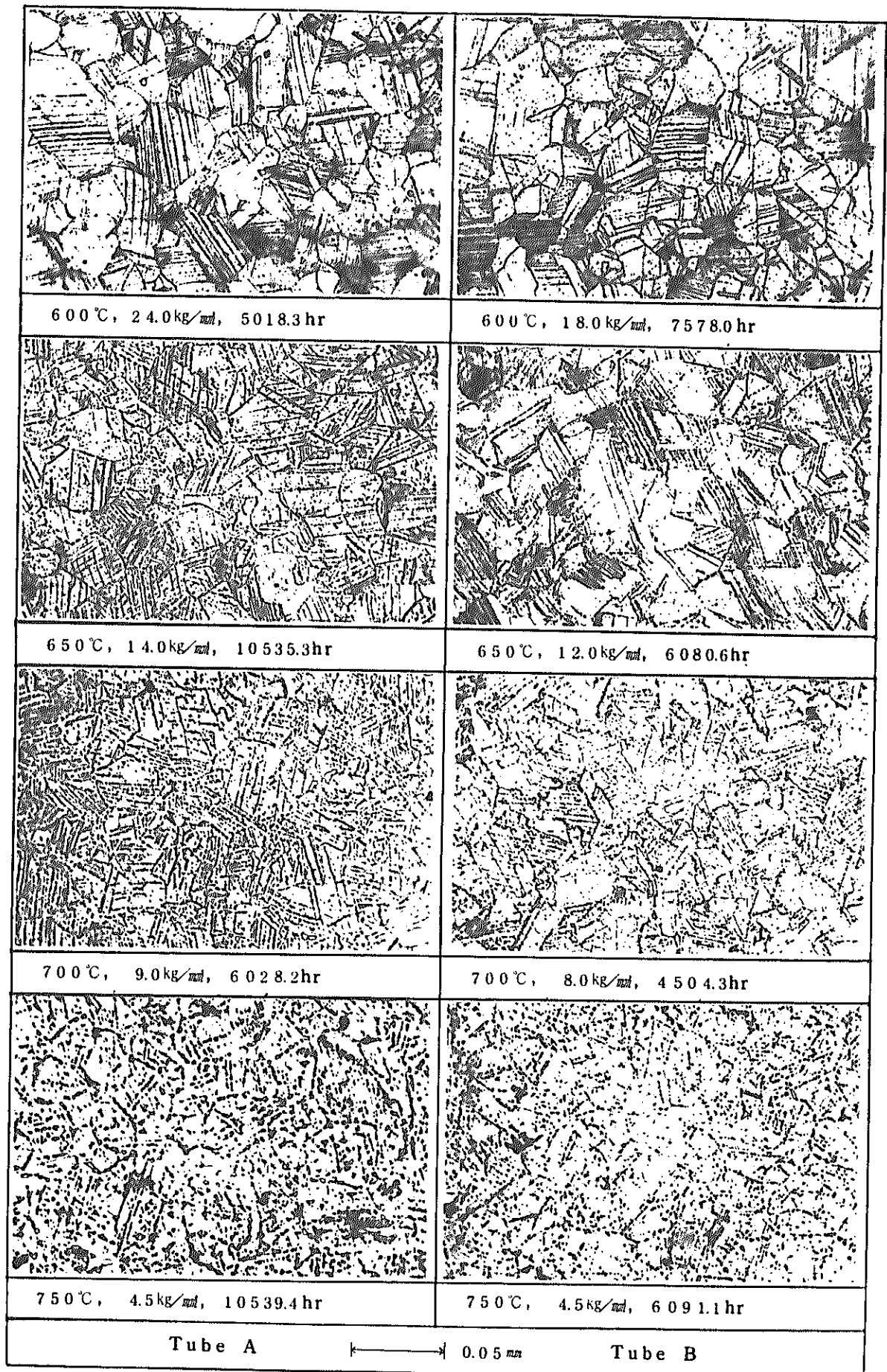|	
6 0 0 ℃, 2 4.0 kg/㎜, 5 0 1 8.3 hr	6 0 0 ℃, 1 8.0 kg/㎜, 7 5 7 8.0 hr
6 5 0 ℃, 1 4.0 kg/㎜, 1 0 5 3 5.3 hr	6 5 0 ℃, 1 2.0 kg/㎜, 6 0 8 0.6 hr
7 0 0 ℃, 9.0 kg/㎜, 6 0 2 8.2 hr	7 0 0 ℃, 8.0 kg/㎜, 4 5 0 4.3 hr
7 5 0 ℃, 4.5 kg/㎜, 1 0 5 3 9.4 hr	7 5 0 ℃, 4.5 kg/㎜, 6 0 9 1.1 hr

Tube　A　　｜←————→｜ 0.0 5 ㎜　　Tube　B

Photo. 5　　Photomicrographs of specimens of long-term rupture at each
temperature tested under uniaxial tension (longitudinal).

- 7 5 -

Specifications for Experimental Fast Reactor Fuel Claddings

November 28, 1968

POWER REACTOR AND NUCLEAR FUEL DEVELOPMENT CORPORATION

C O N T E N T S

1. Scope

   This Specifications specifies AISI #316 stainless steel seamless pipes used for fuel cladding tubes for fast experimental reactor.

   Unless otherwise specified, products under this Specifications shall conform to the requirements of A-450 of the ASTM.

2. Reference Standards

   ASTM A-450   General Requirement for Alloy Steel Tubes
        E-165   Liquid Penetrant Inspection
        A-370   Mechanical Testing of Steel Products
        E-112   Estimating the Average Grain Size of Metals
        E- 45   Determining Inclusion Content of Steel
        A-262   Intergranular Attack in Stainless Steel

3. Manufacture

   3.1 Melting

        Material shall be vacuum-melted.

   3.2 Heat Treatment and Cold Working

        After processed by solution heat treatment, products shall be treated with cold working of 8% to 15%. If necessary, products shall be treated with stress relief annealing.

4. Chemical Composition

   The chemical composition of products shall conform to the requirements of Table 1.

Element		Weight percent
Carbon		0.06 - 0.08
Manganese	(maximum)	2.00
Phosphorus	(")	0.03
Sulfur	(")	0.03
Silicon	(")	0.75
Nickel		11.00 - 14.00
Chromium		16.00 - 18.00
Molybdenum		2.00 - 3.00
Cobalt	(maximum)	0.10
Boron	(")	0.001
Nitrogen	(")	0.035
Iron		Balance

Table 1.   Chemical Composition

The suppliers shall make analysis of each heat, shall confirm that the specifications are met, and shall submit report thereof to the purchasers. The suppliers shall also make analysis of each lot of products in accordance with the sampling method and sampling rate specified by the purchasers, and shall submit report thereof to the purchasers.

4.1   Definition of Heat

Heat shall be defined as a single and uniform melt.

Lot shall mean products of same dimensions and same thickness continuously manufactured from same heat, annealed it same annealing batch, and inspected continuously.

5.   Mechanical Properties

Products shall have mechanical properties conforming to those specified in Table 2. Sampling method and sampling rate shall be specified by the purchasers.

A. Mechanical Properties at Room Temperature (Minimum Value)

Tensile strength (kg/mm^2)	0.2% Yield strength (kg/mm^2)	Elongation – 50 mm (%)
60	40	25

B. Mechanical Properties at 650°C (Minimum Value)

Tensile strength (kg/mm^2)	0.2% Yield strength (kg/mm^2)	Elongation – 50 mm (%)
30	20	15

Table 2.   Mechanical Properties

6. Structure

6.1 Grain Size

Test shall be made in accordance with the method specified by the ASTM E-112, and with the sampling method and at the sampling rate specified by the purchasers, and maximum grain size shall not be more than ASTM #6.

6.2 Inclusions

Material and inclusion in final products shall be inspected in accordance with the requirements of ASTM E-45.

Sampling method, sampling rate and criterion for judgement shall be specified by the purchasers.

7. Dimensional Accuracy

7.1 Straightness

Products shall be free of breaks or twists. Bend shall not be more than 0.75 mm per 1,000 mm. Inspection shall be made to all products.

7.2 Circularity

Circularity is defined as the difference between the maximum value and the minimum value of inside diameters. Circularity shall not be more than 0.05 mm in all products.

7.3 Dimensional Tolerance

Inside diameter, outside diameter and thickness shall be within the limits of the following tolerances. Inspection shall be made on all products.

Inside diameter (mm)	± 0.025
Outside diameter (mm)	± 0.030
Thickness (mm)	± 0.030
Length (mm)	+10 - 0

8. Surface Finish

Inside and outside surfaces of products shall be free of harmful deposits or stains including oxides. Surface roughness shall not be more than JIS 3S.

9. Cleaning

In cleaning, use of cleaning agent containing chlorine is not desirable. The suppliers, when determined or intended to use cleaning agent containing chlorine, shall inform the purchasers thereof at the time of inquiry and shall state in inspection report that residual chlorine on the surface of products is not more than 0.008 mg per 10 cm^2 surface area. Inspection method shall be approved by the purchasers. Inspection method shall be approved by the purchasers.

10. Test and Inspection

10.1 Mechanical Strength Test

10.1.1 Flattening Test

Flattening test shall be made in accordance with the testing method specified by ASTM A-450 and the sampling method specified by the purchasers.

10.1.2 Flaring Test

Flaring test shall be made in accordance with the testing method specified in the ASTM A-450, and with the sampling method and sampling rate specified by the purchasers.

10.1.3 Hardness Test

Hardness shall be tested in accordance with the sampling method and sampling rate specified by the purchasers.

10.1.4 Hydraulic Test

All products shall be hydraulically tested at room temperature under the pressure determined by the following equation:

$$P = \frac{2St}{D}$$

P : Pressure

S : One half of 0.2% yield strength in Table 2.

t : Nominal thickness

D : Nominal outside diameter

10.1.5 Hydraulic Burst Test

Hydraulic burst test shall be made in accordance with the sampling method and the sampling rate specified by the purchasers, and the burst pressure shall not be less than 800 kg/cm^2 and the yield pressure shall not be less than 650 kg/cm^2.

10.2 Flaw Detecting Test

10.2.1 Permeability Test

All products shall have permeability test made on their surface in accordance with the method specified by the ASTM E-165, and shall not have any visual defect.

10.2.2 Ultrasonic Flaw Detecting Inspection

Ultrasonic flaw detecting inspection shall be performed on all products using suitable apparatus, and those products to which defective signal equivalent to or more than the signal in the standard specimen was given shall be unacceptable. Said standard specimen shall have an artificial defect 0.025 mm deep and 0.75 mm long longitudinally and laterally.

10.3 Corrosion Test

10.3.1 Grain Boundary Corrosion

The sections of specimens sampled in accordance with the method and rate specified by the purchasers shall be observed under a microscope of 100 magnifications without etching, and shall show no grain boundary corrosion.

10.3.2 Corrosion Resistance

Corrosion test shall be made on products in accordance with the ASTM A-262. This test shall include tests for grain boundary corrosion produced by the precipitation of chromium carbide and by sigma deposit. The criterion for acceptance shall be specified by the purchasers.

11. Sampling Method and Sampling Rate

The sampling method and the sampling rate shall conform to the requirements of the Quality Control Regulations set forth by the purchasers.

12. Handling, Packing and Transportation

Products shall be carefully handled, packed and transported to be protected from damage on their surface.

Products shall be individually packed in paper or polyethylene and shall be transported in containers capable of protecting them from bending or damaging force.

- 6 -

The transportation containers shall have the following marking clearly shown:

1) Order number
2) Name of supplier
3) Grade
4) Dimension
5) Lot and heat or ingot numbers

13. Documents Required for Submission

The suppliers shall submit the purchasers the following documents and specimens on designated date and shall have them approved by the purchasers.

Item	No. of Copies	Submission Date
Manufacturing Procedures		Prior to preceding test
Quality Control Regulations		"
Descriptions of Manufacturing Equipment		"
Manufacturing & Quality Controlling Form		"
Manufacturing Schedules		"
Preceding Specimens		"
Test & Inspection Results	3	Within 30 days after test or inspection
Lot Records	3	Within 30 days after manufacture (lot)

Creep Tests on Fuel Claddings

for Experimental Fast Reactor, "JOYO"

- the Primary Test -

Abstract

As a part of investigating high temperature characteristics of "JOYO" fuel claddings, made of AISI 316 stainless steel, creep rupture tests under internal pressure, creep and creep rupture tests under uniaxial tension are presented in this report.

Two kinds of test cladding tubes, A and B, were prepared and tested at 600°C, 650°C, 700°C and 750°C with the target maximum rupture time of 3,000 to 10,000 hr. The results were as follows:

1) Some difference was observed in the creep characteristics between A and B claddings.

2) With regard to creep rupture tests under internal pressure, no significant difference was observed between the data obtained at the cooperating firms and institute. No difference in data due to argon gas atmosphere itself, moreover, was found out between those at 650°C and at 700°C, test time for both being about 3,000 hr.

3) Review on the results of creep rupture tests under internal pressure and of those under uniaxial tension indicated that the both were well correlated each other in the mean diameter equation.

4) Comparing the creep rupture strengths obtained in our experiment with those by ISO, it was suggested that, with regard to non-cold-worked cladding, our data were somewhat larger than ISO ones in the shorter time side while the former were closer to the latter in longer time side.

November, 1971

Creep Sub-Group

FBR Materials Subcommittee

FBR Fuel Design Committee

PNC

The work was undertaken by ten sub-group members, each two of them being the representatives of five organizations; they are National Research Institute for Metals, Kobe Steel, Ltd., Sumitomo Metal Industries, Ltd., Hitachi, Ltd. and Power Reactor & Nuclear Fuel Development Corp.